January 2010

Light-harvesting and the Primary Photochemistry of Roseiflexus castenholzii

Aaron Collins
Washington University in St. Louis

WASHINGTON UNIVERSITY IN ST. LOUIS

Department of Chemistry

Dissertation Examination Committee:

Robert E. Blankenship, Chair
Dewey Holten
Robert G. Kranz
Joshua A. Maurer
Liviu M. Mirica
Yinjie J.Tang

LIGHT-HARVESTING AND THE PRIMARY PHOTOCHEMISTRY OF *ROSEIFLEXUS CASTENHOLZII*

by

Aaron Michael Collins

A dissertation presented to the
Graduate School of Arts and Sciences
of Washington University in
partial fulfillment of the
requirements for the degree
of Doctor of Philosophy

August 2010

Saint Louis, Missouri

ABSTRACT

Photosynthetic organisms have evolved diverse antennas to harvest light of various qualities and intensities. Anoxygenic phototrophs can have bacteriochlorophyll Q_y antenna absorption bands ranging from about 700-1100 nm. This broad range of usable wavelengths has allowed many organisms to thrive in unique environments. *Roseiflexus castenholzii* is a niche-adapted, filamentous anoxygenic phototroph (FAP) that lacks chlorosomes, the dominant antenna found in all green bacteria. Light-harvesting is realized only in the membrane with BChl *a* and a variety of carotenoids. Through biochemical and spectroscopic methods, a model for the size and organization of the photosynthetic antenna is presented.

Despite the wide distribution of antennas, photochemistry occurs in the reaction center (RC), which can be separated into two groups distinguishable by the identity of the terminal electron acceptor. These are the Fe-S type or type-I and the quinone-type or type -II RCs. All known anoxygenic phototrophs have evolved to utilize only one type of RC. *R. castenholzii* contains a type-II RC. Through the successful isolation of the RC the kinetics of electron transfer have been investigated by ultrafast pump-probe spectroscopy.

Lastly, the energetics of some of the RC cofactors were determined by using redox titrations. The combination of the antenna model and RC kinetics and energetics allows for a nearly complete model of the primary photochemistry in *Roseiflexus castenholzii* and the expansion of photosynthetic data available among FAPs.

ACKNOWLEDGMENTS

There are many individuals that without their help and guidance, this thesis would not have been possible. It is a pleasure to convey my gratitude to those who deserve special acknowledgement.

First and foremost, my advisor, Professor Robert Blankenship, has set the bar on what it means to be a truly exceptional advisor. Your steadfast support and enthusiasm has made my smallest advances feel important and you have provided the framework for what it means to be a good scientist. Too numerous to list here are all the members of the Blankenship lab, both past and present, for their rich discussions and helpful suggestions, in particular, Martin who provided exceptional mentorship when I first arrived in Tempe, and Yueyong for developing my skills as a biochemist. To Wen, you started out as my lab mate and friend and have become more like my brother. I know you will be successful in any avenue you wish to pursue in life. I have be fortunate to have been part of several fruitful collaborations. I especially thank Drs. Dewey Holten, Chris Kirmaier, and Rich Loomis for experimental assistance that allowed me to dig deeper into my research projects and to Drs. Neil Hunter, John Olsen and Pu Qian. I am very grateful to have had my remarkable and lovely wife, Jessica, with me on this journey. I have cherished your relentless support and encouragement. I am thankful to my parents, Doug and Nancy, who have advocated the exploration of my interests and for their love.

I would like to acknowledge the Department of Energy, Graduate Assistance in Areas of National Need (GAANN) Fellowship and the Photosynthetic Antenna Research Center (PARC) Scientific Exchange grant for financial support.

TABLE OF CONTENTS

LIST OF TABLES

LIST OF FIGURES

ABBREVIATIONS

ACIII	Alternative complex III
bc_1	Ubiquinol:cytochrome *c* oxidoreductase complex
BChl	Bacteriochlorophyll
BPhe	Bacteriopheophytin
CD	Circular dichroism
Chl	Chlorophyll
DAD	N,N,N',N'-tetramethyl-1,4-phenylenediamine
β-DDM	n-dodecyl-β-D-maltopyranoside
EM	Electron microscopy
FAP	Filamentous anoxygenic phototroph
FMO	Fenna-Matthews-Olson protein
GSB	Green sulfur bacteria
IEC	Ion-exchange chromatography
LD	Linear dichroism
LDAO	Lauryl dimethylamine N-oxide
LH	Light-harvesting
LH1	Light-harvesting 1 complex
LH2	Light-harvesting 2 complex
LHCI	Light-harvesting complex I
LHCII	Light-harvesting complex II
LHRC	Light-harvesting – reaction center

MQ	Menaquinone
NIR	Near infrared
PCP	Peridinin-chlorophyll-protein
Phe	Pheophytin
PS1	Photosystem I
PS2	Photosystem II
RC	Reaction center
RR	Resonance Raman
RT	Room temperature
SDS-PAGE	Sodium dodecyl sulfate polyacrylamide gel electrophoresis
TA	Transient Absorption
TCSPC	Time-correlated single photon counting
TMPD	2,3,5,6-Tetramethyl-p-phenylenediamine
UQ	Ubiquinone
VIS	Visible

CHAPTER 1

GENERAL INTRODUCTION TO PHOTOSYNTHSIS

"In essence, science is a perpetual search for an intelligent and integrated comprehension of the world we live in."

Cornelius Bernardus Van Neil

Most of the energy consumed on earth, in the form of fossil fuels, is the result of photosynthesis many hundreds of millions of years ago. It is undeniably from this observation that photosynthesis is not only an ancient process but an invaluable process to understand at the deepest levels. Derived from Greek, photosynthesis literally means "to put together with light" but in more broad terms can be understood as a process that converts light from the sun into stable chemical products.

Oxygenic photosynthesis was the singular great biological invention that resulted in oxygenation of Earth's atmosphere and a radical new environment for all life. The rise in oxygen is thought to have started about 2.45 billion years ago (Bekker et al. 2004). It is likely that some form of anoxygenic photosynthesis was a precursor to the complex machinery necessary for photosynthetic oxygen evolving (Blankenship 1992). Interestingly, there exist today several different groups of organisms that only photosynthesize under conditions of ancient Earth's atmosphere *i.e.* in the absence of oxygen. Belonging exclusively to the bacterial kingdom, modern anaerobic phototrophs

may well be vestiges of some of the earliest photosynthesizers and may also represent model systems to study photosynthesis in its simplest forms.

Photosynthesis is a process that occurs on a time scale spanning at least 12 orders of magnitude (Blankenship 2002). The primary events of photosynthesis can be separated into two distinct processes; energy and electron transfer. Photonic energy is captured by light-harvesting (LH) pigment-protein complexes and the excitation is rapidly transferred to a photochemical reaction center (RC). The RC uses energy delivered from the antenna to facilitate charge separation across the membrane. The primary processes of photosynthesis, involving light capture, excitation transfer and the initial electron transfer reactions, happen on the femtosecond (fs, 10^{-15} s) to picosecond (ps, 10^{-12} s) time scales . Once initiated by energy delivered from the antenna, an electron is rapidly transferred from a primary donor through accessory pigments and subsequently to a terminal acceptor in the RC. Once reduced, the terminal acceptor either passively diffuses out of the RC and enters the electron transport chain or passes the electron to soluble carriers. These event can occur in the nanosecond (ns, 10^{-9} s) to microseconds (μs, 10^{-6} s) regime. Finally the reductions of secondary electron transport proteins spans from milliseconds (ms, 10^{-3} s) to seconds following initial antenna excitation and ultimately results in the formation of stable products.

Chlorophylls and bacteriochlorophylls

Chlorophyll (Chl) and bacteriochlorophyll (BChl) have duel roles in biology and that is to facilitate energy and electron transfer. Chls are a subset of tetrapyrole macrocycles that contain a fifth isocyclic ring E and are usually coordinated by a central Mg atom. Moreover, these pigments typically contain a long-chain hydrocarbon ester at the C-17[3] position (figure 1.1). (B)Chls are nearly ubiquitous among photosynthetic organisms. The physical properties of Chl and BChl in organic solvent are markedly different from their *in vivo* characteristics. For example, free pigments are labile to acids, bases, light and chemical oxidation. The conjugation of the macrocycle gives rise to strong light absorption properties (high extinction coefficients) and relatively long lived excited state lifetimes on the order of a few ns (Connolly et al. 1982). Chls and BChl are thus efficient photosensitizers (especially of oxygen) when illuminated with visible (VIS) to near infrared (NIR) light, thereby generating cytotoxic reactive oxygen species (Elstner 1982).

The absorption properties of Chls and BChls can be fine tuned by substituting for different moieties as well as differences of the oxidation level at particular positions of the macrocycle. These substitutions can either extend or condense the conjugation of the macrocycle along a particular molecular axis. Generally speaking, an increase in conjugation, even if only partial, results in shift in Q_Y absorption to longer wavelengths while the removal of such conjugation extensions has the opposite effect. This can be illustrated by considering that BChl *b* is identical to BChl *a* except that the ethyl group positioned at C-8 in BChl *a* is replaced by an ethylidine group (=CH-CH_3) at the C-8 position in BChl *b*. This subtle change extends the Q_Y absorption maximum of BChl *b*

in solvent by about 23 nm. An overview of Chl structure and the substitutions to the macrocycle observed among a variety of natural pigments is shown in figure 1.1. Additionally, the absorbance spectra of several Chls and BChls in organic solvent are displayed in figure 1.2. The chemical and physical properties of Chl are appreciably changed when interacting with one another or when bound in a protein.

Chl has three principally important photosynthetic functions and each will be addressed sequentially in the order in that they occur. First, Chl functions to capture photons. The oscillating electric field component of a photon may interact with the electrons of a molecule thus causing the electrons of the molecule to change their spatial distribution. Such an event is necessarily based on probability and the transition from one electronic configuration (state) to another configuration is described by the **transition dipole moment**, μ_{0A}

$$\mu_{0A} = \int \Psi_0 \mu \Psi_A dv$$

Where Ψ_0 and Ψ_A are wavefunctions representing the ground and excited state, respectively, μ is the electric dipole-moment operator, and dv is a volume element integrated over all space. Because the electrons of an absorbing molecule are interacting with an oscillating electric field, the transition dipole moment is a vector quantity having a both magnitude and directionality within the molecule, in other words, the transition from a ground state to an excited state is polarized. The relationship between absorption of light by a molecule, A, the oscillating electric field component of a photon (assumed here to be linearly polarized), E, and the transition dipole moment, μ, is given by

$$A \propto \left(\vec{E} \cdot \vec{\mu} \right)^2 = \left| \vec{E} \right|^2 \left| \vec{\mu} \right|^2 \cos^2 \phi$$

with arrows indicating vector quantities and φ is the angle between the electric field and transition dipole moment. It can be seen from this relationship that when $\vec{E}$ and $\vec{\mu}$ are arranged parallel, the absorption of light by the molecule is greatest.

The square of the transition dipole moment above is termed **Dipole strength**, *D*, and is a useful term because it relates to the absorption spectrum and properties of the absorbing molecule by the following relationship

$$D = \frac{9.185 \times 10^{-39}}{n} \int \frac{\varepsilon(v)}{v} dv$$

where *n* is the refractive index of the medium, ε is the molar extinction coefficient integrated over the entire absorption band, and *v* is the frequency. It can be seen from this relationship that *D* and $\varepsilon(v)$ are directly related *i.e.* a large extinction coefficient for a particular transition is associated with large dipole strength.

Chl and BChl molecules are satisfactory photon capturing pigments because of their large extinction coefficients and dipole strength. For example, the molar extinction coefficient of BChl *a* and Chl *a* measured for their respective Q_Y transitions in diethyl ether are about 90 cm^{-1} mM^{-1} (Goedheer 1966; Oelze 1985).

The transition from the ground to an excited state in Chl (or most molecules for that matter) occurs in just a few fs. As mentioned above, the excited state lifetime of free Chl and BChl in solvent is on the order of a few ns. The major competing de-excitation pathways for the excited state of Chl are fluorescence, thermal deactivation,

energy transfer and photochemistry however these processes will only be biologically useful if the rate in that they occur is significantly faster than the intrinsic excited state lifetime of the pigment. Energy transfer and photochemistry are indeed sub-ns processes and have been optimized in photosynthesis to make use of light energy.

This leads to the second principally important quality of Chl, the ability to transfer excitation. Energy transfer is a purely physical process where an excited pigment molecule relaxes back to the ground state by transferring the excitation of the excited state to a neighboring pigment. This process can be extended to the many pigments that make up the LH antenna. The orientation and spatial relationships between adjacent pigments are precisely controlled by coordination from the protein. Additionally, pigments are usually organized in a manner in which the most distal pigments to the RC absorb the highest frequencies of light and pigments closest to the RC usually absorb at lower frequencies. This situation allows excitation in the antenna to be funneled "downhill" or to lower energies as it approaches the RC. This further increases the efficiency of the energy transfer process because the transfer of excitation to pigments of lower energy is thermodynamically favorable.

The concept of energy transfer has been subject to several theoretical treatments (Akihito and Graham 2009; Beljonne et al. 2009; Van Amerongen H et al. 2000). No singular approach is sufficient to describe all of the observed energy transfer events in photosynthesis, however Förster's theory of energy transfer has been successfully applied for a variety of energy transfer processes (Förster 1948; Stryer 1978). Briefly, in Förster theory, two pigments, an excited donor and acceptor in the ground state, are

separated such that excitonic coupling between the two pigments is small (compared to the energies of the individual pigments). Under these circumstances, energy is transferred non-radiatively and in resonance by a dipole-dipole or Coulomb mechanism that follows a $1/R^6$ dependence where R is the distance between the donor and acceptor molecules. Because electron transitions are quantized in each molecule, donor and acceptor molecules must have energy states in common in order for energy to be transferred efficiently. One useful way to visualize this is to consider the overlap of the fluorescence emission band of the donor molecule compared to the absorption band of the acceptor both normalized at their respective maxima. Where the two bands overlap are where common energy states may exist. In addition to the overlap of energetic states between the donor and acceptor, efficient energy transfer depends on the orientation of the transition moments between the molecules. In other words, because the transition to and from excited states are associated with transition dipole moments, and thus have associated directionality, parallel orientation of these transitions will lead to the most efficient energy transfer while orthogonal orientation would be least favorable.

Lastly, the third preeminent property of Chl and BChl is the ability to participate in electron transfer and these events occur in the RC. Often, the excited state of a molecule has vastly different properties than the same molecule in the ground state. For example, the photo-excited states of (B)Chl are strong reducing agents able to donate electrons to nearby acceptor molecules. Electron transfer reactions are ubiquitous in chemistry and biology and their rates depend on the redox potential

difference of the donor and acceptor (ΔG), the coupling of the initial and final states of the system, and the reorganization energy, which can be described as the energy required to structurally change the electronic configuration of the donor to that of the acceptor. The theoretical framework for describing the kinetics and thermodynamics of electron transfer has been described by Marcus (Marcus 1964).

Light-harvesting antennas

Light-harvesting (LH) antennas represent a markedly diverse set of pigment-proteins complexes that all function under that same accord: to capture light energy and funnel the excitation to a photochemical RC. For most LH antennas, protein serves as a scaffold to arrange the pigments spatially and in a particular orientation. A delicate balance of pigment-pigment distance and transition dipole orientation is necessary to maximize energy transfer efficiency. The absorption properties of LH antennas can be fine tuned by altering the pigment identity as well as changing the local environment through electrostatic interactions of the pigment within the protein. The structures of several representative antenna complexes as well as their respective absorption spectra are depicted in Figure 1.3. LH antennas can be broadly categorized as either *integral membrane* (LH1, PS1, PS2, etc) *peripheral membrane* (chlorosomes, FMO, PCP, phycobilisomes etc) or *accessory* (LHCII, LHCI, LH2 etc) antenna complexes. Integral membrane complexes contain protein regions that span the biological membrane. Peripheral membrane antennas are associated with the membrane but do not span the

membrane and are often found in association with integral membrane proteins. Lastly, accessory antenna complexes are always found in conjunction with integral membrane proteins. They can be mobile, exist in variable stoiciometry and are often involved in regulatory processes.

The LH system of purple non-sulfur bacteria

The purple non-sulfur bacteria are anoxyphototrophs that are often found in anaerobic layers of aquatic environments. All purple bacteria posses an integral membrane core-complex that is the combination of its RC and the so-called LH1 complex. LH1 is composed of an inner ring of α-subunits and outer ring of β-subunits that encompass the RC. Each subunit binds one BChl *a* (or BChl *b* in some species) so that the pigments are arranged perpendicular to the plane of the membrane, in a ring between the protein subunits. The combination of BChl *a* or *b* (as apposed to Chl) as well as interactions with the protein push the wavelengths of light utilized by these organisms from ~800 to over 1000 nm. The long wavelength absorption maximum in LH1 with BChl *a* is at about 875 nm. The LH machinery of purple bacteria have been extensively investigated for its structural and kinetic properties (Cogdell et al. 2006).

Intact chromatophores from several species of purple bacteria have been visualized with AFM. These remarkable images revealed RCs that can be completely or partially surrounded by the LH1 ring with 15 or 16 α/β-subunits or even form "S-shaped" core-complex dimers of 26 subunits. The diameter of monomeric LH1 range

from about 90-120 Å while the dimeric core complexes have dimensions of about 100-250 Å (Scheuring 2006). Additionally, the core complex structure from *Rhodopseudomonas palustris* was determined by x-ray crystallography to 4.8 Å resolution (Roszak et al. 2003) (figure 1.4 upper panel).

An accessory integral membrane antenna associated with many but not all purple bacteria is the LH2 complex. The structure of LH2 from *Rhodoblastus acidophilus* (formerly *Rhodopseudomonas acidophila*) and *Phaeospirillum* (formerly *Rhodospirillum*) *molischianum* are known at atomic resolution (Koepke et al. 1996; McDermott et al. 1995; Papiz et al. 2003) (for *R. acidophilus* structure see figure 1.4 lower panel). LH2 is a ring-shaped complex of either eight or nine subunits, depending on species and like LH1, is composed of an inner ring of α-subunits and outer rings of β-subunits. The diameter of LH2 is about 6.5 nm. Each α/β pair binds three BChl *a*, one BChl absorbing around 800 nm (so called B800) towards the cytoplasmic side of the membrane and two strongly coupled BChl absorbing around 850 nm (B850) located towards the periplasmic side of the membrane. The B850 pigments are arranged perpendicular to the membrane plane with the Q_Y transition dipole being in the plane of the membrane. The B800 pigments more-or-less sit flat in the membrane. Despite differences in the orientation of each set of pigments, the Q_Y transition dipole for both B800 and B850 are nearly parallel. From the *R. acidophila* structure, adjacent B800 pigments are separated by a center-to-center distance of 21.2 Å and B800 is separated from the B850 pigments by 17.6 or 18.3 Å (Papiz et al. 2003). Additionally, an extended carotenoid molecule forms a half helix, wrapping around from one subunit to

the adjacent and is in close proximity to both B800 and B850. The carotenoid molecule is considered structurally important and deletion of the carotenoid through mutations lead to LH2s that fail to assemble *in vivo* (Lang and Hunter 1994).

LH2, LH1 (and the LH1RC) have been the subject of numerous spectroscopic investigations. These systems are well suited for such approaches because they are stable, can be purified in large quantities, some species are amenable to genetic manipulation (Hunter 1995), and as mentioned above, there are high-resolution crystal structures to link the spectroscopy to theoretical approaches.

LH system of filamentous anoxygenic phototrophs

FAPs belong to The Family Chloroflexaceae. The first discovered FAP, named *Chloroflexus aurantiacus*, was discovered from thermophilic hot springs and was shown to be clearly distinct from all other photosynthetic bacteria (Pierson and Castenholz 1974). Many species of FAP inhabitat mat communities with cyanobacteria, however other mesophilic FAPs are found in fresh water and yet still other species are found in hypersaline environments, for example *Candidatus* Chorothrix halophila (Klappenbach and Pierson 2004). Interestingly, not all members of the family Chloroflexaceae are photosynthetic. 16S rRNA analysis indicate that Chloroflexaceae are the deepest branching group containing phototrophs (Oyaizu et al. 1987).

The photosynthetic apparatus of FAPs is complex and can be described as chimeric, having themes from both the purple bacteria and green sulfur bacteria (GSB).

Most distal to the RC, some species of FAPs contain a chlorosome. Chlorosomes, in general, are enormous, self-assemblies of BChl *c*, *d*, or *e*, housed in a lipid monolayer. Chlorosomes from GSB are about 110-180 nm long, 40-60 nm wide, and 20-30 nm tall (Frigaard et al. 2004) while those found in FAPs are generally smaller and can vary in size depending on growth conditions (Golecki and Oelze 1987). The number of BChl *c* housed in an average chlorosome from *Chlorobium tepidum* was calculated to be approximately 215,000 ± 80,000 (Montaño et al. 2003a). Chlorosomes are remarkable antenna structures and have warranted much research interest partly due to the fact that the pigments are self-assembled and do not necessitate a protein scaffold for correct assembly (Brune et al. 1987b). Chlorosomes primarily absorb light between 700-760 nm depending on the identity of the BChl pigments within.

Light excitation absorbed by BChl *c* in the chlorosome is funneled into the membrane through the so-called baseplate complex. In FAPs, the baseplate is comprised of a small 5.7 kDa CsmA protein, BChl *a* and β-carotene and has been successfully isolated from the chlorosome (Montaño et al. 2003b). The baseplate complex is thought to reside on the side of chlorosome that faces the cytoplasmic membrane. Recently, cryo-electron microscopy has shown small features attributed to the baseplate that were only visualized on one side of the chlorosome (Psencik et al. 2009). Kinetics studies clearly indicate that the decay of excitation from BChl *c* in the chlorosome interior is matched by a rise of the same kinetics from BChl *a* in the baseplate (Brune et al. 1987a; Savikhin et al. 1998). The baseplate has a Q_Y absorption band at 795 nm.

Though not all FAPs possess chlorosomes, all members of this group have a membrane bound antenna system that has properties of both LH1 and LH2 from purple bacteria. The antenna system from the chlorosome-lacking FAP, *Roseiflexus castenholzii*, is the main subject of this work and will be described in further detail in the following chapters. The membrane bound antenna has a sequence homology to both LH1 and LH2 from purple bacteria (Wechsler et al. 1985; Wechsler et al. 1987). Like most LH2, it contains two long wavelength bands in the near-infrared. It is highly probable that each subunit of the antenna contains three BChl *a*. However, similar to LH1, the complex is associated with a RC (Collins et al. 2009; Yamada et al. 2005). Dynamic light scattering and EM have shown that the purified antenna from *C. aurantiacus* may be circular in shape and have a diameter larger than that of LH1 from purple bacteria (Xin et al. 2005). A model of the architecture of the chlorosome containing FAP, *C. aurantiacus* is presented in figure 1.5.

Reaction Centers

RCs are integral membrane complexes that use light energy, usually delivered from the antenna, to catalyze the endergonic transport of an electron across the biological membrane. There are two classes of RCs that are distinguishable by the identity of the terminal electron acceptor. These are the Fe-S type or Type-I and the quinone-type or Type -II RCs. Photosynthetic eukaryotes and cyanobacteria have evolved to utilize both types of RCs connected in series to drive the oxidation of water

while all known anoxygenic phototrophs have evolved to utilize only one type of RC. For example, purple bacteria and FAPs employ a Type-II RC while GSB, heliobacteria and the genus Chloracidobacterium contain a Type-I RC (figure 1.6).

Although differing in the identity of the terminal electron acceptor, the two classes of RCs contain overlapping structural elements. Both types of RCs contain a special pair of (B)Chl that are coupled near the interface of a hetero or homo dimeric RC core protein. The special pair is always located near in the periplasmic side of the member in bacteria or the luminal side of chloroplasts. Additionally, cofactors are precisely orientated around a (pseudo)-C_2 *symmetry* axis along the RC core.

Electrons are preferentially transferred only along one branch of cofactors in the case of Type-II RCs despite having similar or identical cofactors along the inactive branch of the RC. The preference for one branch over the other arises from the protein environment around the cofactors which may alter their redox potentials, thus making electrons transfer to those cofactors unfavorable. Moreover, Type-II RCs can be strong oxidizing agents and in cyanobacteria and photosynthetic eukaryotes, PSII can extract electrons from water. In the case of Type-I RCs, electrons are transferred along both branches of the RC. However, it has recently been observed that unidirectional electron transport was observed in PSI from *Acaryochloris marina* (Itoh et al. 2008). Type-I RCs are powerful reducing agents, for instance the excited state of the special pair, P_{700}, from PSI is estimated to have a redox potential of -1.26 V.

The sequence identity between the two types of RCs are very low, <10%, however the core of each type of RC is structurally similar indicating a common ancestor may have occurred from a gene duplication event (Sadekar et al. 2006).

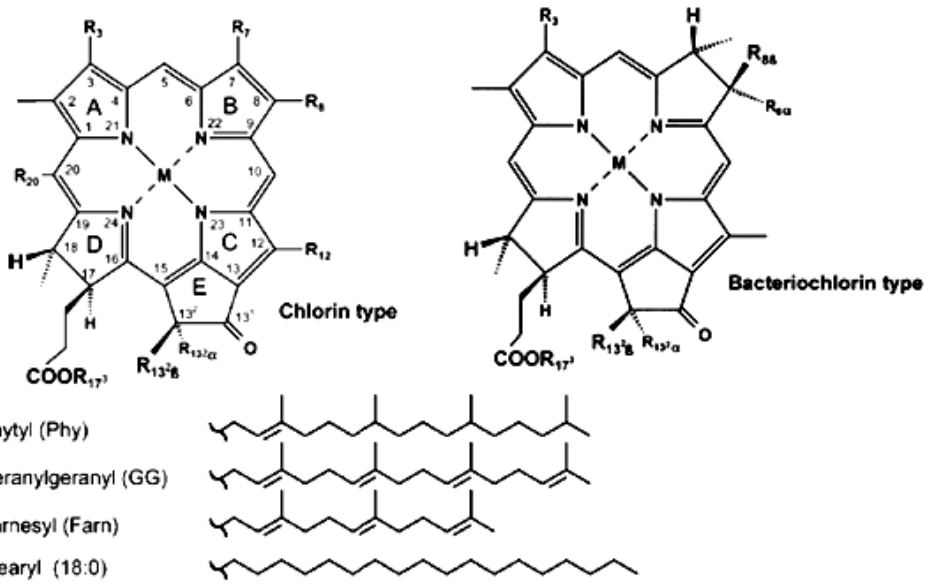

Chlorin Type

Pigment	Abbr.	R_3	R_7	R_8	R_{12}	$R_{13}^2{}_\alpha$	$R_{13}^2{}_\beta$	R_{17}^3	R_{20}
Chlorophyll *a*	Chl *a*	C_2H_3	CH_3	C_2H_5	CH_3	$COOCH_3$	H	Phy	H
Chlorophyll *b*	Chl *b*	C_2H_3	CH_3	C_2H_5	CH_3	$COOCH_3$	H	Phy	H
Chlorophyll *d*	Chl *d*	CHO	CH_3	C_2H_5	CH_3	$COOCH_3$	H	Phy	H
Pheophytin *a*	Phe *a*	C_2H_3	CH_3	C_2H_5	CH_3	$COOCH_3$	H	Phy	H
Bacteriochlorophyll *c*	BChl *c*	CHOH-CH_3	CH_3	$CH_2CH_n(CH_3)_{3-n}$	CH_3/C_2H_5	H	H	Farn/others	CH_3
Bacteriochlorophyll *d*	BChl *d*	CHOH-CH_3	CH_3	$CH_2CH_n(CH_3)_{3-n}$	CH_3/C_2H_5	H	H	Farn/others	H
Bacteriochlorophyll *e*	BChl *e*	CHOH-CH_3	CHO	$CH_2CH_n(CH_3)_{3-n}$	CH_3/C_2H_5	H	H	Farn/others	CH_3

Bacteriochlorin Type

Pigment	Abbr.	R_3	R_7	$R_{8\alpha}/R_{8\beta}$	R_{12}	$R_{13}^2{}_\alpha$	$R_{13}^2{}_\beta$	R_{17}^3	R_{20}
Bacteriochlorophyll *a*	BChl *a*	$COCH_3$	H	H/C_2H_5	CH_3	$COOCH_3$	H	Phy	H
Bacteriochlorophyll *b*	BChl *b*	$COCH_3$	H	=CH-CH_3	CH_3	$COOCH_3$	H	Phy	H
Bacteriochlorophyll *g*	BChl *g*	C_2H_3	H	=CH-CH_3	CH_3	$COOCH_3$	H	GG	H
Bacteriopheophytin *a*	BPhe *a*	$COCH_3$	H	H/C_2H_5	CH_3	$COOCH_3$	H	Phy	H
Bacteriopheophytin *b*	BPhe *b*	$COCH_3$	H	=CH-CH_3	CH_3	$COOCH_3$	H	Phy	H

Figure adapter from Scheer, 2006

Figure 1.1. Chlorin and bacteriochlorin macrocycle structures numbered according to IUPAC nomenclature. The major difference between chlorin and bacteriochlorin type chlorophylls is the presence or absence of a double bond between C-7/C-8 and C-17/C-18. Note that BPhe and Phe molecules are distinguished from BChl and Chl by a lack of a centrally coordinated Mg^{2+}. Data in (A) are from(Scheer 2006).

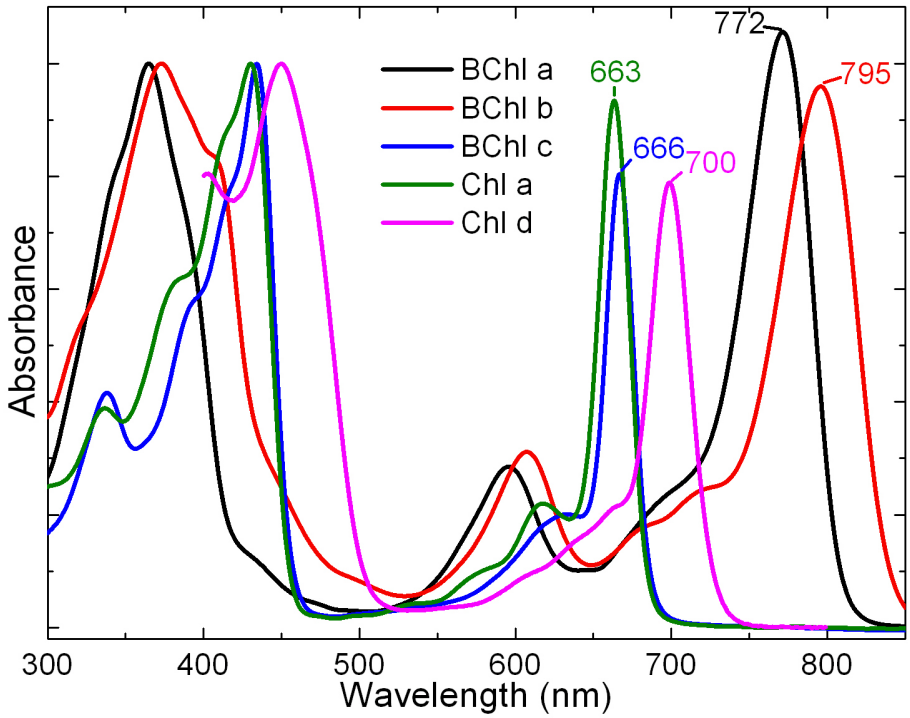

Figure 1.2. Absorption spectra of selected Chls and BChls in Methanol: acetonitrile: ethylacetate normalized in the Soret region. The Q_Y absorption maximum for each pigment is indicated in nm. Coordinates are from (Frigaard et al. 1996)

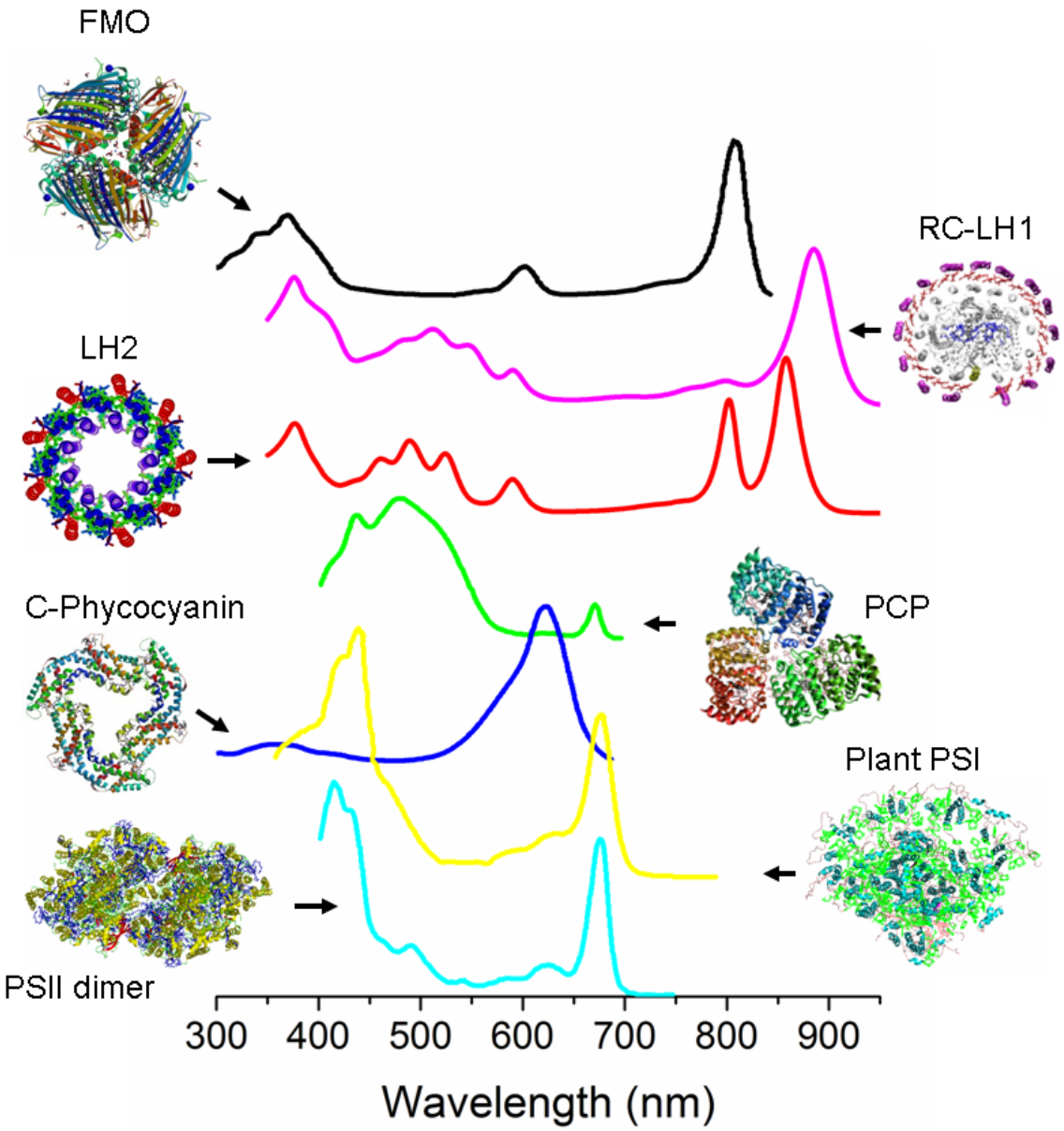

Figure 1.3 – Structures of several representative LH antennas as determined by x-ray crystallography. Starting from the top of the figure; Fenna-Matthews-Olsen (FMO) Protein from *Prosthecochloris aestuarii* (PDB accession 3EOJ). The RC-LH1 complex from *Rhodopseudomonas palustris* (PDB accession 1PYH). LH2 complex from *Rhodopseudomonas acidophila* strain 7050 (PDB accession 1NKZ). The peridinin-chlorophyll-protein (PCP) from *Amphidinium carterae* (PDB accession 1PPR). C-phycocyanin, a phycobiliprotein, from *Cyanidium caldarium* (PDB accession 1PHN). Plant PSI (from *Pisum sativum*) (PDB accession 2WSC) and the PSII dimer (PDB accession 3A0B) from *Thermosynechococcus vulcanus.*

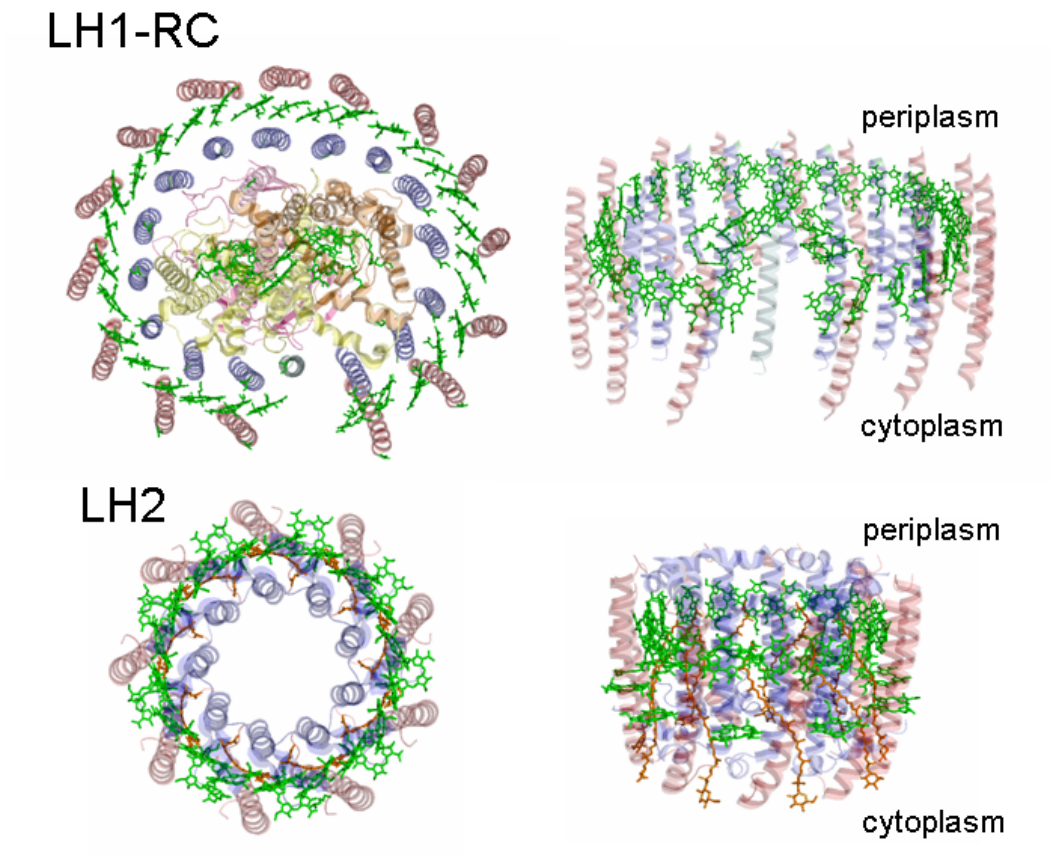

Figure 1.4 – Structures of the LH1-RC from *Rhodopseudomonas palustris* (PDB accession 1PYH) and LH2 from *Rhodopseudomonas acidophila* strain 7050 (PDB accession 1NKZ). Left images are top views looking down into the periplasmic side of each complex. Right images are side view images. In all images, the phytol side chains of BChl *a* have been removed for clarity. The α-polypeptides are blue, and the β-polypeptides are colored red. BChls are colored green and rhodopin glucoside in orange.

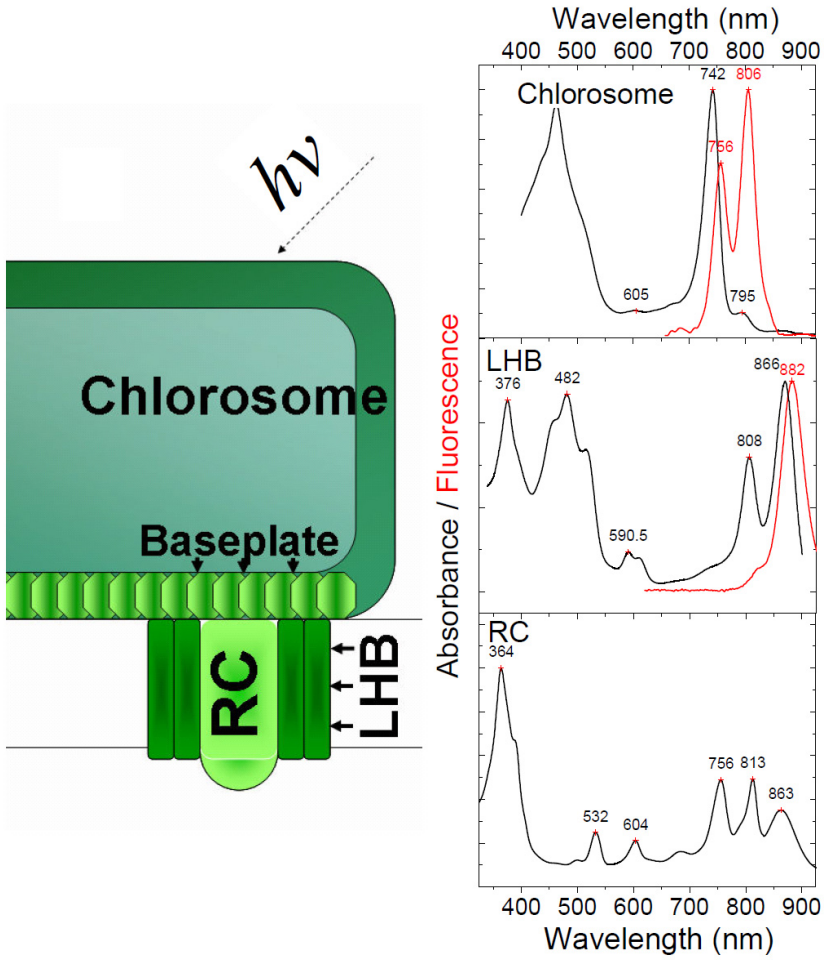

Figure 1.5 – Left - Model of the LH apparatus in *C. aurantiacus*. Right – absorption (black) and fluorescence (red) properties of the isolated chlorosome (top panel), LHB 808-866 (middle panel) and the RC (lower panel). Note that the baseplate absorbance appears at 795 nm as a small peak in chlorosome absorption panel.

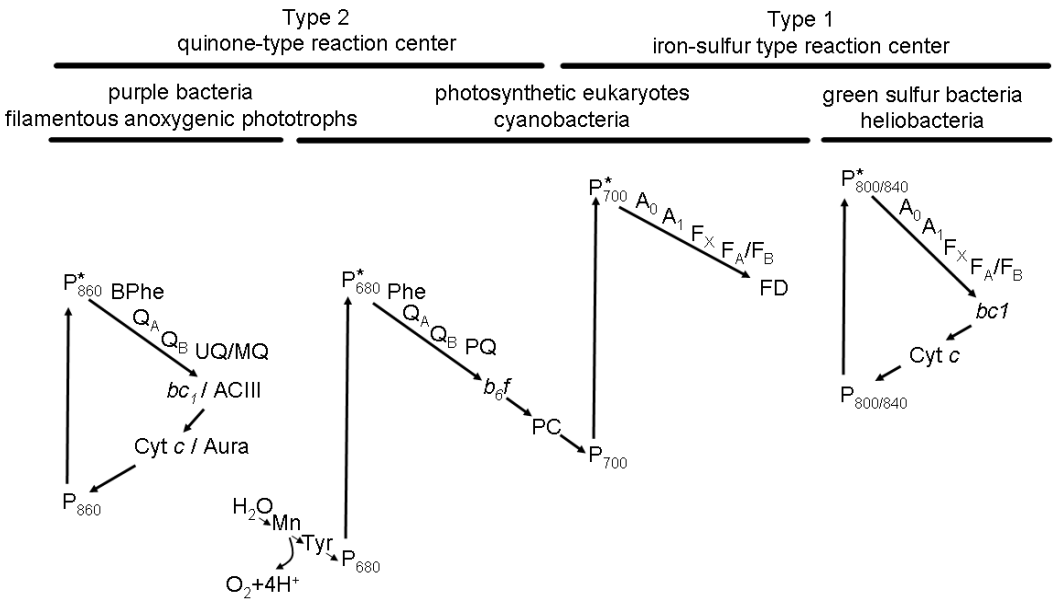

Figure 1.6 – RC cofactors among various groups of phototrophs. P_{860} – the special pair BChl from purple bacteria or FAPs, BPhe – bacteriopheophytin, the primary acceptor in the RC, Q_A - the first quinone acceptor, Q_B – the terminal quinone acceptor. UQ/MQ – the ubiquinone or menaquinone pool, *bc_1* - ubiquinol:cytochrome *c* oxidoreductase complex, ACIII – alternative complex III (menaquinol:auracyanin oxidoreductase), Cyt *c* – cytochrome *c* the immediate donor to the RC of purple bacteria, Aura – auracyanin the proposed immediate donor to the RC in FAPs. Mn – manganese cluster, Tyr – tyrosine Z, P_{680} – PSII special pair Chl, PQ – plastoquinone pool, *b_6f* - cytochrome *b_6f* complex (plastoquinol—plastocyanin reductase), PC – plastocyanin, P_{700} – PSI special pair Chl, A_0 – primary acceptor chlorophyll, A_1 – secondary acceptor quinone, F_X – [4Fe-4S] cluster F_A/F_B – additional [4Fe-4S] clusters residing on the PscA protein, FD – ferredoxin. P_{800} the special pair BChl from heliobacteria, P_{840} – the special pair BChl from green sulfur bacteria.

CHAPTER 2

PIGMENT ORGANIZATION IN THE PHOTOSYNTHETIC APPARATUS OF *ROSEIFLEXUS CASTENHOLZII*

Abstract

The light-harvesting – reaction center (LHRC) complex from the chlorosome-lacking filamentous anoxygenic phototroph (FAP), *Roseiflexus castenholzii* (*R. castenholzii*) was purified and characterized for overall pigment organization. The LHRC is a single complex that is comprised of light harvesting (LH) and reaction center (RC) polypeptides as well as an attached *c*-type cytochrome. The dominant carotenoid found in the LHRC is keto-γ-carotene, which transfers excitation to the long wavelength antenna band with 35% efficiency. Linear dichroism and fluorescence polarization measurements indicate that the long-wavelength antenna pigments absorbing around 880 nm are perpendicular to the membrane plane, with the corresponding Q_y transition dipoles in the plane of the membrane. The antenna pigments absorbing around 800 nm, as well as the bound carotenoid, are oriented at a large angle with respect to the membrane. The antenna pigments spectroscopically resemble the well-studied LH2 complex from purple bacteria, however the close association with the RC makes the light harvesting component of this complex functionally more like LH1.

Introduction

Photosynthetic organisms have evolved to capture sunlight utilizing a variety of light harvesting architectures and pigment compositions that are highly diverse and have evolved to adapt to very different light intensity and light quality environments. Significant progress has been made in elucidating the structure-function relationships of the LH, RC and photosynthetic electron transport complexes among the various classes of phototrophs (Blankenship 2002). However, among the anoxygenic phototrophs, the purple bacteria are by far the best understood and other groups are less well characterized (1995; Cogdell et al. 2006; 2008).

The phylum *Chloroflexi* contains filamentous anoxygenic phototrophs (FAPs) which are typified by *Chloroflexus* (*Cf.*) *aurantiacus* and harvest light primarily using bacteriochlorophyll (BChl) *c* located in the chlorosome (Frigaard and Bryant 2006). The photosynthetic apparatus of most recently isolated species have not yet been characterized (Keppen et al. 2000; Klappenbach and Pierson 2004; Weller et al. 1992). Among these, the newly described *Roseiflexus castenholzii* is one of just a few known FAPs that lack chlorosomes (Hanada and Pierson 2006; Hanada et al. 2002). Recently, a crude RC preparation from *R. castenholzii* was described which has similar absorption characteristics to the RC of *Cf. aurantiacus* and protein sequence homology both to *Cf. aurantiacus* and to purple bacteria (Yamada et al. 2005). This same report determined that the *puf* gene arrangement was in the order of *pufB*, -*A*, -*L*, -*M*, and –*C*. This is more analogous to the arrangement of the *puf* operon in purple bacteria rather

than that in *Cf. aurantiacus,* which have the same genes located on two distinct operons, *puf1* and *puf2* (Watanabe et al. 1995). The genome sequences of several FAPs, including both *Cf. aurantiacus* and *R. castenholzii* have recently been determined.

Cf. aurantiacus contains, in addition to the peripheral chlorosome, a membrane-bound light-harvesting complex (B808-866) that is in close association with the RC. The B808-866 complex, named according to its Q_y absorption maxima, is thought to contain 3 BChl *a* per two antenna polypeptides, which are similar to the α- and β-subunits of LH1 and LH2 from purple bacteria (Wechsler et al. 1985; Wechsler et al. 1987). The absorbance of the antenna resembles LH2, however, the close association with the RC suggests that its function is related to LH1 (Vasmel et al. 1986; Xin et al. 2005). The Q_y transitions of the 866 nm pigments were determined to be approximately in the plane of the membrane while the 808 nm transitions are oriented at ~45° to the membrane plane (Novoderezhkin and Fetisova 1999; Vasmel et al. 1986). *R. castenholzii* lacks chlorosomes but also contains a membrane-bound antenna that is generally similar to that found in *Cf. aurantiacus,* however its absorbance maxima are at about 800 and 880 nm (Hanada et al. 2002; Yamada et al. 2005).

Chloroflexi are the earliest branching phylum of bacteria that contains phototrophs, so they may have a central importance in understanding the origin and evolution of photosynthesis (Oyaizu et al. 1987). However, with the exception of *Cf. aurantiacus,* relatively little has been done to characterize this very diverse group of bacteria. The following objectives for the present analysis are: (a) to purify the LHRC

complex from *R. castenholzii* and (b) provide initial characterization the LHRC complex in terms of pigment composition and organization. Our results demonstrate an overall similarity between the antenna pigments in *R. castenholzii* and *Cf. aurantiacus,* but with some significant differences. Lastly, the LHRC from *R. castenholzii* provides a unique opportunity to study the antenna-reaction center complex of an FAP without the complication of the chlorosome.

Materials and methods

Purification of the LHRC from *R. castenholzii*

Roseiflexus castenholzii strain HLO8^T was a kind gift from Dr. Yusuke Tsukatani and cells were grown photoheterotrophically according to Hanada et al. (Hanada et al. 2002). Purification of the LHRC was performed as follows: whole membranes (OD = 50 cm^{-1} measured at 880 nm) were solubilized with 2% n-dodecyl-β-D-maltopyranoside (DDM) by incubation for 30 minutes in the dark at 4ºC and then ultracentrifuged at 200,000g for 2 hours. Solubilized membranes were subjected to ion-exchange chromatography (IEC) on a column packed with QSFF resin (GE Healthcare, Uppsala, Sweden) followed by gel filtration (Sephacryl S-400 HR resin, GE Healthcare, Waukesha, WI) and a second round of IEC (QSHP resin, GE Healthcare, Uppsala, Sweden). All columns were equilibrated with 0.02% DDM in 20mM Tris-HCl, pH = 8.0 and eluted with NaCl in the same detergent solution. The purified LHRC used for these analyses were concentrated and the 280/880 nm ratio was measured to be

≤ 0.66. Sucrose gradients containing between 5 – 25 % sucrose in 0.02% DDM and 20mM Tris-HCl, pH = 8.0, were prepared and 1 mL of the LHRC was loaded and ultracentrifuged for 15 hours at 150,000g. SDS and native PAGE were performed according to the methods of Schägger and von Jagow (Schägger and von Jagow 1987, 1991).

Pigment extraction and identification

Pigments were extracted by diluting the LHRC 10-fold (v/v) in 7:2 acetone: methanol, followed by centrifugation. The supernatant liquid was taken and the pellet was resuspended in fresh solvent and subjected to a second round of centrifugation. The above procedure was repeated until the pellet was colorless. The resulting supernatant liquid was dried and resuspended in methanol for pigment composition analysis and for HPLC analysis. Pigment ratios were determined using the molar extinction coefficients ε_{462} = 167 mM^{-1} cm^{-1} (Young and Britton 1993) and ε_{772} = 60 mM^{-1} cm^{-1} (Oelze 1985) for γ-carotene and BChl *a*, respectively. Reverse-phase HPLC was performed with an Agilent 1100 system using a Zorbax Eclipse XDB-C18 column with an isocratic flow rate of 1 ml/min with 100% methanol. The identities of the eluted carotenoids were determined using MALDI-TOF mass spectrometry on a 4700 Proteomics Analyzer (Applied Biosystems Inc, Foster City, CA, USA) and masses were compared to published values (Takaichi et al. 2001).

Steady-State Spectroscopy

Absorption spectra were recorded using a Perkin Elmer Lambda 950 spectrophotometer (Waltham, Massachusetts, USA). Light-minus-dark difference absorbance spectra were generated using the following protocol: equal concentrations of sample were placed in two equivalent cuvettes in the sample and reference chamber respectively, and a baseline was recorded. Then light from a projector lamp was filtered through a 700 nm short pass filter and piped through a fiber optic cable, illuminating the bottom of the sample cuvette.

Fluorescence and fluorescence excitation spectra were recorded using a Photon Technology International fluorometer (Birmingham, NJ, USA), equipped with a red-sensitive avalanche photodiode detector (Advanced Photonics Inc., Camarillo, CA). Excitation spectra were corrected by measuring the output of the source with a calibrated reference diode and dividing the raw fluorescence data by these values. For fluorescence polarization measurements, linearly polarized light was generated using polarizers (Meadowlark Optics, Inc. Frederick, CO, USA) and the emission monochromator was removed and replaced by an interference filter. Fluorescence polarization is defined as:

$$P = \frac{I_{II} - I_{\perp}}{I_{II} + I_{\perp}}$$

Calibration of the polarizers was performed as previously described (Lakowicz 1983) and also checked by measuring a dilute solution of BChl *a* and comparing the resulting polarization to published values (Breton et al. 1981).

Circular dichroism (CD) spectra were recorded on a Jasco J-815 spectropolarimeter (JASCO Inc.Easton, MD, USA) using two different photomultiplier detectors: one sensitive to visible light (model R376, Hamamatsu Photonics, Hamamatsu, Japan), and the other to NIR radiation (model R316, Hamamatsu Photonics, Hamamatsu, Japan). Samples were measured in quartz cuvettes.

Low temperature linear dichroism (LD) spectra were measured by suspending membranes in a 10% acrylamide gel according to Dolan *et al*. (Dolan et al. 2001)with 66% glycerol added to the final mixture to ensure a clear glass upon cooling. The gel, which was cylindrical in shape, was compressed in a 1 cm x 1 cm cuvette to 60% its original height and in doing so, expanded along its stretching axes to fill the cuvette. The sample was then cooled in a cryostat. LD is defined as

$$LD = A_{II} - A_{\perp}$$

Where A_{II} and $A_{\perp}$ refer to absorbance due to linear polarized light that is parallel or perpendicular to the stretching axis, respectively (Abdourakhmanov et al. 1979). The reduced LD is LD/3A, where A is the isotropic absorption of an identical sample in an uncompressed gel.

Low temperature environments were created using a liquid nitrogen cryostat (OptistatDN, Oxford Instruments, Bucks, UK). A final concentration of 66% glycerol was added to all samples prior to cooling.

Results

Sample Purification and Characterization

The purification protocol produced a single complex from *R. castenholzii* that contains LH and RC peptides as well as an attached *c*-type cytochrome. The purified complex runs as a single band on a continuous sucrose density gradient, while analysis by native PAGE shows a predominant band at about 450 kDa (figure 2.1). The value from Native PAGE is similar to that observed for the LH1-RC monomer from *Rhodobacter sphaeroides* (Suzuki et al. 2007). SDS-PAGE analysis shows five bands which have been identified previously (Yamada et al. 2005) and include the LH α and β polypeptides, RC subunits L and M as well a tetraheme *c*-type cytochrome based on the gene sequence. It should be noted that the RC from *R. castenholzii* lacks the H-subunit found in the RC of purple bacteria as is also the case with *Cf. aurantiacus*. The dominant carotenoid (>70%) found in the LHRC was determined to be keto-γ-carotene. The amount varied slightly for various preparations and may indicate low specificity for carotenoid binding. The molar ratio of BChl *a* to carotenoid was determined to be 3:2 based on the extinction coefficients for BChl *a* and γ-carotene. This ratio is only tentatively assigned because the extinction coefficient for keto-γ-carotene is, to our knowledge, unknown and therefore the extinction coefficient of γ-carotene was used for the calculation.

Absorption and Circular Dichroism

The absorption spectra of the LHRC at room temperature (RT) and 77 K are presented in figure 2.2A. At RT, the Q_y absorption bands are centered at 802 and 882

nm (herein these bands are termed B800 and -880 for convenience), respectively, while only one Q_x band was resolved at 593 nm. At 77 K, the two Q_y bands red-shift to 806 and 890 nm respectively, accompanied by an increase in absorption intensity for both bands. Additionally, a band is clearly resolved at 760 nm and is ascribed to the RC bacteriopheophytin (BPhe) *a*. Two bands in the Q_x region are observed at 605 and 593 nm respectively in the low temperature spectra. The carotenoid region displays peaks at 519, 482 and 457 nm and the shoulder at 410 nm is due to oxidized cytochrome *c*. The light-minus-dark difference spectrum reveals a photoactive RC underneath the dominant antenna absorption bands (figure 2B). The Q_y RC region resembles that of the *Cf. aurantiacus* RC (Pierson and Thornber 1983) as well as results published previously for *R. castenholzii* (Yamada et al. 2005). In the purified LHRC the special pair bleaches at 860 nm, however, in the isolated complex this value is reported to be 865 nm (Yamada et al. 2005). The slight discrepancy in wavelength most probably arises from detergent effects (Fathir et al. 1998; Müh et al. 1998). Minima are observed at 423, 524, and 554, which are assigned to Soret, beta- and alpha- bands of cytochrome *c*.

The NIR CD of the LHRC is dominated by the antenna pigments, while subtle contributions from the RC can also be seen (figure 2.3). The BPhe *a* absorption peak at 760 nm splits in the low temperature CD spectra into a negative lope centered at 755 nm and a positive lobe at 772 nm. Increasing in wavelength across the Q_y transitions of the antenna pigments, the CD signature is + – + – which resembles the “type 2” or “molischianum”-like CD from LH2 in purple bacteria (Georgakopoulou et al. 2002)

and the purified LHB 808-866 complex from *Cf. aurantiacus* (Xin et al. 2005). Interestingly, the carotenoid region has a CD signature more similar to the LH complexes from many purple bacteria (Cogdell and Scheer 1985) than *Cf. aurantiacus* (Vasmel et al. 1986). In addition, the B880 long wavelength band has a 5nm red shift in the CD zero-crossing at RT and 77K (887nm and 895nm respectively). The red-shift in zero-crossing has been modeled to represent a delocalization of an exciton over a "ring" of BChl molecules in LH2 (Koolhaas et al. 1997; Sauer et al. 1996).

Fluorescence Emission, Excitation and Polarization

The vast majority of fluorescence from the LHRC is emitted from the long wavelength Q_y band of B880 at RT and 77K (figure 2.4), independent of the excitation wavelength tested (470, 590, 600, 800 nm). The emission bands are centered at 898 nm and 911 nm at RT and 77K, respectively. A shoulder is observed on the blue side of RT emission band and decreases below the experimental noise at 77 K (figure 2.4 – inset). The shoulder was fit to a single Gaussian revealing a peak centered at 817 nm and is attributed to fluorescence from B800. The ratio of the 817 / 898 nm emission bands is approximately 1/70 at RT, indicating efficient energy transfer from B800 to B880. A similar emission shoulder is observed in membranes of *C. aurantiacus* devoid of chlorosomes (Vasmel et al. 1986) as well the purple bacterium *Rhodobacter* s*phaeroides* (Kramer et al. 1984b).

Energy transfer efficiency was revealed by comparing the 77 K fluorescence excitation to a calculated absorption (1 – T) spectrum (figure 2.5). Nearly 100% energy

transfer efficiency is observed from B800 pigments to the long wavelength band, while energy transfer from the carotenoid region is about 35% efficient. The lack of energy transfer from the peak at 760 nm and the 410 nm shoulder supports the assignments of these bands to the RC BPhe *a* and cytochome *c*, respectively. The negative polarization value at 590 nm clearly identifies this band as the Q_x transition of the B880 pigments (figure 2.5). The polarization of the B800 band is also negative indicating that the transition dipole moment of these pigments forms a large angle with respect to B880. The polarization of the B880 pigments is positive (0.09) and increases slightly over the absorbance band, indicating the possibility of rapid exchange of excitation over these pigments. The fact that the polarization for the long wavelength band is not as large as those measured for membranes of *Cf. aurantiacus* (Vasmel et al. 1986) or LH2 (Kramer et al. 1984b) and LH1 (Kramer et al. 1984a) from purple bacteria may indicate isotropic distribution of these pigments, or losses in polarization due to instrumental limitations.

Linear Dichroism

The LD along with the reduced LD (LD/3A) of membranes from *R. castenholzii,* recorded at 77K has many prominent features (figure 2.6). Considering the antenna bands, the overall shape of the LD is strikingly similar to that of *Phaeospirillum* (*Ph*.) (formerly *Rhodospirillum*) *molischianum* with the exception of the B800 Q_y transitions (Visschers et al. 1995). We chose to use membranes as opposed to the purified LHRC complexes for these measurements because membranes in *Cf.*

aurantiacus form disc-like fragments in suspension (Schmidt 1980) and should become optically anisotropic upon compression whereas the isolated complex is of unknown geometry. The Q_y transition moments comprising B880 have a very large and positive LD. Comparison to the 77K absorbance data (figure 2.2, solid line) indicates these transition moments are oriented essentially in the plane of the membrane. In addition, the reduced LD, is essentially constant over the entire absorbance band suggesting that these transitions all have the same orientation with respect to the symmetry axis. The LD of the Q_x transition of B880 (which was identified by fluorescence polarization) at 590nm is clearly negative, making these transitions more or less perpendicular to the membrane. The combination of the Q_y and Q_x dipoles makes the B880 pigments perpendicular to the membrane plane, as is the case for the B850 pigments in LH2 (Koepke et al. 1996; McDermott et al. 1995; Papiz et al. 2003). The B800 and carotenoid transitions appear to form a large angle with respect to the membrane plane as has been demonstrated in membranes of *Cf. aurantiacus* (Vasmel et al. 1986).

The transition dipole moments can be calculated for disc-like particles using the reduced LD (Abdourakhmanov et al. 1979; Georgakopoulou et al. 2003) and follows the relationship

$$\frac{LD}{3A} = \left\langle \frac{1}{2}(3\cos^2\alpha - 1) \right\rangle \varphi$$

where A is the isotropic absorption measured on an uncompressed gel of the same optical pathlength and sample concentration, α is the angle between the transition dipole and the normal to the membrane plane (symmetry axis), $\langle ... \rangle$ represent weighted

averaging of all transitions contributing to the absorption at a particular wavelength and φ is an orientation factor that relates to how well the sample is oriented in the gel. The value of φ can not be determined from the LD measurement. However, if the angle of one dipole transition can be estimated, then a ratio of reduced LD between two dipoles allows for the orientation factor to cancel. This is exploited by assuming the Q_Y transition dipole for B880 to be 80° or 90° with respect to the normal of the membrane plane and calculating the other dipole angles (Table 2.2). Selecting 80° or 90° for the Q_Y transition of B880 is considered appropriate because this band possesses the strongest LD and only changes the other calculated dipole angles by a maximum of three degrees. Figure 2.7 is a proposed model of the BChl orientation in a single antenna subunit based on the reduced LD calculation.

Discussion

The light harvesting α- and β-apoproteins from *R. castenholzii* and *Cf. aurantiacus* have conserved residues important for BChl-binding when compared with the analogous peptides from both LH1 and LH2 (fig 2.8.). The dimer of BChl in LH1 and LH2 is coordinated by a His in both the α- and β- apoproteins. In LH1 as well as LH2 of *Ph. molischianum*, αW_{+11} and βW_{+6} make H-bonds to the C3-acetyl group of ring A of BChl *a* (Sturgis et al. 1997). All of these residues are conserved in both *R. castenholzii* and *Cf. aurantiacus,* which might explain the observed spectroscopic similarities of the B880 and B866 pigments of *R. castenholzii* and *Cf. aurantiacus* to

the B850 and B870 pigments of LH1 and LH2, respectively.

The obvious differences between the B800 pigment orientation in *R. castenholzii* and LH2 probably indicates a different mode of BChl binding. The 2.0 Å structure of LH2 from *Rhodoblastus* (*Rdb.*) *acidophilus* shows that the Mg^{+2} of the B800 is coordinated at the N-terminus by a modified methionine on the α-chain as well as hydrogen bonds with αN_{-29}, αQ_{-28}, and βH_{-18}. The C3-acetyl carbonyl of ring A in B800 forms a H-bond with βR_{-10} (Papiz et al. 2003). LH2 from *Ph. molischianum* is known to bind the B800 BChl *a* in a different manner than that of *Rdb. acidophilus*. The Mg^{+2} of B800 is coordinated via αD_{-28} with hydrogen bonds from a water molecule and βH_{-18}, resulting in the Q_y transitions being oriented 20° out of the plane of the membrane and rotated 90° with respect to B800 in *Rdb. acidophilus* (Koepke et al. 1996). *R. castenholzii* shares the conserved βH_{-18}; however, this residue is also maintained in LH1, which does not bind an additional pigment similar to B800. There is no evidence at this time that the α-chain necessarily binds the B800 pigment in *R. castenholzii* and the distance between the N-terminus and the conserved αH_0 is shorter than the α-chain in LH2. Interestingly, the β-chain in *R. castenholzii* is longer than the β-chain in LH2 and has several residues that could serve as potential coordinators to Mg^{+2} of B800. Further work is required to resolve the coordination of B800 in *R. castenholzii.*

The purification of the LHRC from *R. castenholzii* allows the unique opportunity to study a compact and complete photosystem from a member of the FAPs without the complication of the chlorosome. The light-harvesting antenna

spectroscopically resembles LH2; however, its close association with the RC demonstrates its function is more similar to LH1. The co-purification of an attached tetraheme cytochrome in the LHRC is unique among FAPs (Dracheva et al. 1991; Freeman and Blankenship 1990). The predominant carotenoid found in the LHRC is keto-γ-carotene and it transfers excitation to the long wavelength band with 35% efficiency. The amount of carotenoid bound in the LHRC per BChl *a* is twice that of what is found in the LH2 complex from *Rhodopseudomonas acidophila* (1:3 rhodopin-glucoside to BChl) (Andrew et al. 2006), Although many of the initial measurements on the carotenoid to BChl *a* stoiciometry in purple bacteria were overestimates (Gardiner et al. 1993; Germeroth et al. 1993), we obtained the same ratio as was determined for the purified B808-866 complex from *Cf. aurantiacus*. *Chloroflexus*- and *Roseiflexus*-like organisms are often found in mat communities in symbiosis with cyanobacteria where they are exposed to hyperoxic conditions due to oxygen trapped in the mat (Hanada et al. 2002) and the additional carotenoids may serve a photo-protective role against high levels of oxygen.

The red-shift in the CD zero-crossing for the B880 band, at RT and 77K, may indicate that the LHRC complex is organized in a ring-like structure. This conclusion is based on a LH2 modeling study by Koolhaas et al., where the observed red-shift in the zero crossing in B850 from LH2 could only be reconstructed by modeling an energy mismatch between α and β-bound BChl *a* in the B850 pigments as well as exciton delocalization over more than half of the ring structure (Koolhaas et al. 1997). Further

structural studies will be necessary to determine the geometry of the LHRC from *R. castenholzii*.

In this work we describe the LHRC from *R. castenholzii* which has similar spectroscopic properties to membranes of *Cf. aurantiacus* devoid of chlorosomes. The B880 pigments are proposed to lie perpendicular to the membrane plane with the Q_y transitions more or less parallel in the membrane. Both fluorescence polarization and LD measurements demonstrate that the B800 pigments form at a large angle in the membrane as does the carotenoid.

RT	77K	Light-minus-dark
882 (42)	890 (28)	860 (-)
802 (27)	806 (27)	831 (+)
593	760	821 (-)
483	605	808 (+)
376	593	760 (+)
	519	605 (-)
	482	554 (-)
	457	524 (-)
	376	423 (-)

Table 2.1. Wavelengths of absorbance maxima (in nm). The measured FWHM are in parentheses along with peaks and valleys for the difference spectra indicated with + and –, respectively.

Dipole	Wavelength (nm)	LD/3A	LD/3A Normalized		α Experimental	
Qy B880	890	0.197	-0.500	-0.450	90	80
Qy B800	800	-0.134	0.340	0.306	42	43
RC BPhe *a*	760	-0.128	0.325	0.292	42	43
Qx B800	610	0.073	-0.185	-0.166	63	62
Qx B880	590	-0.274	0.696	0.625	27	30
Keto-γ-carotene	480	-0.189	0.480	0.431	36	38

Table 2.2. Position, wavelength, reduced LD, and calculated angle for the given dipole. LD/3A were normalized so that the angle of the B880 transition dipole is 80° or 90° and all other dipoles were calculated using these values as references.

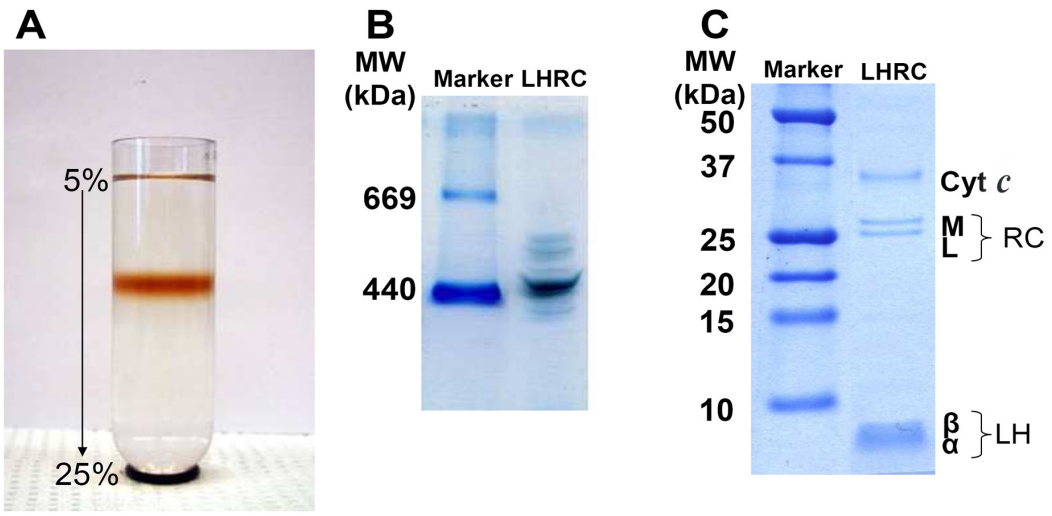

Figure 2.1. Estimate of the size and composition of the LHRC. (A) Sucrose density gradient (5-25%) showing a single pigmented band at 12% sucrose. (B) Native PAGE and (C) SDS-PAGE of the LHRC from *R. castenholzii* (right lane) and the molecular marker (left lane). Cyt *c*, M, L, β and α represent cytochrome *c*, M-, L-, β- and α-polypeptides, respectively.

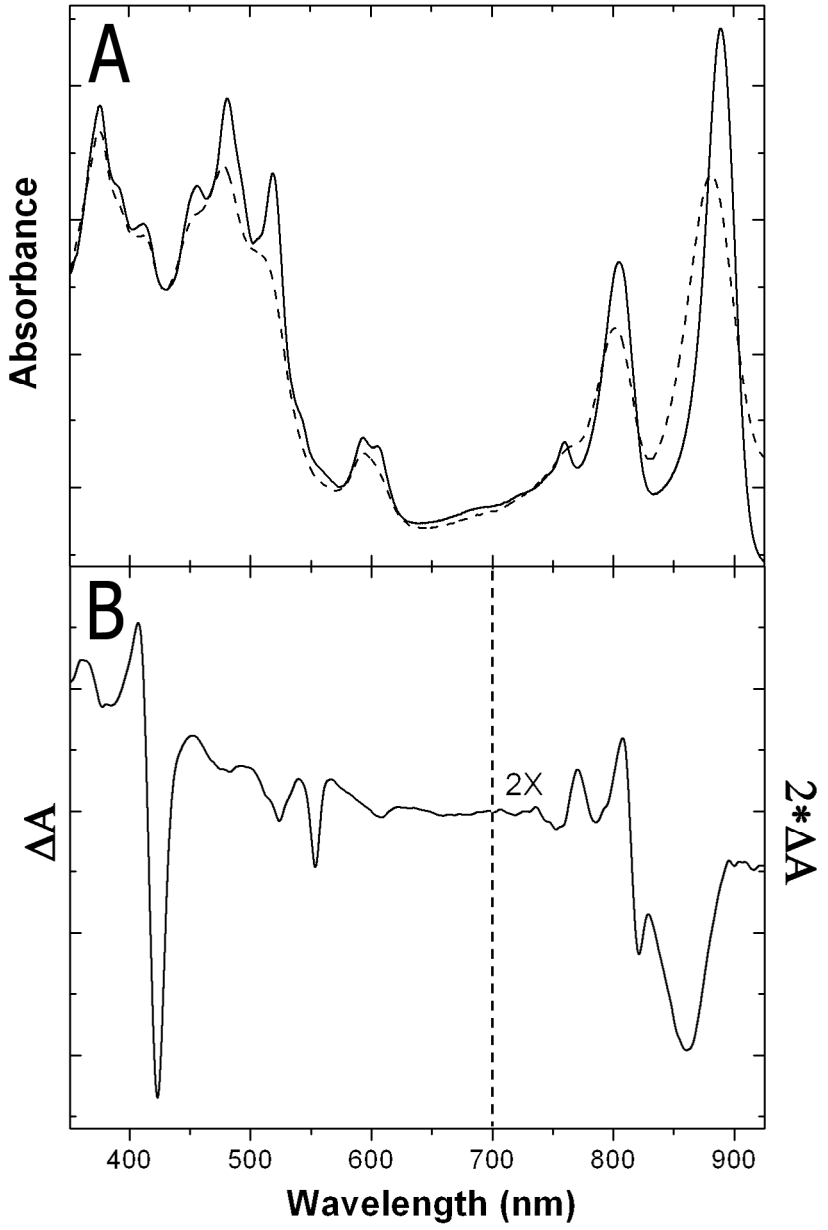

Figure 2.2. Absorption (A) of the LHRC measured at RT (dash) and the same sample cooled to 77K (solid). Light-minus-dark difference spectra (B) recorded at RT. Wavelengths above 700 nm in the difference spectrum have been scaled by two for clarity. Absorbance maxima and minima are in Table 1.

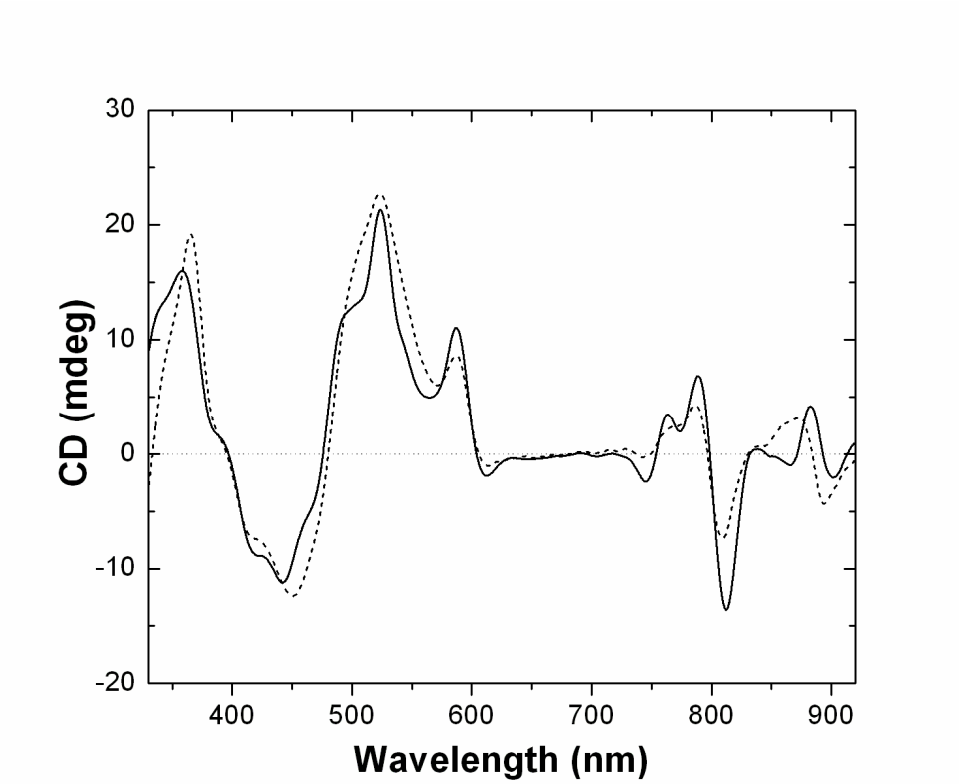

Figure 2.3. Circular dichroism of the LHRC from *R. castenholzii* measured at RT (dotted) and the same sample cooled to 77 K (solid). The sample OD was 0.6 cm^{-1} at 880 nm measured at RT. Zero-crossing for the B880 Q_y band RT and 77K are 887 and 895 nm, respectively.

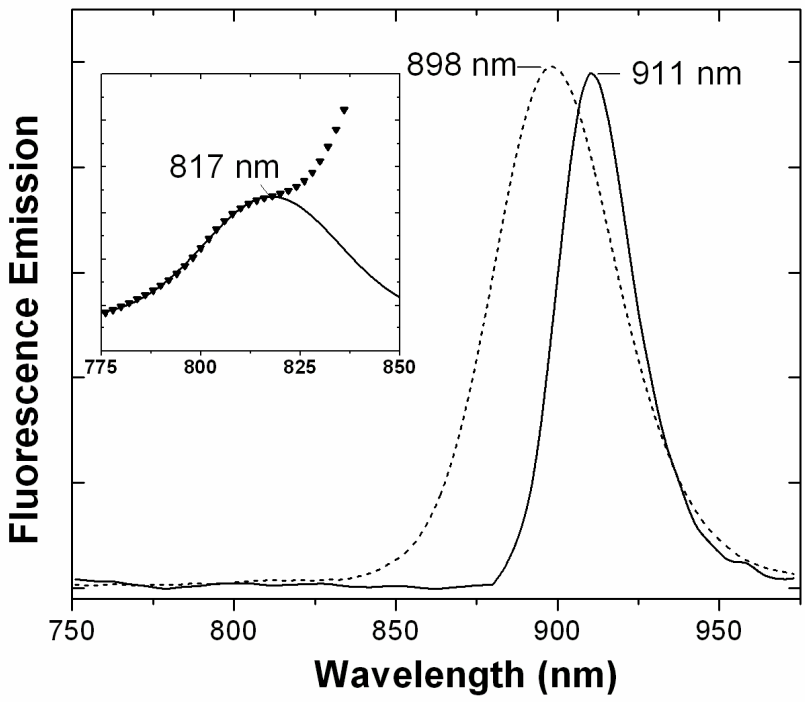

Figure 2.4. Fluorescence emission from *R. castenholzii* LHRC complex recorded at RT (dashed line) or 77 K (solid line). Excitation wavelength was 470 nm. Data are normalized at the emission maximum. Inset – 15 fold expansion of the RT emission (triangles) with a Gaussian fit (solid line) to the spectra revealing a weak emission band centered at 817 nm.

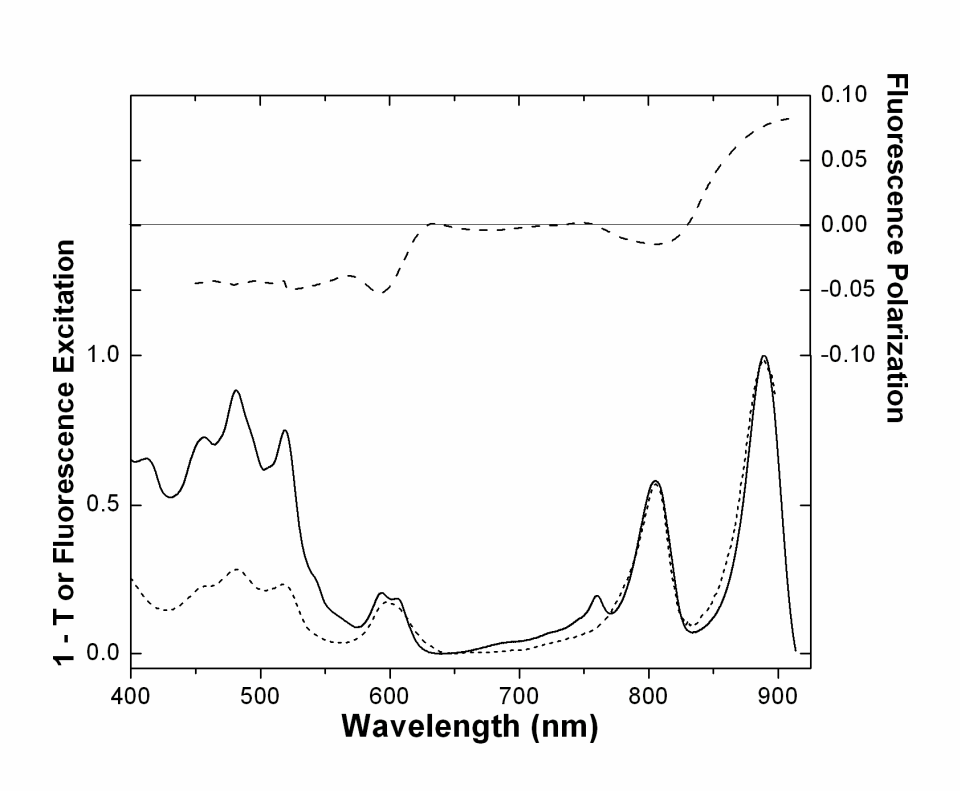

Figure 2.5. Fluorescence excitation (dotted) detected at 925 nm and absorption (1 – T) (solid) spectra on the same sample recorded at 77 K. Both spectra are normalized to 1.0 at the long wavelength band. Fluorescence polarization (dashed) detected at 925 nm is presented in the top panel. Bandwidths for absorption and fluorescence measurements were 1 and 4 nm, respectively.

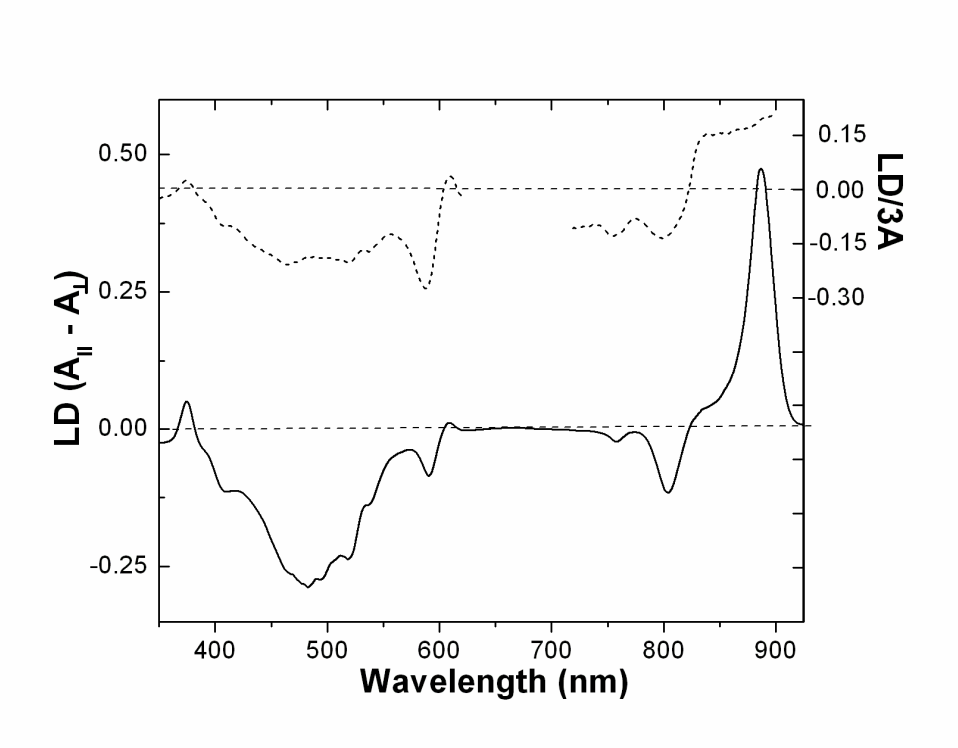

Figure 2.6. Linear dichroism spectrum of membranes at 77K from *R. castenholzii* (solid) and the reduced LD (LD/3A) (dotted), which is only shown in regions of appreciable absorption. The membranes were embedded in a 10% acrylamide gel that was compressed to 60% of the original gel height. The optical density of the uncompressed gel was 0.75 cm^{-1} for B880.

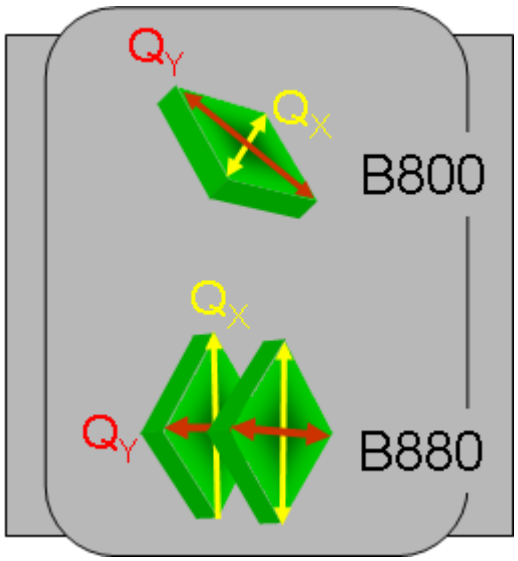

Figure 2.7. BChl orientation in one subunit of the LHRC based on the reduced LD (Table 2.2). Each subunit is proposed to contain a monomeric BChl *a* absorbing around 800 nm and oriented at ~45° with respect to the plane of the membrane. Two BChls are responsible for the absorption at 880 nm and are suggested to be oriented perpendicular to the plane of the membrane with the Q_Y dipole in the plane of the membrane.

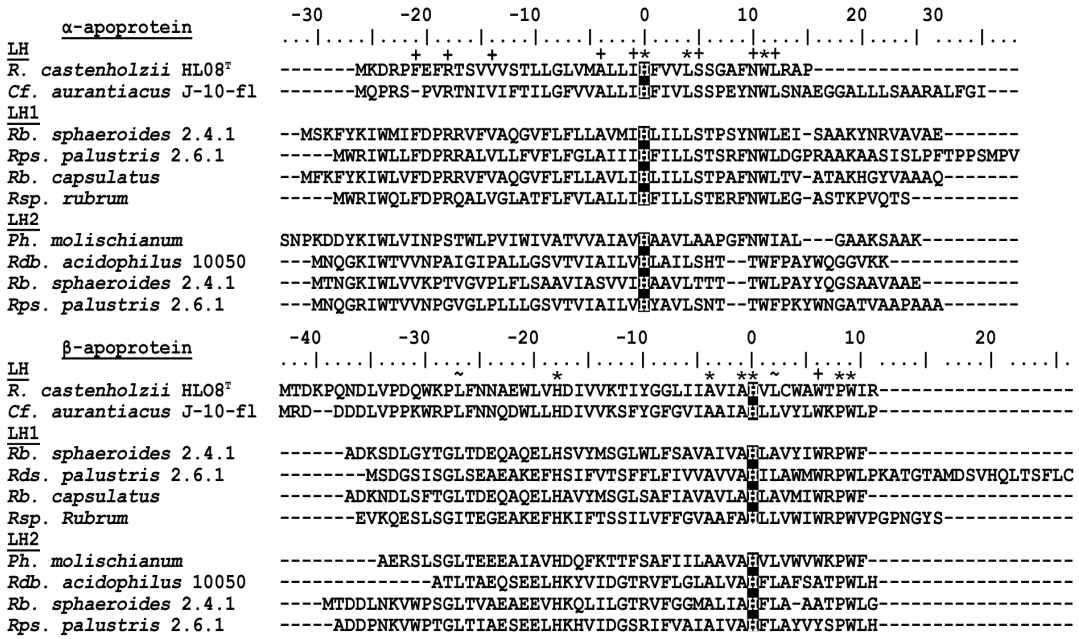

Figure 2.8. Sequence alignments of the α- and β-apoproteins of the LH complex from *R. castenholzii* and *Cf. aurantiacus* and the LH1 and LH2 complexes from various purple bacteria. The sequences from purple bacteria are from peptides while those of *R. castenholzii* and *Cf. aurantiacus* are deduced from gene sequences. Each set of apoproteins are aligned to the His that coordinates the central Mg^{2+} of BChl *a* in LH1 and LH2 and are highlighted in black. Residues conserved among all LH sequences are indicated by asterisks and those conserved among *Roseiflexus* and LH1 or *Roseiflexus* and LH2 are indicated by plus signs and tilde, respectively. Sources: *Rhodobacter* (*Rb.) sphaeroides*, *Rhodospirillum* (*Rsp*.) *rubrum, Rhodoblastus* (*Rdb.*) *acidophilus* and *Rhodopseudomonas* (*Rps.*) *palustris* (LH2) (Zuber and Cogdell 2004), *Phaeospirillum* (*Ph*.) *molischianum* (Germeroth et al. 1993) and *Rb*. *capsulatus* (Youvan et al. 1984)

CHAPTER 3

PURIFICATION AND CHARACTERIZATION OF THE REACTION CENTER, LIGHT-HARVESTING-ONLY AND THE CORE COMPLEX FROM *ROSEIFLEXUS CASTENHOLZII*

Abstract

The organization and composition of the light-harvesting (LH) antenna from the filamentous anoxygenic phototroph, *Roseiflexus castenholzii* isolated and characterized. By comparison of the bacteriochlorophyll (BChl) to bacteriopheophytin (BPhe) ratio of the core-complex and the RC, the number of subunits that comprise the antenna can be determined. These analyses resulted in 15 ± 1 subunits and an antenna that contains 45 BChl *a* esterified with phytol. The LH-only antenna was also investigated by resonance Raman spectroscopy and displayed stretching modes that indicated the 3C-acetyl groups of BChl *a* are all involved in molecular interactions probably in a similar manner to those of LH1 from purple bacteria. Finally, two-dimensional projections of the core-complex and LH-only generated from single particle analysis of electron micrograph images revealed a closed elliptical ring of ~120-150 Å in diameter.

Introduction

The photosynthetic machinery of filamentous anoxygenic phototrophs (FAPs) has overlapping elements with other groups of phototrophs. The Light-harvesting

antenna is usually exemplified by the chlorosome, enormous, self-assemblies of BChl *c*, *d*, or *e*, housed in a lipid monolayer can contains relatively little protein. However, not all FAPs contain chlorosomes (Hanada and Pierson 2006). Chlorosomes are also found in green sulfur bacteria (Frigaard and Bryant 2006) and more recently in genus Chloracidobacterium (Bryant et al. 2007). Both of these examples contain species with type-I or Fe-S-type RCs.

An integral membrane antenna complex termed B808-866 in the chlorosomes-containing, *C. aurantiacus* and B800-880 in the chlorosome-lacking *R. castenholzii* have been biochemically and spectroscopically described (Collins et al. 2009; Xin et al. 2005). The membrane-bound antenna complex has sequence similarity and spectroscopically resembles LH2 from some purple bacteria. However, there is also sequence homology to LH1 and the complex is intimately associated with a RC, in the manner of LH1.

FAPs possess a type-II or quinone-type RC (Blankenship et al. 1983) that embody only three sunbunits, L-, M- and C- . The L- and M- subunits have low sequence homology to those of purple bacteria (~25-30%) while the C-subunit is most almost certainly a tetra-heme cytochrome *c* (Dracheva et al. 1991; Freeman and Blankenship 1990; Yamada et al. 2005)

While several kinetic studies have been performed on the integral membrane antenna from *C. aurantiacus* (Griebenow et al. 1991; Novoderezhkin and Fetisova 1999; Novoderezhkin et al. 1998) structural data has been elusive. Complications arise in *C. aurantiacus* because the dominant chlorosome antenna can be difficult to separate

from the membrane and only a few purification procedures for the B808-866 complex have been described (Griebenow et al. 1991; Xin et al. 2005). Here were present a full description of the purification of the LHRC (core-complex), LH-only and RC from *R. castenholzii* an organism that does not contain chlorosomes. This provides a unique opportunity to prepare a full complement of LH and RC complexes from a representative member of the FAPs.

In the absence of high-resolution structural data, the number of antenna subunits can be determined indirectly by comparing the amount or ratio of BChl to BPhe in the core and the isolated RC. Such approaches have given estimates to the number of subunits in the detergent solubilized antenna from *Rhodobium marinum* (Francke and Amesz 1995; Qian et al. 2000) and a variety of other purple bacteria containing only LH1 (Akiyama et al. 1999). These methods utilize pigment extraction followed by separation and quantification by HPLC and rely on knowing the ratio of BChl to BPhe in the RC and the number of BChls in each antenna subunit. These values are 2:1 in the purple bacterial RC and 2 BChl for each LH1 antenna subunit, respectively (Picorel et al. 1983; Straley et al. 1973) and is most likely 1:1 BChl:BPhe and 3 BChl in each subunit of the LH antenna in FAPs (Blankenship et al. 1983; Vasmel et al. 1986).

Additionally, resonance Raman can provide structural information by reporting the stretching modes of C3-acetyl and $C13^1$-keto groups of BChl among many others (Robert 2009). The Raman stretching frequencies of these groups are shifted by many tens of cm^{-1} if they are involved in intermolecular interactions as compared to their unbound states giving insight to the local environment around the antenna pigments.

In this work we show that the LH antenna from *R*. *castenholzii* contains 15 ± 1 α/β protein subunits and has Raman features akin to LH1 indicating that the environment around the B880 pigments is likely similar. The results herein and those of Chapter 2 allow us to construct a model of the antenna RC complex of *R*. *castenholzii*.

Materials and methods

Preparation of whole membranes

R. *castenholzii* strain HLO8^{T} was grown anaerobically and photosynthetically at 50 °C on 02YE media (Hanada et al. 2002) under continuous illumination from four 60 w incandescent light bulbs in a 15 L fermentor (Bioengineering, Wald, Switzerland) for seven days. Cells were harvested by centrifugation. These conditions repeatedly yield approximately 3 grams of cells per liter of media.

Cells were resuspended in 20mM tris buffer, pH=8.0 (buffer A), mixed thoroughly and disrupted using a Branson sonifier (Model 250, Danbury, CT). The lysate was centrifuged at 16,000 x g for 20 minutes to remove unbroken cells and large debris. The supernatant liquid was ultracentrifuged at 225,000 x g for 2 hours to pellet membranes. The resulting pellet was homogenized using a minimal amount of buffer A with an overhead stirrer. The membranes were adjusted to have a final OD measured at 880 nm to be ~20-30 cm^{-1}. Membranes were used immediately or frozen at -80 °C.

Purification of the RC

Whole membranes described above were mixed with lauryldimethylamine n-oxide (LDAO) drop wise from a concentrated stock (30%) to a final concentration of 0.45 % (w/v) and stirred at 0°C for 90 minutes. The mixture was diluted to a final LDAO concentration of 0.1% before being subjected to ultracentrifugation at 200,000 x g for one hour. This resulted in a supernatant liquid that was enriched in RCs, a soft pellet that contained primarily the LHRC and some RC, and a pellet that was still somewhat colored. The supernatant liquid was removed and care was taken to avoid the soft pellet. This mixture was filtered through a 0.22 μm filter and immediately loaded to an IEC Q-sepharose HP column (GE Healthcare, Uppsala, Sweden) that was pre-equilibrated with 0.1% LDAO in buffer A. After loading, the column was washed extensively with 0.1% LDAO in buffer A followed by 2 column volumes of 1% LDAO in buffer A. After re-equilibrating the column with 0.1% LDAO in buffer A, the RC was eluted by a linear gradient of NaCl in 0.1% LDAO in buffer A. The RC eluted with 175 - 200mM NaCl. The best RC fractions as judged by the absorption spectrum were pooled and concentrated and applied to a Superdex 200 (GE Healthcare, Uppsala, Sweden) column equilibrated with 0.02% n-dodecyl-β-D-maltoside (β-DDM) and 100 mM NaCl in buffer A and eluted with a flow rate of 0.5 mL/min. If further purification was needed, the RCs were diluted to reduce the NaCl concentration and loaded to a Mono-Q IEC column (Bio-Rad Lab, Richmond, CA) and eluted with a linear gradient of NaCl in β-DDM in buffer A. The best RC fractions had an 814 nm / 280 nm ratio of 2.2.

Purification of the LH-only and LHRC

The LHRC was purified using a variety of methods and detergents. The following method is a good compromise for large scale purification while not consuming expensive detergents until the later stages of purifications.

Whole membranes ($OD_{880\ nm}$ =20-30 cm^{-1}) were mixed to a final LDAO concentration of 1% and stirred for 60 minutes at 0°C. The mixture was diluted two times with buffer A and ultracentrifuged at 225,000 x g for one hour. This resulted in a dark red to brown supernatant liquid and a pellet that was largely devoid of color. The supernatant was diluted two times further in buffer A and then filtered through a 0.22 μm filter. The solubilized material was loaded to a IEC Q-sepharose HP column (GE Healthcare, Uppsala, Sweden) that was pre-equilibrated with 0.1% LDAO in buffer A. The bound material was washed with 50mM NaCl in 0.1% LDAO in buffer A for several hours to remove weakly bound proteins and free BChl *a* and carotenoids. The NaCl was increased to 100 mM and washing was continued. The NaCl concentration was increased to 180 mM and this released some RCs, and the LH-only. The eluent was collected for further purification of the LH-only. Finally, the NaCl concentration was increased to 250 mM the LHRC was eluted off the column.

The LH-only and LHRC was both further purified separately by gel filtration and a final IEC as described for the purification of the RC above. The final ratio of 880 nm / 280 nm for the LHRC was 1.5 and the final ratio of 884 nm / 280 nm was 1.7.

SDS-PAGE was performed according to the methods of Schägger and von Jagow (Schägger and von Jagow 1987).

Pigment extraction and subunit determination by HPLC

The number of subunits in the LH antenna was a determined using a modification method described by Qian et al (Qian et al. 2000). 50 µl of the purified LHRC (OD_{880} = 4 cm^{-1}) or purified RC (OD_{814} = 1 cm^{-1}) were suspended in 500 µl of ice cold 8:2 (v/v) methanol:acetone and stored at -20 °C in the dark for 30 minutes. The mixture was then centrifuged at 14,000 x g in a microfuge. The supernatant was drawn off and dried under a stream of argon gas in the dark before being resuspended in 100 µl of 8:2 methanol:acetone and immediately injected into the HPLC (Agilent 1100 system). Centrifugation and drying of the pigments took less than 20 minutes to complete. Additionally, the single extraction described above was enough to extract essentially all of the pigments from the protein as determined by resuspending the pellet and measuring the OD. Reverse-phase HPLC was performed with a Zorbax Eclipse XDB-C18 column with an isocratic flow rate of 1 ml/min with 8:2 methanol:acetone and the eluent was monitored from 200-850 nm using an array detector.

Under the conditions above, the eluted BChl *a* and BPhe *a* were separated by several minutes and the area under each elution peak was integrated.

Fluorescence lifetime measurements

A tunable Ti:sapphire oscillator laser system with pulse durations of □150 fs at 800 kHz was used in the spectrally resolved time-correlated single photon counting (TCSPC) experiments. The emission intensity decay profiles were acquired with a temporal resolution of 40 ps using a multi-channel plate photomultiplier tube coupled with a TCSPC system. The photon detection rate was kept at <1 % of the excitation rate, and excitation energy densities ranging from 35-559 □J cm^{-2} were used. Excitation wavelengths utilized were 380, 404 and 808 nm and emission was monitored at several wavelengths in the NIR, 800, 820, 850 and 900 nm. Data was acquired until at least 5,000 counts were achieved. A bin channel resolution of 6.5 ps was used. Several excitation wavelengths were selected and all gave very similar kinetics. However only a single emission band was observed at 900 nm. The fluorescence kinetics were fit to a sum of exponential functions and the quality of the fits were determined by the reduced χ^2 function as well as the residual plot.

Resonance Raman

The resonance Raman (RR) measurements were performed on the LH-only sample contained in tightly sealed 1 mm i.d. capillary tubes that were mounted directly onto the cold tip of a closed-cycle liquid He refrigeration system (ADP Cryogenics DE-202). The excitation wavelength was 364 nm. Spectra were acquired with a triple spectrograph (Spex 1877) equipped with a holographically etched 2400 grooves/mm grating in the third stage. The excitation wavelengths were provided by the discrete outputs of an argon ion (Coherent Innova 400-15 UV) laser. The scattered light was

collected in a 90° configuration using a 50mm f/1.4 Canon camera lens. A UV-enhanced charge-coupled device (CCD) was used as the detector (Princeton Instruments LN/CCD equipped with an EEV1152-UV chip). The data acquisition times were ~ 2 h (40 x 180s scans). Cosmic ray spikes were removed prior to addition of the data sets. The laser power was ~ 5 mW, respectively and the spectral resolution was ~ 2 cm^{-1}. The frequencies were calibrated using the known frequencies of indene. Further details of the experimental setup can be found elsewhere (Palaniappan et al. 1993).

Electron microscopy (EM) and particle analysis

Before analysis by EM, the LHRC and LH-only was passed over a final high-resolution gel filtration column (BioSep-SEC-S 3000, Phenomenex) using 0.03% β-DDM in 10 mM Hepes buffer (pH = 7.5) to ensure sample purity. The protein samples were applied separately to glow discharged, carbon-coated copper grids (Agar Scientific), blotted, stained with 0.75% (w/v) uranyl formate, blotted, and dried in air. Electron micrograph was recorded on a Philips CM100 electron microscope fitted with 1K x 1K Gatan Multiscan 794 CCD camera at 52,000 magnification

Single particle analysis was performed using the IMAGIC-5 software package (Image Science Software GmbH) (van Heel et al. 1996; van Heel and Keegstra 1981). Totally, 8394 single particle projections were boxed from electron micrographs using a box size of 64 x 64 pixels (250 x 250 Å). Particles were subjected to iterative normalization and band-pass filtering before alignment.

Results

Purification of the RC, LH-only, and LHRC

The RC, LH-only, and LHRC were separated and purified from *R. castenholzii*. The respective absorption spectra are shown in figure 3.1. The absorbance features of the LHRC have been described in detail in chapter 2. The LH-only lacks absorption shoulders at 410 and 760 nm that are ascribed to the Soret band of oxidized cytochrome *c* and the Q_X band of the RC associated BPhe *a*, respectively. Additionally, the Q_Y band of B880 redshifts 4 nm to 884 nm when the RC is removed. Moreover, there is a slight shift in the carotenoid region, suggesting a possible difference in the carotenoid environment for this sample. Lastly, the RC has a NIR absorption spectrum very similar to the RC of *C. aurantiacus* (Blankenship et al. 1983; Xin et al. 2007). However, the VIS portion of the spectrum clearly identifies an oxidized *c*-type cytochrome that co-purifies with the RC and will be described in more detail in chapter 4.

The purity as well as the peptide composition of the RC, LH-only and LHRC can be assessed by SDS-PAGE analysis (figure 3.2). These bands have been identified previously (Yamada et al. 2005) as: The RC C-subunit (37,000 kDa), L-Subunit (26,000 kDa), M-subunit (24,000 kDa) and antenna α-subunit (5,000 kDa) and β-subunit (7,000 kDa). The presence of minor stained bands in the background indicate a small amount of contaminating protein.

Fluorescence lifetimes in the LH-only and LHRC

Kinetic fluorescence measurements are useful to determine the trapping time of excitation in the antenna by the RC as well as the endogenous lifetime of the antenna itself (figure 3.3). The fluorescence lifetimes were measured using excitation into the Soret band of BChl *a* (380 nm), the higher vibronic bands of the carotenoid region (404 nm) and the red edge of B800 (808 nm) for the LHRC with emission monitored at 900 nm. In the absence of exogenous electron acceptor and donors and regardless of excitation wavelength tested the lifetimes were fit satisfactorily to the sum of 2 exponential decays of 60 ± 10 ps (92% amplitude) and 900 ± 50 ps (8% amplitude). The LH-only could be fit to a single exponential decay of 910 ± 50 ps. The dominant 60 ps decay component represents trapping of antenna excitation by "open" RCs. This value is accord with trapping by the RC from chromatophores from *C. aurantiacus* (Montaño et al. 2004), *Rhodospirillum rubrum* and *Rhodobacter sphaeroides* (Borisov et al. 1985) and membranes of the BChl *b*-containing *Rhodopseudomonas viridis* (Zhang et al. 1992). When the RC is absent from the LH antenna, the lifetime of the excited state is considerably longer (910 ps). The fact that the same long lifetime is present in the LHRC sample might indicate that a small fraction of the sample lacks the RC or that RC is uncoupled from the antenna. The fluorescence lifetime of the purified B808-866 complex from *C. aurantiacus* has been fit to multiple components with the most dominant being ~800 ps (Griebenow et al. 1991; Montaño et al. 2004). The fluorescence lifetimes of LH1 in purple bacteria has been observed to be principally

monoexponential and decay in about 650 ps (Bergström et al. 1988; Freiberg and Timpmann 1992).

The number of BChl *a* and subunits in the LH antenna

The number of antenna subunits and subsequently the quantification of BChl *a* within the LHRC can be determined by the separation of extracted pigments by HPLC. A representative chromatograph for the isolated RC and LHRC recorded at 750 nm is presented in figure 3.4. The peak ascribed to BChl *a* matched the elution time of BChl *a* esterified with phytol, isolated from *Rhodobacter sphaeroides* (result not shown) demonstrating that phytol is the esterifying alcohol in the antenna and the RC in *R. castenholzii*.

It has been determined that the ratio of BChl *a* to BPhe *a* in the RC of *C. aurantiacus* is 1:1 (Blankenship et al. 1983). This almost certainly indicates that there are 3 BChl *a* and 3 BPhe *a* divided amongst the RC L- and M- subunits. The ratio of BChl to BPhe (X) from pigments extracted from the isolated RC can be represented as

$$X = \frac{A_{BChl}(RC)}{A_{BPhe}(RC)} = \frac{3\varepsilon_{BChl}}{3\varepsilon_{BPhe}} = \frac{\varepsilon_{BChl}}{\varepsilon_{BPhe}}$$

where A_{BChl} and A_{BPhe} are the integrated absorbances from the HPLC chromatograph for BChl and BPhe, respectively and ε_{BChl} and $\varepsilon_{\mathrm{BPhe}}$ are extinction coefficients for BChl and BPhe at the detection wavelength of 750 nm.

If we assume that LHRC is composed of 1 RC and *n* antenna subunits and that in each antenna subunit there are 3 BChl *a*, then the ratio of BChl to BPhe for the LHRC (Y) from the chromatograph may be represented as

$$Y = \frac{A_{BChl}(LHRC)}{A_{BPhe}(LHRC)} = \frac{(3n+3)\varepsilon_{BChl}}{3\varepsilon_{BPhe}} = (n+1)\frac{\varepsilon_{BChl}}{\varepsilon_{BPhe}}$$

where *n* represents the number of antenna subunits. Combining the above two equations and solving for the number of subunits *n*, yields $n = (Y/X - 1)$. Six separate extractions of the LHRC (Y) and three for the isolated RC (X) yielded values in Table 3.1. Solving for the number of antenna subunits yields a value of 14.9 ± 0.9 subunits. If three BChl are bound in each subunit, then there are 45 ± 3 BChl that comprise the antenna complex.

Hydrogen bonding in the antenna

One of the most interesting features of the LH antenna from FAPs is that spectroscopically it resembles the peripheral antenna LH2 from purple bacteria, however functionally, is more akin to LH1. An explanation for these findings is not apparent from a superficial examination of the primary sequence of the α- and β-subunits. However, resonance Raman is a suitable spectroscopic method to investigate the interactions of BChl ring constituents with the protein environment.

Resonance Raman (RR) spectra were recorded for the LH-only complex at 30 K with an excitation wavelength of 364 nm. The 1600-1720 cm^{-1} region is sensitive to conjugated carbonyls and in the context of BChl *a* reports on C3-acetyl and $C13^1$-keto

groups. Considering the carbonyl stretching region, the dominant stretching frequency observed was a symmetric band at 1613 cm^{-1} and is consistent with the methine bridge stretching frequency for a pentacoordinated BChl (Cotton and Van Duyne 1981). An additional band is clearly resolved at 1641 cm^{-1} and two minor bands of approximately the same amplitude are observed at 1666 and 1672 cm^{-1} (figure 3.5). The distinct but asymmetric band centered at 1520 cm^{-1} most likely represents the C=C stretch of the antenna carotenoid molecules.

A survey of 7 LH1 complexes, investigated by RR all produce a band close to 1645 cm^{-1} that is though to exclusively originate from bound C3-acetyl groups (Robert and Lutz 1985). Interestingly, No reported LH2 complex had a RR stretching band in this region with the exception of *Ph. molischianum* which is known to have sequence homology to LH1 (Germeroth et al. 1993).

From the same report by Robert and Lutz, all LH1 complexes had a weak mode around 1667 cm^{-1} and a yet smaller mode near 1676 cm^{-1}. These bands were provisionally assigned to 13^1-keto carbonyls involved in inequivalent hydrogen bonding (Robert and Lutz 1985) but can also occur from unbound C3-acetyls. Moreover, many LH2 complexes also possess a mode around 1660-1670 cm^{-1} that it proposed to originate from the B850 pigments. Two bands of nearly equal magnitude were observed in this same region for the *R. castenholzii* LH-only (1666 and 1672 cm^{-1}). The additional band intensity on the higher frequency mode may reflect contributions from the B800 pigments in *R. castenholzii* that are not present in LH1.

Some LH2 complexes display a band at 1700 cm^{-1} (for example *R. sphaeroides*) that is indicative of free $C13^1$-keto carbonyls and is thought to arise from the B800 pigments because RR analysis of LH2s that were depleted of B800 did not contain this stretching frequency (Robert and Lutz 1985). The clear absence of a 1700 cm^{-1} mode in the antenna of *R. castenholzii* suggests that the 13^1-keto groups of all the BChl are involved in intermolecular interactions.

Overall, the RR spectrum of the LH-only from R. *castenholzii* is more similar to LH1 and LH2 from *Ph. molischianum* than other LH2s and probably reflects a very similar BChl environment for B880 pigments.

Single particle analysis of negatively stained the LHRC

Single LHRC and LH-only particles were directly imaged by EM (figure 3.6A and B). With images of the LHRC, the majority of particles appeared to sit flat on the carbon support film of the EM grid (figure 3.6A, green box). However, some particles appeared to be side views (figure 3.6A, red box). Of the top viewed particles, some were observed to be circular and other more elliptical and the average diameter was measured to vary between 120-140 Å. Many of the side view projections had a clear projection extending from only one side of the complex. This is presumed to be the C-subunit which co-purifies with the RC. However, it can be noted that the presence of the presumed C-subunit was not always obvious. The height of the side projections with and without the C-subunit was measured to be 110-115 Å and 70-75 Å, respectively while the width is consistent with the those of the top projection.

EM images of the LH-only revealed some circular and elliptical particles with most lacking density in the center, confirming the lack of the RC (figure 3.6B, green box). The dimensions of closed rings observed for the LH-only were approximately the same as the LHRC. There appeared to be many fewer side projections and many of the rings were not complete (figure 3.6 red box).

In total, several thousand single projections were boxed (figure 3.6B and C) and used to create image classes that are the average of several hundred particles. Three projections for each the LHRC and the LH-Only are shown in figure 3.7. Of these classes of particles, three projections assumed; 1- a bottom projection looking down into the periplasmic side of the complex, 2 – a top projection looking down into the cytoplasmic side of the complex and 3 – a side view, presumably in the plane of the ring. Most obvious of these projections were the side views (figure 3.7C and F). The C-subunit is well established in the side view of the LHRC and extends perpendicular to the plane of the ring structure. The top and bottom projections are ambiguous to determine but reveal that the circular or elliptical structure is a closed ring. The LHRC from *R. castenholzii* lacks the H-subunit found in all purple bacteria but maintains a large C-subunit. One side of the complex should most likely have a protrusion representing the C-subunit while the opposite side could be relatively flat. The C-subunit might be responsible for the weak staining that is observed in the center of the complex that extends to the edge of the ring (figure 3.7D). If this is indeed the C-subunit protrusion, it is interesting that it is observed to orient along the short axis of the elliptical ring.

Discussion

The study of photosynthetic membrane complexes among FAPs has been largely limited to *C. aurantiacus* due to its relative ease to grow and lack of other species that can be cultured in high yield. However, *C. aurantiacus* contains chlorosomes that often dominate the optical properties of samples. Despite this, procedures have been developed to prepare cytoplasmic membranes devoid of chlorosomes (Feick et al. 1982). The discovery and isolation of *R. castenholzii* by Hanada et al provides an opportunity to study a representative member of the FAPs without chlorosomes (Hanada et al. 2002). Here we present a full description of the purification of a full complement of photosynthetic complexes from *R. castenholzii*: the RC, LH-only, and the LHRC.

The fluorescence lifetime measurements of the LHRC are consistent with a nearly uniform decay of antenna excitation by RC trapping. Several different excitation were used to directly excite various electronic bands of the LHRC and LH-only. All of the difference excitations produced essentially the same emission kinetics and probably reflects a rapid decay of excitation to the lowest excited energy level, S_1, of B880. When the RC is not present in the sample, then the lifetime of the B880 antenna pigments is considerably longer and decays monoexponentially in about 900 ps.

Model of the LH antenna in *R. castenholzii*

Pigment extraction followed by HPLC to quantify the ratio of BChl to BPhe pigments allowed for the number of subunits in the antenna to be determined. It is assumed that the isolated RC contains 3 BChl and 3BPhe while the antenna is comprised of 3*n BChl, where n is the number of subunits. This method affords the advantage of not needing to determine extinction coefficients to quantify the total amount of pigments in the sample. This is advantageous considering that fact that extinction coefficients can depend strongly on the solvent system used. Based on 6 extractions of the LHRC and 3 from the isolated RC, it was determined that the antenna contains 15 ± 1 subunits. Using a similar HPLC method, it was shown that there were 16 subunits in the detergent-solubilized antenna of *Rhodobium marinum* (Qian et al. 2000). The 8.5 Å projection structure of the RC-LH1 from *Rhodospirillum rubrum* revealed a ring of 16 subunits completely surrounding the RC (Jamieson et al. 2002) while the crystal structure of the RC-LH1 from *Rhodopseudomonas palustris* exposed an elliptical ring of 15 antenna subunits surrounding the RC (Roszak et al. 2003). It can be noted, however, that in all of these cases, purified complexes were analyzed. When native membranes have been imaged directly using atomic force microscopy, monomeric RC-LH1s are shown to contain 15 or 16 subunits depending on species and to be circular or elliptical in shape while some species have dimeric "S"-shaped antenna RC complexes that are composed of 26 antenna subunits and 2 RCs (Scheuring 2006).

The antenna α- and β-subunits from *R. castenholzii* have sequence homology to both LH1 and LH2 (Collins et al. 2009). The resonance Raman spectrum for the LH-

only had features similar to those measured for LH1 rather than most LH2 (with the exception of *Ph*. *molischianum*, see below). The differences in the Raman spectra for LH2 and LH1 are manifested in the hydrogen bonding differences for the B850 and B880 pigments, respectively. From the crystal structure of LH2 from *Rhodopseudomonas acidophila*, the BChl pigments that make up B850 are centrally coordinated by His residues on the α- and β-subunits. An H-bond is present between the C3-acetyl group on ring A of BChl *a* and αTrp_{+14}. Another H-bond is formed between the C3-acetyl of the other BChl and αTyr_{+13} of an adjacent protomer. In other words, each α-subunit H-bonds two BChl C3-acetyl groups of BChl *a* but the two pigments are not in the same antenna subunit.

The situation is different for the H-bonding pattern in the B880 from LH1. Both the α- and β- subunits coordinate a BChl with His (Olsen et al. 1997). Although there is no high resolution crystal structure for LH1, resonance Raman and mutagenesis have clearly demonstrated that the C3-acetyl groups of BChl *a* in LH1 are hydrogen bonded to αW_{+11} and βW_{+6} and that these interactions are internal to the same α/β pair (Olsen et al. 1994; Sturgis et al. 1997). In fact, LH2 from *Ph*. *molischianum* was shown to have Raman features similar to LH1 and peptide sequence that conserves both αW_{+11} and βW_{+6} (Germeroth et al. 1993). The crystal structure later confirmed the participation of these two residues in H-bonding to the B850 pigments (Koepke et al. 1996). While the resonance Raman spectrum can not determine unequivocally for *R*. *castenholzii* that both αW_{+11} and βW_{+6} are maintained (see figure 2.8 of Chapter 2). It is probably the case that the molecular interactions of the BChl that embody B880 in *R*. *castenholzii*

are similar to those of LH1. The interactions of the BChls in the B800 band are not determined here. It is still unknown to which residue it is coordinated and how it is interacting with its environment.

The structural significance of the H-bonding differences between LH1 and LH2 have been speculated to allow flexibility in LH1 and specifically to permit the escape of quinol formed by RC photochemistry (Bahatyrova et al. 2004; Jamieson et al. 2002). The similar H-bonding pattern for the B880 pigments in *R. castenholzii* and its analogous functionality indicate that an antenna organization surrounding the RC may be expected.

Images generated of the LHRC and LH-only by single particle analysis revealed circular and elliptical complexes that appeared to be closed rings that were slightly larger than the dimensions reported for most purple bacterial reaction center-antenna complexes (~10.5 Å) (Jamieson et al. 2002; Roszak et al. 2003).However, negatively stained, detergent-solubilized complexes will have an increased measured diameter due to bound detergent molecules (Boonstra et al. 1993; Timmins et al. 1988). For example, negatively stained, core-complexes from *Phaeospirillum molischianum*, solubilized in β-DDM were measured to have a diameter of 14.1-14.6 nm (Boonstra et al. 1994). However, the LH1 ring in its native membrane environment, for this same species was measured using AFM to have short and long-axis diameters of 8.5 and 9.5 nm, respectively (Gonçalves et al. 2005). Images of individual LH-only complexes displayed rings of variable diameter and what appeared to be portions of rings. This result might not be unexpected because LH1 without the RC was observed to have

variable number of subunits in *Rhodobacter sphaeroides* and this was attributed to flexibility and the weak association of the antenna subunits when the RC is not present (Bahatyrova et al. 2004; Westerhuis et al. 2002).

The results herein and those of Chapter 2 allow for the construction of a structural model of the size and pigment organization in the antenna of *R. castenholzii* (figure 3.8). There are 15 ± 1 subunits in the antenna and each subunit binds 3 BChl *a* (all esterified with phytol), 2 carotenoids, and the α- and β-subunit. The B880 pigments are proposed to be oriented vertically with the Q_Y transitions in the plane of the membrane. Each of these pigments is likely coordinated by His residues with H-bonds to the C3-acetyl groups of each BChl provided by αW_{+11} and βW_{+6} and these bonds are internal to each subunit. The additional BChl pigment that absorbs around 800 nm is oriented at ~45° with respect to the membrane plane and its coordination is unknown.

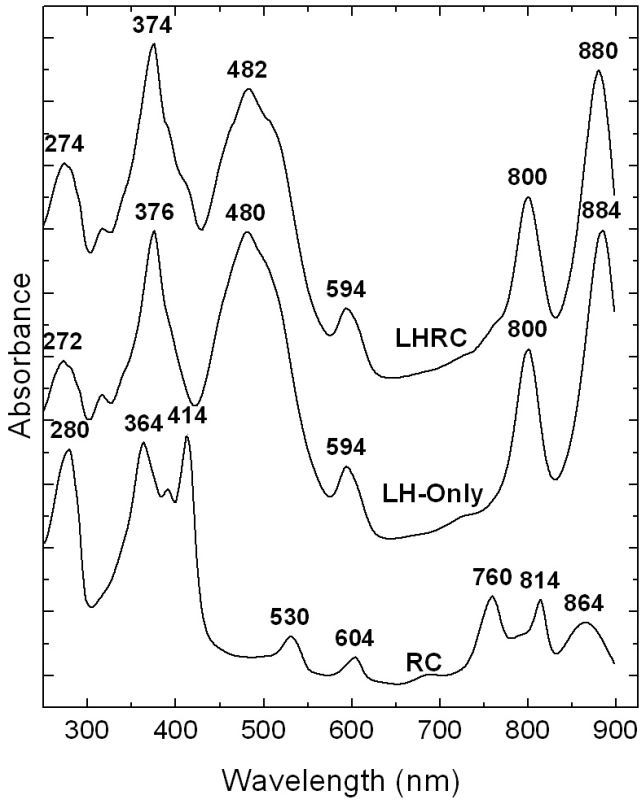

Figure 3.1 Absorption spectra of the isolated LHRC, LH-only and RC from *R. castenholzii* with wavelength maxima indicated in nm. The spectra have been vertically displaced for clarity.

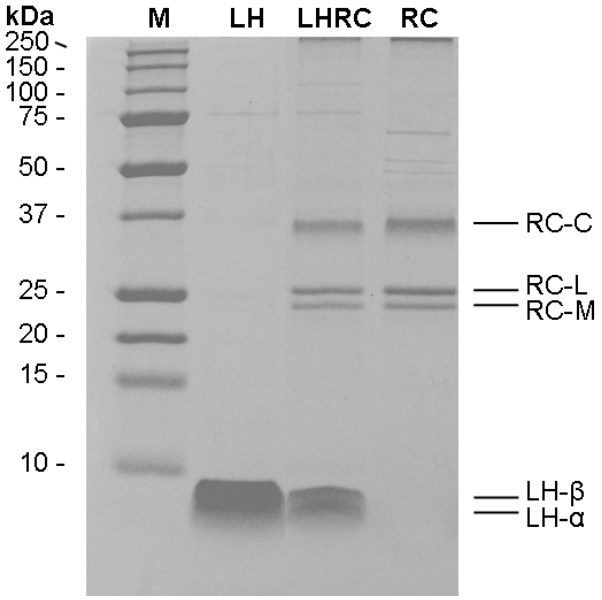

Figure 3.2. Coomassie stained SDS-PAGE of the LH-only, LHRC and RC from *R. castenholzii* along with a molecular mass marker (M). The apparent masses determined from the gel are: the RC C-subunit (37,000 kDa), L-Subunit (26,000 kDa), M-subunit (24,000 kDa) and LH α-subunit (5,000 kDa) and β- subunit (7,000 kDa).

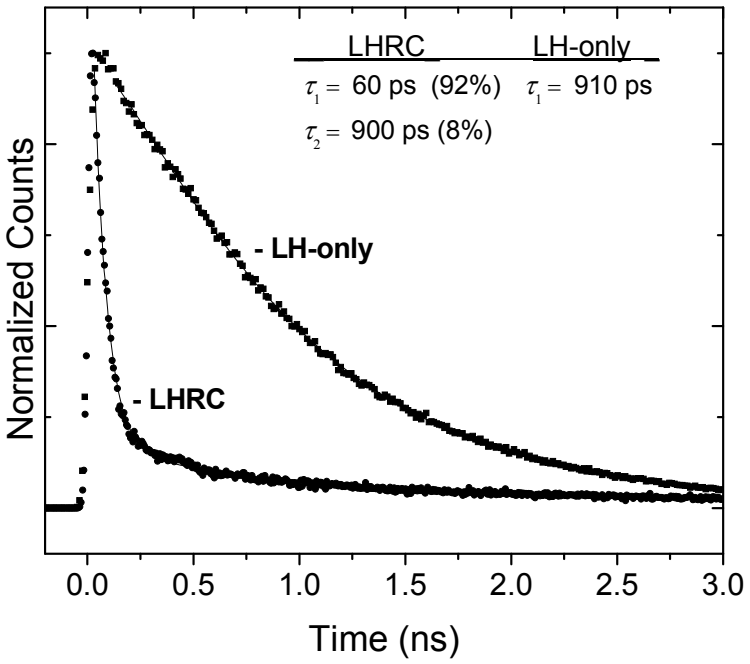

Figure 3.3. Fluorescence lifetime kinetics of the LHRC and the LH-only. Excitation was into the soret band of BChl *a* at 380 nm and emission was monitored at 900 nm. kinetic fits for the LHRC yielded two single exponential kinetic components, 60 ps (92% amplitude), and 900 ps (8% amplitude) while the LH-only kinetics could be satisfactorily fit to a single exponential decay of 910 ps and are represented by smooth lines.

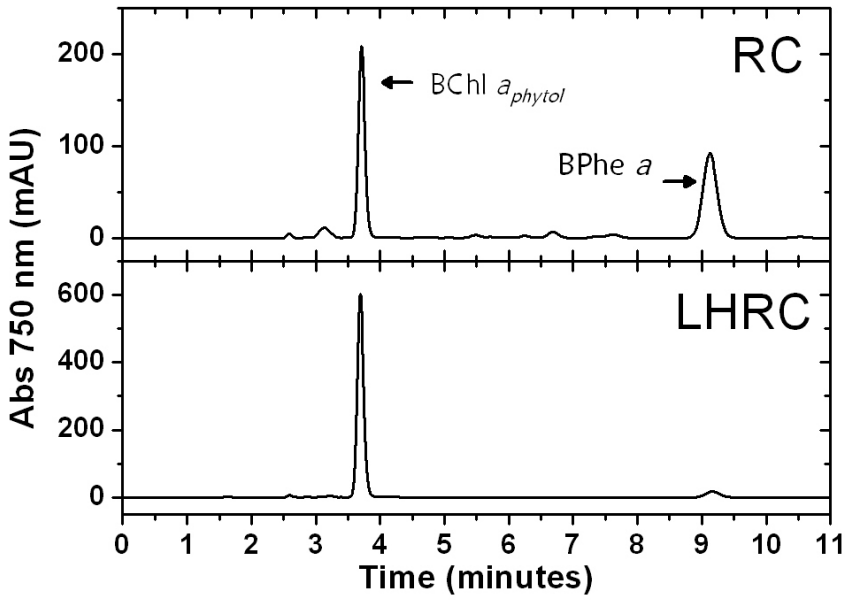

Figure 3.4. Representative HPLC elution profiles, monitored at 750 nm, for pigment extracted from the purified RC (top panel) and the LHRC (bottom panel). The solvent system was an isocratic flow of 80:20 (v/v) methanol:acetone.

Complex	BChl *a* / BPhe *a* (750 nm)	Ave. ± SD
LHRC	*Y* = 15.5, 15.9, 16.6, 16.2, 16.6, 16.2	16.2 ± 0.4
RC	*X* = 1.02, 0.99, 1.04	1.02 ± 0.03

Table 3.1. Ratio of the integrated absorption peaks of BChl *a* / BPhe *a* from HPLC chromatographs from six separate extractions of the LHRC and three separate extractions of the isolated RC.

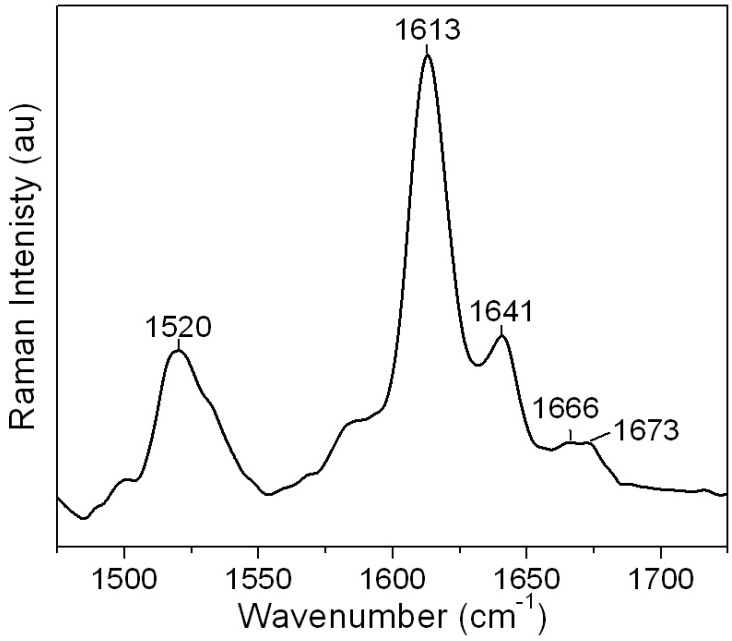

Figure 3.5. Resonance Raman spectrum of the LH-only recorded for the high frequency region recorded at 30 K with an excitation wavelength of 364 nm.

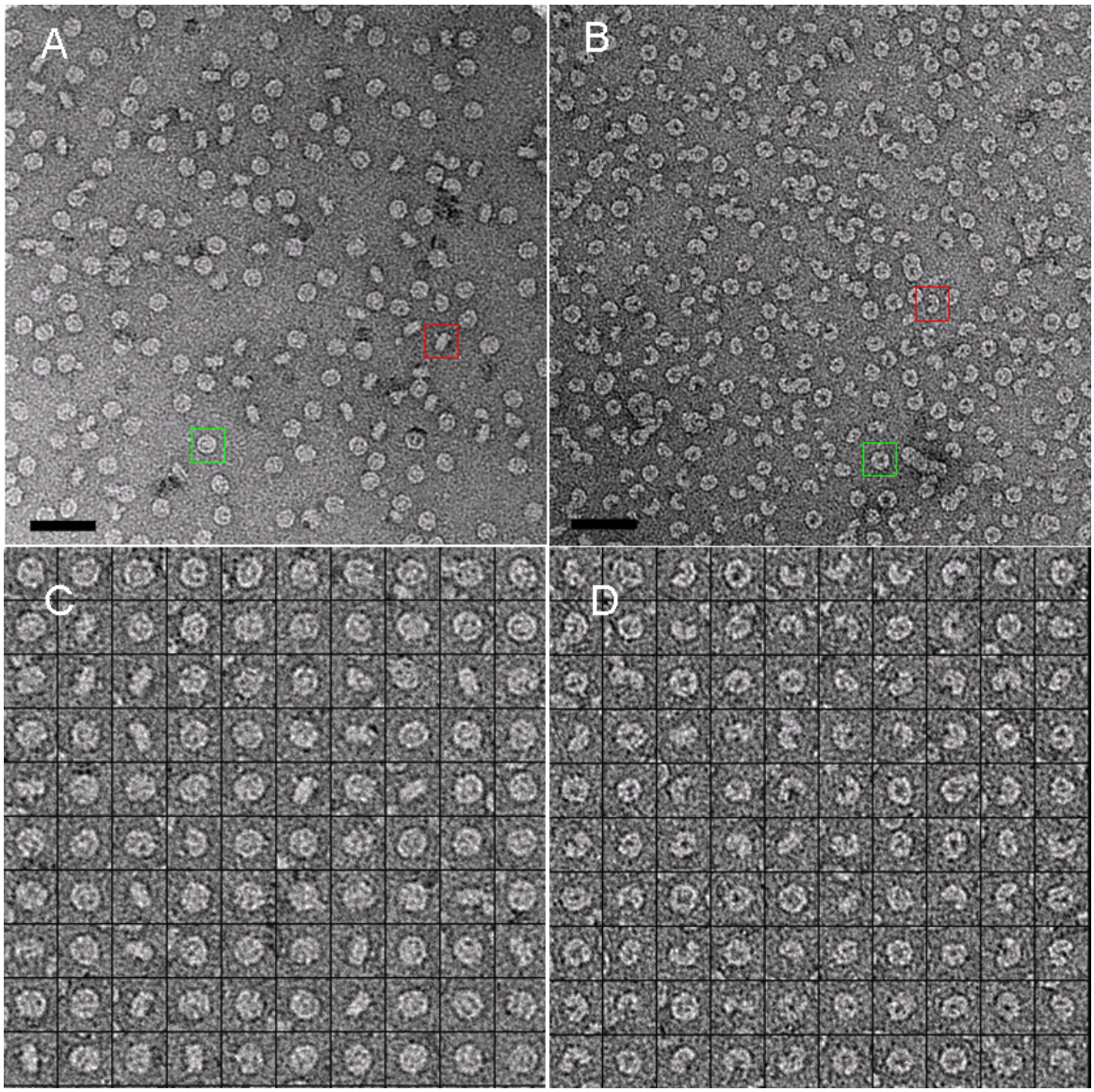

Figure 3.6A. Representative electron micrograph at 52,000 magnification of the detergent solubilized LHRC. B – Same as (A) only for the LH-only. An example of a top or bottom view of the LHRC is shown in a green box while the presumed side view is shown in a red box in (A). In (B), the green box represents top or bottom view of the LH-only, while the red box shows an incomplete ring. The scale bar represents 50 nm. B and C – 100 selected single particles for the LHRC and LH-only, respectively. Each box is 25 x 25 nm.

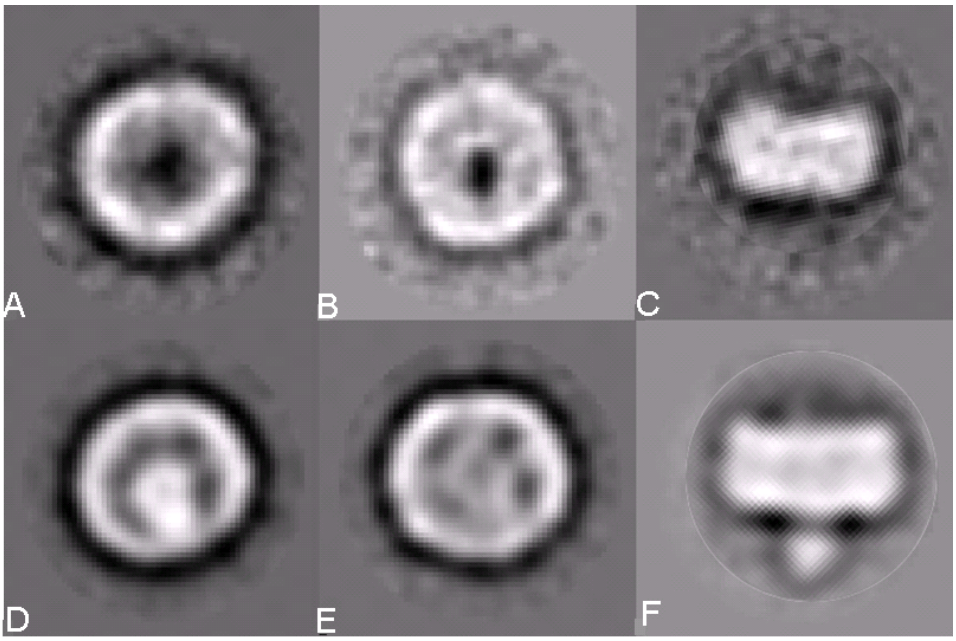

Figure 3.7. Top panel – Presumed periplasmic (A), cytoplasmic (B) and side projection (C) of the LH-only. Lower panel – Presumed periplasmic (D), cytoplasmic (E) and side projections (F) of the LHRC. Each box is 25 x 25 nm. Each image is the average of > 100 individual particles.

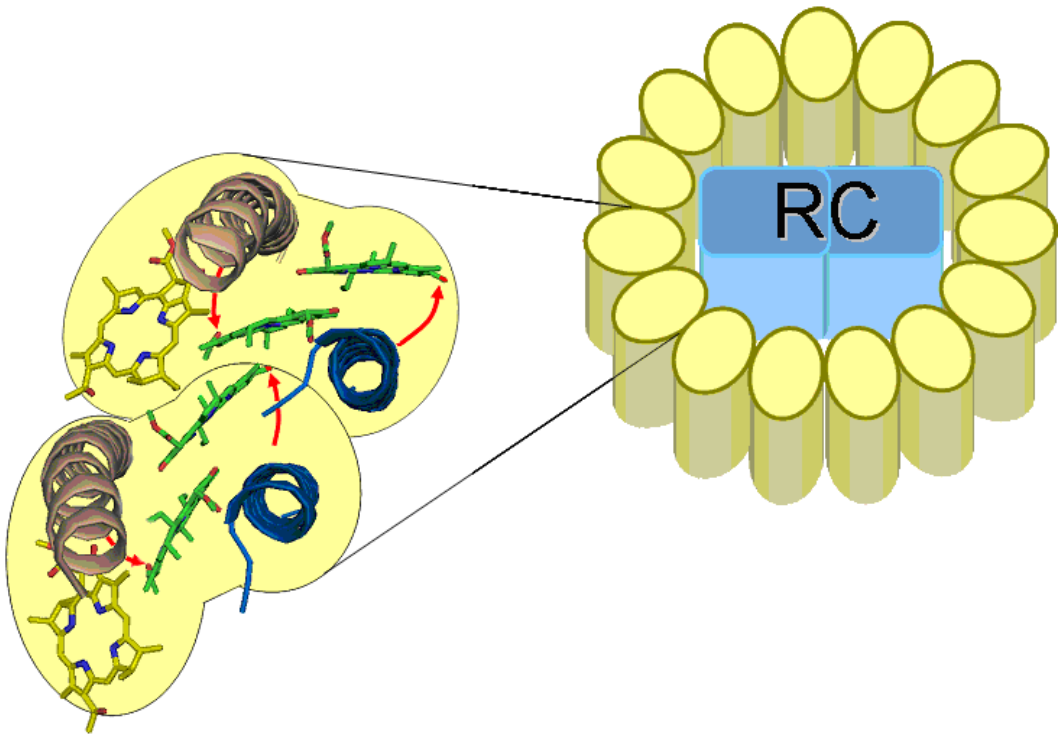

Figure 3.8. Model of the size and organization of the LHRC from *R. castenholzii*. Each subunit of the antenna contains the α-(blue) and β-(brown) polypeptides that coordinate three BChl *a*. Two BChl embody the B880 pigments (green) while the monomeric BChl represents B800 (yellow). Proposed H-bonds from each LH subunit to the C2-acetyl group of the B880 BChls are indicated in red and are internal to each subunit. Overall, 15 ± 1 subunits are proposed to surround the RC. Each subunit contains carotenoid but is omitted due to the uncertainty of its location.

CHAPTER 4

THE REACTION CENTER KINETICS AND ENERGETICS OF *ROSEIFLEXUS CASTENHOLZII*

Abstract

Integral membrane pigment-protein complexes that facilitate light-induced electron transfer are called reaction centers (RCs). Upon excitation, a specialized pair of chlorophyll molecules rapidly donates an electron to a neighboring acceptor molecule and thus initiates charge separation across the membrane. The electron is transported to additional acceptor molecules and the oxidized special pair is reduced by an electron donor to the RC, resetting the system and allowing for the entire process to occur again. The kinetics of charge separation in the purified RC from the chlorosome-lacking filamentous anoxygenic phototroph, *Roseiflexus castenholzii* have been determined at room temperature and 77°K by transient absorption difference spectroscopy. Additionally, the energetics of the P/P^+ and RC-bound cytochrome subunit midpoint potentials were measured by redox potentiometry.

Introduction

R. castenholzii is a niche-adapted, filamentous anoxygenic phototroph (FAP) that lacks chlorosomes, the primary light-harvesting architecture in green bacteria.

Light-harvesting is realized only in the membrane antenna (B800-880) complex which is in close association with the RC. Bacteriochlorophyll (BChl) *a* and carotenoids are organized in a similar manner to the B808-866 complex from *Chloroflexus aurantiacus* but also share many spectroscopic and functional similarities to LH1 and LH2 from purple bacteria (Collins et al. 2009).

Among FAPs, only the RC from *C. aurantiacus* has been extensively studied and when compared to its closest analog, the RC from purple bacteria, there are many similarities as well as significant differences in the energetics and kinetics of electron transfer. The purified RC from *C. aurantiacus* contains only L- and M- subunits and is thought to be organized with a approxiamte-C_2 symmetry as is the case for the purple bacterial reaction center (Deisenhofer et al. 1985). The L- and M-subunits from *R. castenholzii* shows moderate homology to the analogous subunits in *C. aurantiacus* (52% and 44%, respectively) and fairly low homology to the L- and M-subunits of the well-studied purple bacteria (~25-30%) (Yamada et al. 2005). The RC from *C. aurantiacus* is proposed to contain three BChl *a* and three bacteriopheophytin (BPhe) *a* held by the L- and M- protein subunits (Blankenship et al. 1983; Pierson and Thornber 1983) whereas there are four BChl *a* and two BPhe *a* in the purple bacterial reaction center. The RC cofactor arrangement in the RC of purple bacteria is shown in figure 4.1. The special pair, P, is composed of a dimer of BChls. Two accessory BChls reside in the B_A or B_B site of the RC, two BPhe occupy the H_A and H_B sites, and Q_A and Q_B represent the primary and secondary quinones, respectively. “A” and “B” subscripts in the above nomenclature represent cofactors along the A- or active branch and B-branch

of the RC, respectively. The active branch cofactors are primarily associated with the RC L-subunit. In *C. aurantiacus* it is generally thought that the cofactor arrangement along the active branch of the RC is the same as the L-subunit in purple bacteria (Blankenship et al. 1983; Ivancich et al. 1996) because the His residue that serves as an axial ligand to BChl *a* in the B_B site of the purple bacterial RC is replaced by a leucine in *C. aurantiacus* (Ovchinnikov et al. 1988) (isoluecine in *R. castenholzii*) (Yamada et al. 2005). These substitutions most likely result in the incorporation of the additional BPhe instead of BChl in the RC in the analogous B_B site (termed Φ_B.). However, this assignment is not certain and recent transient absorption measurements utilizing Soret region excitation led Xin et al to speculate the additional BPhe could reside in the B_A site (Xin et al. 2007).

The kinetics of electron transfer in the reaction center from several species of purple bacteria, including many mutants, have been extensively studied (for review see (Wachtveitl and Zinth 2006)). At room temperature, the excited special pair, P^*, facilitates electron transfer (presumably through B_A) to form the $P^+H_A^-$ charge separated state with a time constant of about ~ 3-4 ps (Breton et al. 1986; Holzapfel et al. 1990). Electron transfer proceeds to Q_A with a time constant of about 200 ps. Electron transfer in the RC terminates after Q_B has received two electrons from Q_A and two protons, diffusing out of the reaction center as a quinol and is replaced by a new quinone from the membrane pool. Interestingly, the rates of the first electron transfer reactions are increased at low temperatures (Kirmaier et al. 1985).

The electron transfer intermediates, P^* and $P^+H_A^-$, are also observed in the RC of *C. aurantiacus*, only their respective decay rates are slower (for review (Feick et al. 1995)). At room temperature, stimulated emission from P can be fit to a single exponential of 7 ps and electron transfer to Q_A occurs with a time constant of about ~300 ps (Kirmaier et al. 1986; Xin et al. 2007). Differing from purple bacteria, these kinetic components seem to be largely independent of temperature (Becker et al. 1991).

In purple bacteria, donation to the special pair is achieved through a small soluble cytochrome c_2 or through an RC-attached tetraheme cytochrome depending on species (for reviews see (Axelrod et al. 2009; Nitschke and Dracheva 2004)). In the tetraheme complex of the purple bacterial RC, the potential of the individual hemes are arranged as pairs of alternating high and low potentials and can span a potential range of ~-80- +350 mV. For some species, the high and low potential hemes can be spectroscopically distinguished (Dracheva et al. 1988). The RC from *C. aurantiacus* contains a tetraheme cytochrome subunit, however it readily is dissociated from the RC during purification (Freeman and Blankenship 1990). In membrane fragments as well as the purified cytochrome complex, four poteniometrically distinct *c*-type cytochromes can be resolved. However, unlike the case for purple bacteria, the individual hemes appear to be spectroscopically identical (Freeman and Blankenship 1990). The cytochome complex in *C. aurantiacus* also appears to span a more narrow range (0-300 mV) (Freeman and Blankenship 1990; van Vliet et al. 1991).

Among FAPs, the overwhelming majority of kinetic data has been accumulated for *C. aurantiacus.* Few other organisms for this interesting and diverse group of

phototrophs have been studied. In this work, we have investigated the kinetics and energetics of electron transfer in the isolated RC from *R. castenholzii*. Electron transfer kinetics were investigated using pump-probe spectroscopy at room temperature and at 77 °K. Poteniometric titrations revealed the midpoint potentials for P/P^+ as well as the RC associated cytochrome *c* complex.

Materials and methods

Reaction center purification

R. castenholzii was grown anaerobically and photoheterotrophically on 02YE medium (pH 7.5) (Hanada et al. 1995)in a 15 L fermentor (Bioengineering, Wald, Switzerland). Cells were harvested and then washed in 20 mM Tris, pH = 8.0 (buffer A). Whole membranes were prepared by suspending whole cells in buffer A in a 1:4 (w/v) ratio followed by three cycles (four minutes each) of sonication with a power output of 6 (Model 350, Branson, Danbury, CT). The mixture was centrifuged at 16,000 x g for 20 minutes to separate unbroken cells and the lysate was further centrifuged at 200,000 x g for 2 hours to isolate whole membranes. To isolate the RC, membranes were resuspended in buffer A to an optical density of 10 in 1 cm at 880 nm and lauryl dimethylamine N-oxide (LDAO) was added dropwise from a concentrated stock (30%) to a final concentration of 0.45% (v:v). The mixture was incubated with gentle stirring for 90 minutes at room temperature, then diluted to a final concentration of 0.1% LDAO with buffer A and centrifuged at 200,000 x g for 1 hour. The

supernatant, which was enriched in RCs, was filtered through a 0.22 μm vacuum-driven filter and immediately applied to an ion-exchange chromatography (IEC) column packed with Q-sepharose resin (GE Healthcare) pre-equilibrated with 0.1% LDAO in buffer A. The column was then washed extensively with 1% LDAO in the same buffer to remove nonspecifically bound carotenoids and BChl *a*. After the column was re-equilibrated with 0.1% LDAO in buffer A the reaction centers were eluted with a linear gradient of NaCl. Appropriate fractions, as judged by the absorbance spectrum, were concentrated and subjected to gel filtration chromatography (Sephacryl 200 HR resin, GE Healthcare) using 0.1% LDAO in buffer A with 100 mM NaCl. If further purification was necessary, a final IEC step was employed. The RCs used in these studies reported below had 280/816 nm absorbance ratios ≤ 2.5.

Redox Titrations

Potentiometric titrations on purified RCs were performed in the dark by bulk-electrolysis using a thin layer quartz glass spectroelectrochemical cell with a Pt gauze working electrode. Ag-AgCl / 3M KCl was used as the reference electrode and was calibrated against a saturated solution of quinhydrone at various pH values. All potentials are stated relative to the standard hydrogen electrode (SHE). The potential was controlled by a CH 620 C potentiostat (CH Instruments Inc.) and an absorption spectrum (375-900 nm) was recorded after the sample equilibrated for several minutes at each potential. Oxidative and reductive titrations were performed with 65mM KCl and 20μM of the following mediators to accelerate the equilibrium between the

working electrode and the RCs: potassium ferricyanide, N,N,N',N'-tetramethyl-1,4-phenylenediamine (DAD), 2,3,5,6-Tetramethyl-p-phenylenediamine (TMPD), 1,2-Napthoquinone, and phenazine ethosulfate, phenazine methosulfate, 2-hydroxy-1,4-anthroquinone, 1,2-napthoquinone, 1,2-napthoquinone-4-sulfonic acid and 2-Methyl-1,4-naphthoquinone (menadione).

Spectroscopy

Steady-state absorption spectra were recorded on a Perkin Elmer, Lamda 950 spectrophotometer. For low temperature measurements a liquid nitrogen cryostat (OptistatDN, Oxford Instruments) was used and samples contained glycerol at 50% volume.

Ultrafast transient absorption measurements were performed on a system described previously (Kirmaier and Holten 1991; Yang et al. 2000). 2.5-3 mL of 25-35 μM RCs were flowed from an ice-cooled reservoir through a 2 mm path length cuvette. The sample temperature was approximately 285 °K. The sample was excited at 10 Hz with 130 fs pulses of excitation light (either 605, 860, or 870 nm) and probed with white light of the same pulse duration. For kinetics recorded at 77K, concentrated RCs were mixed with an equal volume of glycerol and placed in a home-build acrylic cuvette (~2 mm path length) and frozen in the dark in an Oxford Instruments cryostat. For all experiments, the excitation energy was kept low enough so that each pulse did not cause more than ~20% bleaching for the sample.

Results

Ground-State Absorption

The RC had near infrared absorption bands at 864, 816, and 760 nm at room temperature and ambient potential, in a ratio of 0.6 : 1.0 : 1.0. These bands are attributed to the Q_y transitions of the special pair of BChls, the accessory BChl *a* and the three BPhe *a* of the RC (figure 4.2). The purified RC does not contain carotenoid. Both the 816 and 760 nm bands are red-shifted (3 and 4 nm, respectively) when compared to the isolated reaction center from *C. aurantiacus* (Shiozawa et al. 1987). The Q_x transition of all of the RC BChl *a* coalesce at 605 nm. The region between ~500-550 nm has contributions from the Q_x bands of BPhe *a* and the RC-associated cytochrome complex and were resolved in the 77 °K spectra (see below). The Soret band of the RC-associated cytochrome complex has a strong peak around 415 nm while the bands observed below 400 nm are mixed Soret contributions from BChl and BPhe and displays peaks around 392 and 365 nm at RT.

At 77°K, the Q_y transition of the special pair red-shifts to 887 nm, while a band is resolved at 788 nm. If analogy to *C. aurantiacus* can be made, this band is due to BChl *a* (Shiozawa et al. 1987). Additionally, there is a shoulder on the blue side of the 760 nm BPhe band and the Q_x bands of BChl *a* is became asymmetric. The Q_x region of BPhe *a* has considerable overlap with the α- and β-bands of the RC-associated cytochrome. However, these could be resolved at low temperature and ambient potential (figure 4.2, inset). The two peaks at 542 and 532 nm are assigned to the Q_x

bands of BPhe *a* and appear in a nearly 1:2 ratio, respectively. The 552 nm band and a shoulder around 524 nm are attributed to the α- and β-bands of the RC associated cytochrome, respectively. This assignment is corroborated by the subsequent redox titration of these bands (see below). The position of the Soret bands of the RC-associated cytochrome, BChl *a* and BPhe *a* are essentially unchanged at both room temperature and 77°K.

Potentiometric Titrations of the RC

Redox titrations of P, monitored as a change in absorption at 865 nm as a function of potential, yields a midpoint potential of 390 ± 5 mV at pH = 8.0 (Figure 4.3A). This value is in accord with the purified RC from *C. aurantiacus* (Shuvalov et al. 1986) as well as isolated cytoplasmic membranes (Bruce et al. 1982) and is about 100 mV lower than the P/P^+ potential from most purple bacteria. Moreover, the potentials of the of the RC-associated cytochomes were calculated by monitoring absorbance changes in the α-band at 554 nm. The titration was fit best to the sum of two n=1 Nernst curves with potentials of 85 ± 5 and 265 ± 5 mV. The relative amplitude of each potential component was calculated to be 0.55 and 0.45, respectively, indicating a nearly equal contributions from both components. Additionally, absorption changes of the β-band of cyt *c* monitored at 524 nm yielded potentials within the uncertainly of the α-band titration (result not shown). To highlight the small absorption changes in the α-band at several different potentials, the difference spectrum between the potential tested and the fully reduced (-100 mV) sample is shown in figure 4.3B.

The difference spectrum nearly removes all of the contributions from the BPhe absorption in this region.

The gene sequence of the RC-associated cytochrome from *R. castenholzii* indicates the presence of four hemes and an overall low sequence identity (27%) when compared the RC C-subunit of *C. aurantiacus* (Yamada et al. 2005). It is possible that the hemes are separated into two pairs of hemes with similar potentials as is the case of many of the tetra-heme cytochromes associated with the RC of purple bacteria (Nitschke and Dracheva 2004). Furthermore, all four hemes are spectroscopically identical. Regardless of the potential tested, a single α-band was observed at 553 nm (figure 4.3B). This was also the case for cytochome *c*-554 from *C. aurantiacus*. However, in this case the cytochrome complex was purified separately form the RC and the midpoint potentials for each of the four cytochromes were unique with values of 0, +120, +220 and +300 mV vs SHE (Freeman and Blankenship 1990).

Overview of Charge Separation at 285 °K

Primary charge separation in *R. castenholzii* can be separated into two kinetically observable phases; the decay of P* and $P^{+}H_{A}^{-}$. Following 130 fs excitation flashes (either at 605 or 860 nm), P is removed from the ground state as P* is formed. The transient absorption (TA) is characterized by the bleaching of the Q_x and Q_y bands of P at 605 and 860 nm, respectively (P* spectra, figures 4.4A and 4.4B, black line). Stimulated emission of P is maximally observed around 920 nm on the long-

wavelength side of P bleaching. This wavelength nearly coincides with the isosbestic point ($\Delta A = 0$) in P^+H^- and $P^+Q_A^-$ NIR TA spectra.

The decay of stimulated emission of P is assigned to electron transfer from P^* to H_L^- in wild-type RCs of purple bacteria as well as the RC of *C. aurantiacus* if 100% yield is assumed. These time constants are ~3-4 ps in purple bacteria (Kirmaier and Holten 1987) and ~7 ps in *C. aurantiacus* (Becker et al. 1991; Xin et al. 2007). In the purified RC of *R. castenholzii*, the decay of stimulated emission monitored between 860-960 nm can be fit to convolution of the instrument response, a constant and a single exponential yielding 3.3 ± 0.4 ps (for representative kinetics see figure 4.5A). Because bleaching of P contributes to stimulated emission in the TA spectrum, we cannot rule out ≤ 10% decay of P^* to the ground state, thus indicating that the yield of charge separation is ≥ 90%.

The difference spectrum at 20 ps following excitation (figure 4.4A and 4.4B, red line) is representative of the $P^+H_A^-$ charge separated state. Bleaching of the photoactive RC BPhe is observed at 542 nm and broad absorption due to an anion of BPhe is seen at 662 and 943 nm. The kinetics data between 500-700 nm were fit by the sum of two exponentials plus convolution of the pump and probe pulses and a constant. The fitted time constants were 3.6 ± 0.4 ps (P^* lifetime) and 200 ± 20 ps ($P^+H_A^-$ lifetime). Representative data are shown in figures 4.5 B and C. The 3.6 ± 0.4 ps P^* lifetime measured here agrees well with that determined in the NIR stimulated emission. $P^+H_A^-$ decays to give $P^+Q_A^-$ (figures 4.4A and 4.4B, red and blue lines) with a yield determined to be ≥ 95%. This state is characterized by the disappearance of the

H_A bleaching (542 nm) and anion bands (662 nm) and the appearance of a small positive feature around 547 nm that may reflect a red-shift in the ground state absorption of BPhe resulting from electrostatic interactions with Q_A^- (Vermeglio and Clayton 1977). The magnitude of bleaching in the Q_x band of P is essentially unchanged ($\geq$ 95% constant). In the RC of purple bacteria and *C. aurantiacus*, $P^+H_A^-$ decays with a time constant of about ~200 ps (Kirmaier et al. 1985) and ~300 ps (Becker et al. 1991; Kirmaier et al. 1986; Xin et al. 2007), respectively.

Overview of Charge Separation at 77 K

The kinetics of electron transfer in the isolated RC are more complicated at low temperature. P* is formed upon excitation at 870 nm (figure 4.6 – blank line). Within 0.5 ps a portion of P^* has already decayed to form $P^+H_A^-$ indicated by the bleaching of the H_A band at 543 nm and the appearance of the anion band around 665 nm. The $P^+H_A^-$ spectrum (20 ps, fig 4.6 – red line) has bleaching of H_A at 543 nm that is not symmetric as there is a shoulder on the blue side of this band that grows in with the bleaching at 543 nm and remains relatively constant throughout the measurement (see spectra at 3 ns, fig 4.6 – blue line). Deconvolution of this peak into two Gaussians revealed peaks at 543 and 537 nm (results not shown). This wavelength is probably too long to originate from the additional BPhe in the RC. The additional RC BPhe is presumed to reside in the B_B site in the RC (see Discussion) and in the H_B site because these bands were identified in the 77K ground state absorption at 532 nm (figure 4.2). The asymmetry of the bleaching observed between 535-545 nm at longer times in the 77 °K TA kinetics

way reflect an electrochromic shift observed in the ground state absorption of BPhe when presumably Q_A is reduced. Such an effect, albeit smaller, has been seen in wild type reaction centers of purple bacteria (Chuang et al. 2008). The spectra at later times (500 ps and 3 ns, fig 5) demonstrated that a portion of $P^+H_A^-$ still persisted and had not decayed to form $P^+Q_A^-$ which is in contrast with the results at RT. Fitting of the kinetics of the H_A bleaching around 542 nm could be done satisfactorily by the sum of 4 exponential decays (Fig 4.7). The initial decay of this band was fit to 1.0 ± 0.1 ps (76% amplitude) and 6 ± 1 ps (24 % amplitude). The disappearance of the bleaching could be fit best by fixing one decay at 20 ns (37% amplitude) while optimizing for the second, 220 ± 20 ps (63% amplitude). The former value, 20 ns, was selected because it corresponds to the lifetime of $P^+H_A^-$ in purple bacterial RCs when Q_A is pre-reduced (τ = 20 ns) at 90 K (Schenck et al. 1982) or when Q_A was depleted (τ = 21 ns) at ~ 90 - 100 K (Ogrodnik et al. 1988). Fixing the long decaying component to 10 ns or 30 ns does not significantly change the other measured lifetimes (results not shown). Moreover, comparison of the magnitude of P bleaching around 600 nm (figure 4.6) suggests ≥ 80% yield of charge separation at 77 °K for at least the formation of $P^+H_A^-$.

Discussion

Here, we have presented kinetics and energetics of electron transfer in the isolated RC from *R. castenholzii*. A schematic energy level and kinetic diagram based on the results of redox titrations, TA, and the assumption of certain equivalencies with

other RCs is displayed in figure 4.8. The ground state absorption (figure 4.2) is similar to that of *C. aurantiacus* with the exception of the cytochrome contribution, in particular, the strong Soret band absorption. It is possible from the low-temperature steady-state and TA spectra to suggest which branch of the RC is photoactive. In the RC of *Rhodobacter capsulatus,* an H-bond from Glu L104 to the $C13^1$-keto group of H_A is responsible for the 15 nm red-shift in the Q_x absorption of H_A compared to H_B at 77 K (Bylina et al. 1988). When L104 was mutated into Leu or Gln the red-shift in H_A was reduced to 0 and 9 nm, respectively, with the latter mutation resulting in bands centered at 531 and 540 nm. The RC from *R. castenholzii* and *C. aurantiacus* both contain Gln at the equivalent residue of L104 and a BPhe occupying H_A. The 77°K Phe Q_x absorbance region of *R. castenholzii* is also resolved at 77 K into two bands at 532 and 542 nm respectively. Since the 542 nm band showed bleaching in the transient absorption spectrum, we suggest by analogy, that the L-subunit of the *R. castenholzii* RC is the photoactive branch. This would indicate that the additional BPhe associated with the reaction center, termed Φ, is proposed to reside in the analogous B_B of the RC (Φ_B) because the M-subunit lacks the His axial ligand. In the *Chloroflexus* RC, the Q_x bands of Phe are only resolved into two distinct bands at 4 K (Vasmel et al. 1983).

In the purple bacterial RC, estimates of the energy of the $P^+B_B^-$ state is calculated to be about 0.24 eV above P* (Parson et al. 1990) making this state inaccessible for electron transfer. However, BPhe has an intrinsically more positive reduction potential than BChl (Watanabe and Kobayashi 1991). All things being equal, this might place the potential of $P^+\Phi_B^-$ near or below P* and make Φ_B a possible

electron acceptor in the FAP RC. This exact situation was tested by Katilius et al. who introduced a luecine residue in place of the BChl-coordinating histidine at position M182, resulting in the incorporation of BPhe at the B_B position in *Rhodobacter sphaeroides* (Katilius et al. 1999). This cofactor change resulted in about 35% electron transfer to the BPhe occupying B_B with a time constant of 200 ± 20 ps. Moreover, the additional BPhe resulted in an absorption band at 785 nm whereas H_A and H_B absorb around 760 nm. While there is identical cofactor composition between this mutant and *R. castenholzii*, there are clearly many amino acid differences suggesting the protein environment compensates to support ≥ 90% charge separation.

The kinetics of electron transfer at 285 ° K in the isolated RC from *R. castenholzii* seem to be more similar to the kinetics determined for purple bacteria rather than *C. aurantiacus.* The P^* and $P^+H_A^-$ lifetimes were measured to be ~3.5 ps and 200 ps. In the RC of purple bacteria, Tyr-M210, is in the proximity of P, B_A and H_A and is thought to influence primary charge separation down the A-branch by lowering the energy of the $P^+B_A^-$ state (Parson et al. 1990). Mutation of this residue to Leu resulted in a significant slowing of the time constant for the formation of $P^+H_A^-$ (Finkele et al. 1990; Hamm et al. 1993; Nagarajan et al. 1990). Leu occupies the equivalent M210 position in the RC of *C. aurantiacus* had has been used to explain the slower kinetics of initial charge separation. However, *R. castenholzii* also maintains Leu in this same position yet has kinetics congruent with wild type purple bacterial RCs.

At 77 °K, the decay of P^* was best fit by the sum of two exponentials (1 ± 0.1 and 6 ± 1 ps). Multi-exponential decays have been used to describe the decay of P^* in purple bacteria (Du et al. 1992) and in *C. aurantiacus* (Becker et al. 1991) although the molecular origins of such an effect have not been delineated. The decay of $P^+H_A^-$ was also fit to two exponentials of 220 ps and a fixed component of 20 ns. Because a portion of the $P^+H_A^-$ state did not decay during the measurement, this strongly suggest that either a portion of the RCs lacked the primary quinone, Q_A or that it was pre-reduced. The complexity of the 285 and 77 °K kinetics suggests that a simple analogy to *C. aurantiacus* or the well-studied RC from purple bacteria is insufficient and that the kinetics are influenced by more than just a few amino acid residues.

The potential of P/P^+ is considerably influenced by H-bonds to the keto carbonyl and acetyl groups of the BChl that comprise P (Lin et al. 1994). Native RCs from purple bacteria contain a single H-bond from His-L168 to the acetyl group of the L-side BChl *a* of P (where the P/P^+ midpoint potential is ~500 mV). Replacement of this residue to Phe resulted in a decrease in the P/P^+ potential to 410 mV while that addition of three H-bonds increased the midpoint potential 260 mV over the wild type. The P/P^+ midpoint potential was determined to be 390 ± 5 mV for *R. castenholzii*. bacteria. In the RC of *R. castenholzii* and *C. auranticus* a Phe occupies the analogous position to L168, and thus, no H-bonds are created between the substiuents on P and the protein scaffold. This observation can reconcile the difference in potentials measured for the RC of FAPs and the purple bacterial. A slightly lower P/P^+ midpoint potential but a similar Q_y ground state absorption maximum for P at 865 nm, compared

to the RC of BChl *a*- containing purple bacteria, might reflect a slightly more reducing excited state redox potential for P^* (see figure 4.8).

Redox titration of the α- and β-bands of the tetraheme cytochrome *c* bound to the RC revealed two waves, that likely represents pairs of high and low potential hemes and were successfully fitted to the sum of two Nernst (n=1) equations of 85 ± 5 and 265 ± 5 mV. Early measurements on the cytochrome subunits from *Rhodopseudomonas viridis* (Clayton and Clayton 1978) or *Chromatium* (Thornber and Olson 1971) suggested that the cytochrome subunit probably contained four hemes. However, only two different potentials were measured. It was later shown in *Rhodopseudomonas viridis* that the α-band of each heme in the complex absorbed at a slightly different wavelength and that each of the hemes were poteniometrically distinct (Dracheva et al. 1988). The redox properties of the C-subunit from *R. castenholzii* differ from those of *C. aurantiacus* which was determined to contain 4 hemes of unique midpoint potentials. Another difference is that the cytochrome subunit purifies with the RC in *R. castenholzii* but not in *C. aurantiacus* (Freeman and Blankenship 1990). This should allow for ready measurements of the rates of inter-cytochrome and cytochrome to P^+ electrons transfer.

The energetics and kinetics of the primary photochemistry in *R. castenholzii* have similarity to both *C. aurantiacus* and purple bacteria. We propose that the L-subunit corresponds to the active branch for electron transfer in the RC with a yield of $P^+Q_A^- \geq 90\%$ at 285 °K. This places the additional BPhe in the analogous B_B site of the RC and it does not appear to participate in forward electron transfer. Additional kinetic

studies to determine the rate of electron transfer from Q_A^- to Q_B as well as the re-reduction of P^+ by the C-subunit cytochrome would be constructive for a complete picture of the RC electron transfer kinetics in *R. castenholzii*.

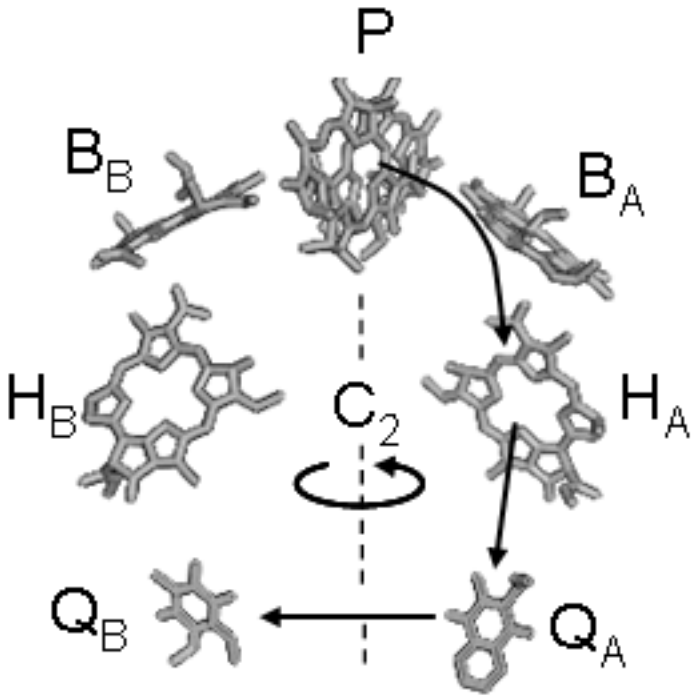

Figure 4.1 Cofactor arrangement and in the RC from purple bacteria. Model is based off of the crystal structure from *Rhodopseudomonas viridis* (PDB accession 2PRC). The RC C-subunit cofactors have been removed for clarity. Electron transfer in the RC is along the A-branch of cofactors and is indicated with arrows. Cofactors are P, the special pair of BChl, B_A and B_B, are the sites of the accessory BChls along the A- and B-branch, respectively, H_A and H_B, are the sites of the RC BPhe along the A- and B-branch, and Q_A and Q_B are the primary and secondary quinones, respectively.

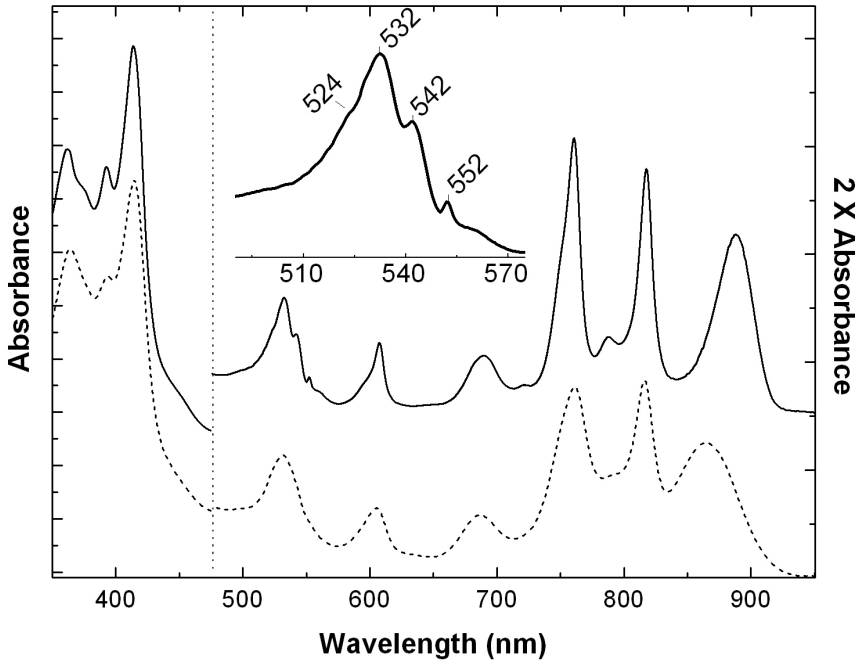

Figure 4.2 –Absorption spectra of isolated RCs from *R. castenholzii* at RT and ambient potential (dashed line) and the same sample cooled to 77 °K. The low temperature spectrum has been offset by 0.1 AU for clarity and both spectra have been scaled by a factor of 2 for wavelengths above 475 nm. The inset expands the 77 °K spectrum between 500-575 nm with wavelengths indicated in nm. The absorbance maxima are given in the text.

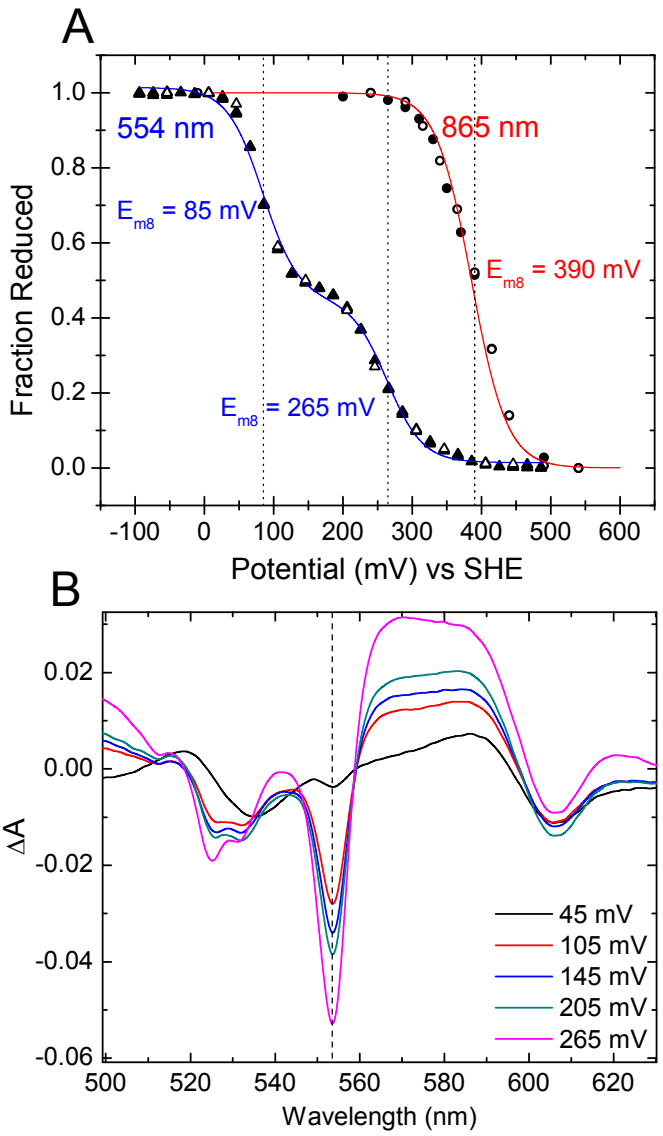

Figure 4.3. A – Potentiometric titration of the RC with absorption detected at 554 nm (triangle) and 865 (circles). Closed and open symbols represented oxidative and reductive titrations, respectively. B – Difference spectrum (potential indicated minus fully reduced, -100 mV) for the α- and β-band region.

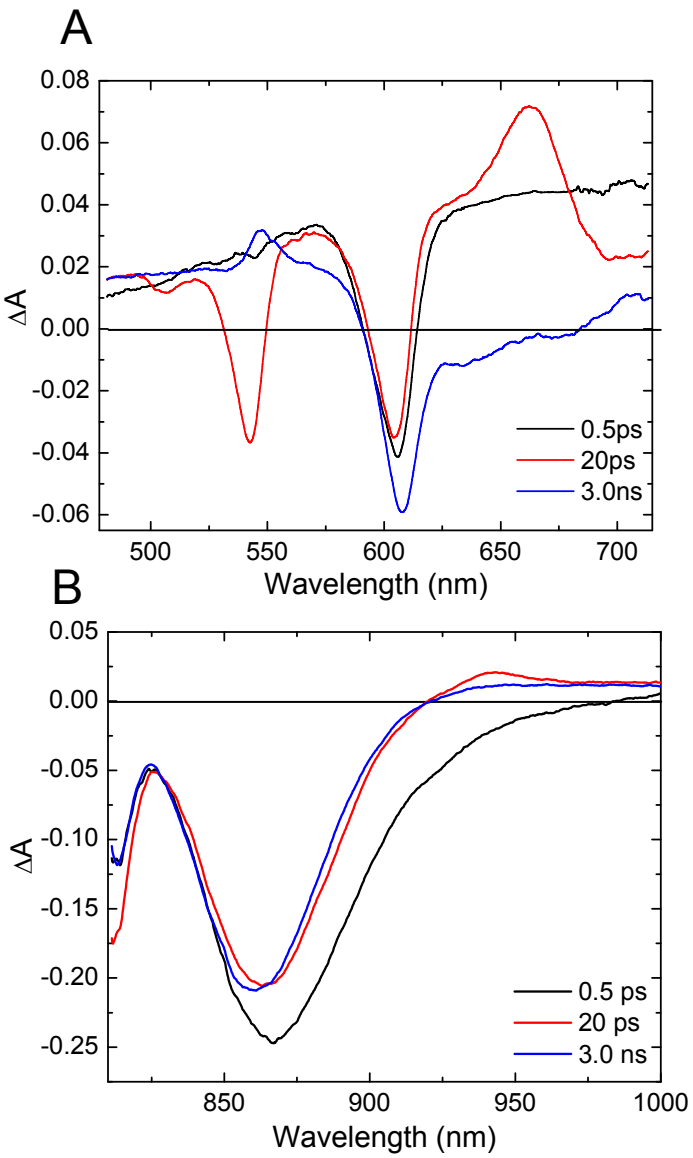

Figure 4.4 – Time-resolved difference spectra obtained at various times after a 130 fs excitation flash at 860 nm (A) or 605 nm (B). The sample $OD_{865\ nm}$ = 0.5 or 1.0 cm^{-1} measured in a 2 mm cuvette (A) and (B), respectively.

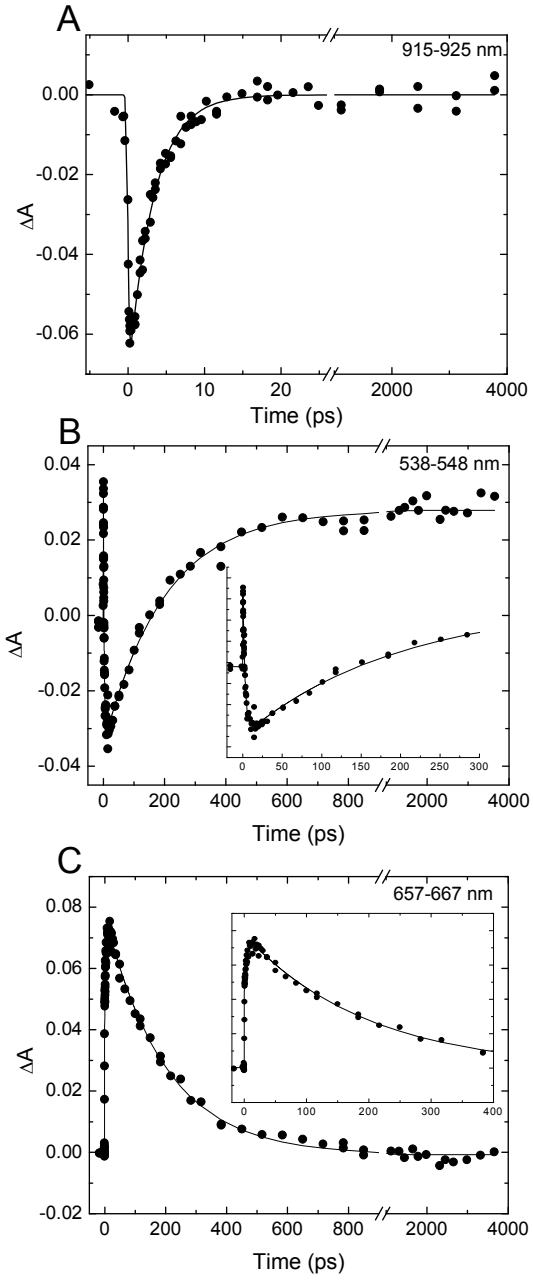

Figure 4.5 – Representative kinetics for the decay of P^* and $P^+H_A^-$. Stimulated emission between 915-925 nm (A). The appearance and decay of the Q_x band of H between 538-548 nm (B) and the appearance and decay a BPhe anion band between 657-667 nm (C). Solid line fits represent convolution of the pump and probe pulses with one (A) or two (B and C) exponentials plus a constant. Excitation was at 605 nm in (A) and 860 nm in (B) and (C).

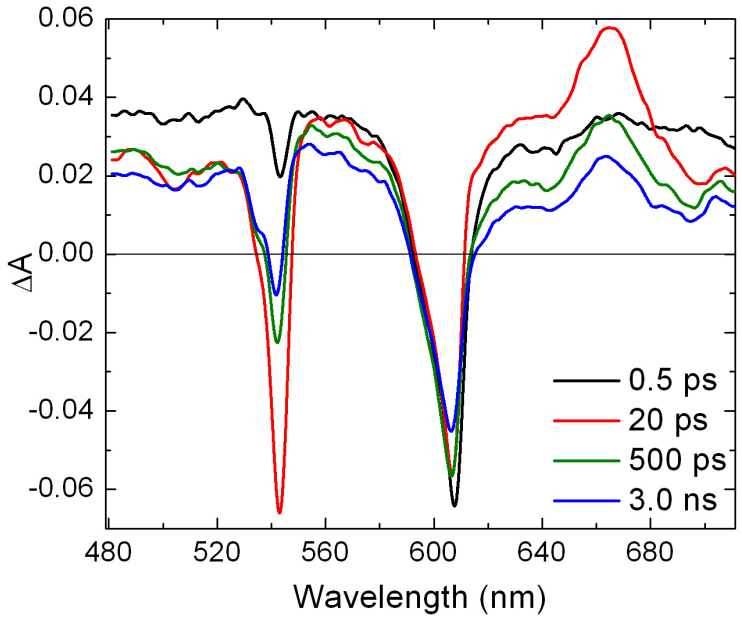

Figure 4.6 – Time-resolved difference spectra obtained at different times after 130 fs excitation at 870 nm measured on isolated RCs measured at 77 °K.

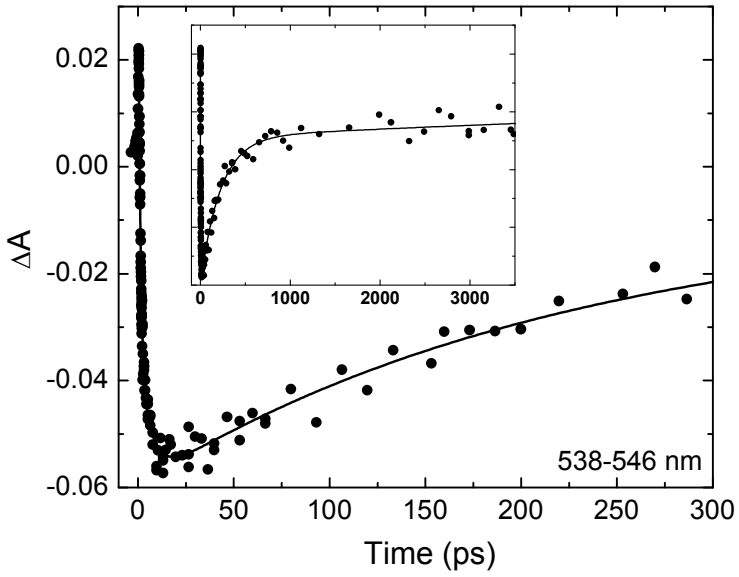

Figure 4.7 – Appearance and decays of the reduction of BPhe at 77 °K for wavelength between 538-546 nm.

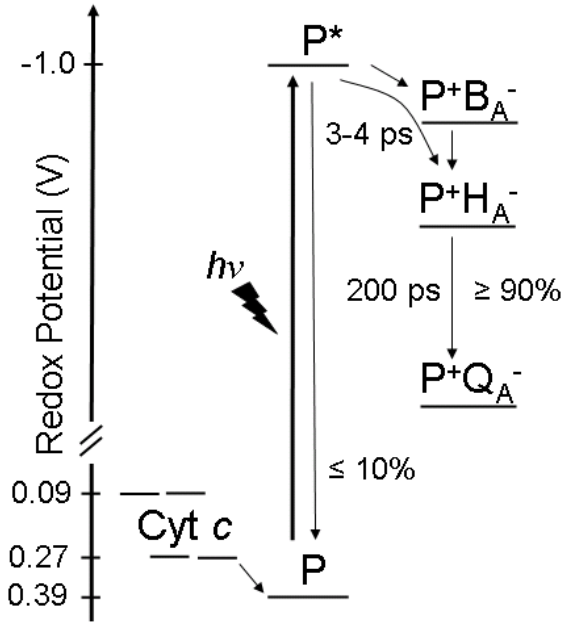

Figure 4.8 – Schematic energy level and kinetic diagram for the *R. castenholzii* RC at 285 °K with determined midpoint potentials (in V vs SHE) indicated and time constants for 90% yield reflect electron transfer from P to H_A and from H_A^- to Q_A, respectively.

CHAPTER 5

CONCLUSIONS AND FUTURE DIRECTIONS

Major findings of this work.

Photosynthetic organisms have evolved to inhabit many biological niches. For example, *R*. *castenholzii* was initially discovered in a bacterial mat from a Japanese hot spring where it was found to grow in symbiosis with cyanobacteria and *Chloroflexus* species (Hanada et al. 2002). The cyanobacteria occupy the surface of the mat and absorb light up to about 700 nm and provide organic matter for species underneath. The layers beneath contain *Chloroflexus* species and *R. castenholii* that absorb primarily around 750 nm (using chlorosomes) and 800-900 nm, respectively. Notably, the LH antennas among these three organisms are different. The remarkable diversity of LH antennas observed among phototrophs (Chapter 1, figure 1.3) demonstrates that nature has solved the problem of light-harvesting using a variety of architectures and pigments. Moreover, even though there are many different antenna types, their functional congruence is to transfer excitation over many nm with high efficiency and deliver it to a RC. Understanding the reoccurring themes in LH antennas would be of considerable interest for the design and implementation of artificial LH devices.

The primary focus of this thesis was to elucidate the initial events of photosynthesis, light-harvesting and initial electron transfer, that occur in *R. castenholzii* because these data are lacking among FAPs. In chapter 2, the LHRC was purified and investigated using biochemistry and a variety of steady-state

spectroscopies. The pigment orientation was calculated from the spectroscopy. Using the primary sequence information of the α- and β-polypeptides and comparison to those of LH1 and LH2 from purple bacteria, a model for the organization of BChl in the antenna was constructed.

In Chapter 3, a full complement of complexes from R. *castenholzii* was prepared. These were the LHRC, the LH-only and the RC. A description of the purification of each complex followed. This allowed for an indirect determination of the number of antenna subunits by comparing the ratio of extracted BChl to BPhe from the LHRC and the RC and yielded 15 ± 1 subunits. The uniformity of the samples was confirmed for the LHRC and LH-only by fluorescence lifetime measurements where both decay by principally monoexponential functions. Additionally, resonance Raman was used to investigate molecular interactions of BChl in the LH-only complex. The stretching modes (in the carbonyl stretching frequency region) observed were very similar to LH1 and not analogous to LH2. This probably reflects a similar mode of BChl binding by the protein between LH1 and the antenna from *R*. *castenholzii*.

The LHRC was then investigated by EM and single particle analysis. Although the resolution is not as high as x-ray crystallography, the size and shape of the complex are easily visualized. The detergent solubilized complex appeared to be a closed elliptical ring and side projections demonstrated the presence of the cytochrome subunit that projects away from the plane of the ring. The size of the ring structure, which including bound detergent, is of sufficient dimension to accommodate the 15 ± 1 subunits determined by pigment extraction. With the number of subunits calculated, the

shape and size of the complex determined by EM, and the pigment orientation within each subunit postulated, a model for the entire LHRC was proposed (figure 3.8).

Finally, the energetics of the P/P^+ and the Cyt/Cyt^+ midpoint potentials of the isolated RC were determined using redox titrations. These values are useful for knowing where on an energetic landscape to place the RC. Moreover, TA spectroscopy allowed for the measurement of the decays of P^* and $P^+H_A^-$ and provided data for the yield of charge separation as well as the rates of electron transfer in the RC.

Future directions

Like most research endeavors there remain unanswered questions. One question that remains is the coordination of B800 in the antenna. In purple bacteria, two crystal structures of LH2 from *Rhodopseudomonas acidophilus* and *Phaeospirillum molischianum* have demonstrated that B800 is centrally coordinated at the N-terminus of the α-subunit by a modified Met (Müh et al. 1998) or Asp located six residues from the N-terminus (Koepke et al. 1996). Analysis of this same region in *R. castenholzii* shows several residues that could be potential BChl coordinating candidates (figure 2.8). However, complicating the issue is that when comparing this region to *C. aurantiacus*, both species preserve an N-terminal Met and two conserved Asp residues near the N-terminus. Without high-resolution structural data, it might be possible to propose how the B800 is coordinated by cloning the N-terminus of the α-subunit from *R. casteholzii* into *Rhodobacter sphaeroides* and seeing if LH2 assembles in the mutant. Assuming this is possible, then a series of mutants could be generated where one or

several residues are replaced with residues not expected to participate in BChl coordination.

The kinetics of electron transfer from the cytochrome complex to P^+ is a ready measurement because the C-subunit co-purifies with the RC. The rates of electron donation to P^+ could only be measured electrometrically in membranes of *C. aurantiacus* and showed an increase in rate when one, two, three or four hemes were reduced prior to the flash (Mulkidjanian et al. 1994). With the RC from *R. castenholzii*, the rate of electron transfer from the cytochrome to P^+ can be measured optically. Additionally, the oxidation of cytochome can be matched by a reduction in P^+ at several different wavelengths to reinforce the measured kinetics.

Preliminary kinetics on the reduction of P^+ by cytochome have been determined on a flash photolysis spectrophotometer (XE920, Edinburgh Instruments Ltd) and will be described fully in a future publication (Niedzwiedzki et al. manuscript in preparation). Briefly, white light generated by a Xe-arc lamp was passed through interference filters (FWHM ~ 10-15 nm) at the desired measuring wavelength. Excitation flashes, at 90 ° relative to the measuring beam, were generated with a tunable laser (OPOTEK Inc.) with a pulse duration of about 6 ns . Triggering of the measuring light and excitation flash were controlled by the system software. Changes in transmission were monitored with a photomultiplier tube with a red sensitive photocathode. The signal was fed into an oscilloscope, digitized and sent to the computer.

Transient kinetics for the isolated *R. castenholzii* RC are shown in figure 5.1. For this measurement, the RCs were mixed with 50 μM TMPD and 1 mM ascorbate. As judge from the absorption spectrum of the RC sample before and after the kinetic measurement, three or four hemes were reduced prior to the flash (result not shown). Under these conditions, the lifetime for the bleaching of the cytochrome α-band and re-reduction of P^+ were similar, yielding 375 and 385 ± 10 ns, respectively. A minor component (20% amplitude) of ~1.5 μs was also observed to contribute to the bleaching of the cytochrome α-band. This component might result from the reduction of whichever heme re-reduced the heme that donated to P^+. A full redox titration of the cytochome region and monitoring by TA would be useful to fully delineate the kinetics of electron transfer in this complex.

The sample experimental setup was also used to monitor charge recombination of $P^+Q_A^-$ and $P^+Q_B^-$ in the *R. castenholzii* RC. To avoid re-reduction P^+ by the C-subunit, neither mediators nor ascorbate was added to the sample. The absorption spectrum of this sample under ambient conditions indicated that at most, one cytochrome was reduced (result not shown). Figure 5.2 displays representative kinetic traces monitored at 865 nm, the maximum of the Q_y transition of P, for RCs from *R. castenholzii* and *C. aurantiacus*. The data for *C. aurantiacus* could be fit to a single exponential of 45 ms and agree well with values published previously for $P^+Q_A^-$ recombination (Venturoli et al. 1991). Moreover this substantiates the finding that purified RCs from *C. aurantiacus* lack Q_B (Blankenship et al. 1983). For *R. castenholzii* the kinetics were fit to 42 ms (70% amplitude) and 1100 ms (30% amplitude) with the

longer component most likely reflecting charge recombination of the $P^+Q_B^-$ state. This indicates that the purified RC from *R. castenholzii* retains at least some Q_B during the purification process. Although the data were normalized for comparative purposes in figure 5.2, the magnitude of bleaching in *R. castenholzii* was about 30% less than that of *C. aurantiacus* despite having comparable OD at 865 nm. Two possible explanations for this observation could be the re-reduction of P^+ by cytochrome that is not observed on these times scales, or that some RCs lacked Q_A. The former seems plausible because of the co-purification of the RC with the C-subunit. Furthermore, the long lifetime component could be completely abolished with the addition of 4 mM *o*-phenanthroline, a known competitor for the Q_B site in *Chloroflexus* (Blankenship et al. 1983) and purple bacteria (Parson and Case 1970) (result not shown).

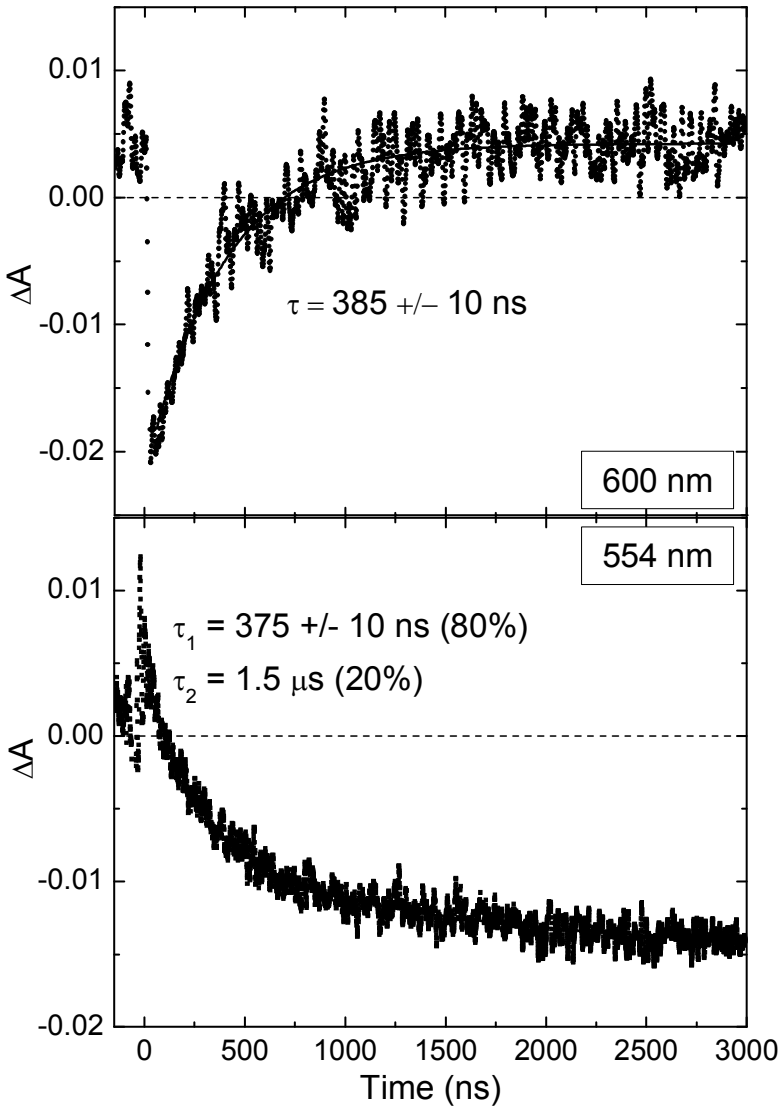

Figure 5.1. The rates of P^+ recovery (top panel) measured in the Q_x band (600 nm) and the bleaching of α-band of cytochrome *c*. The RC concentration was determined to be 2 μM, using an extinction coefficient of 135 mM^{-1} cm^{-1} at 865 nm. The RC were mixed in 0.02% β-DDM, 20 mM Tris, 200 mM NaCl and 50 μM TMPD and 1 mM ascorbate. Both the top and bottom panel were generated by averaging 20 traces at a frequency of 0.067 Hz.

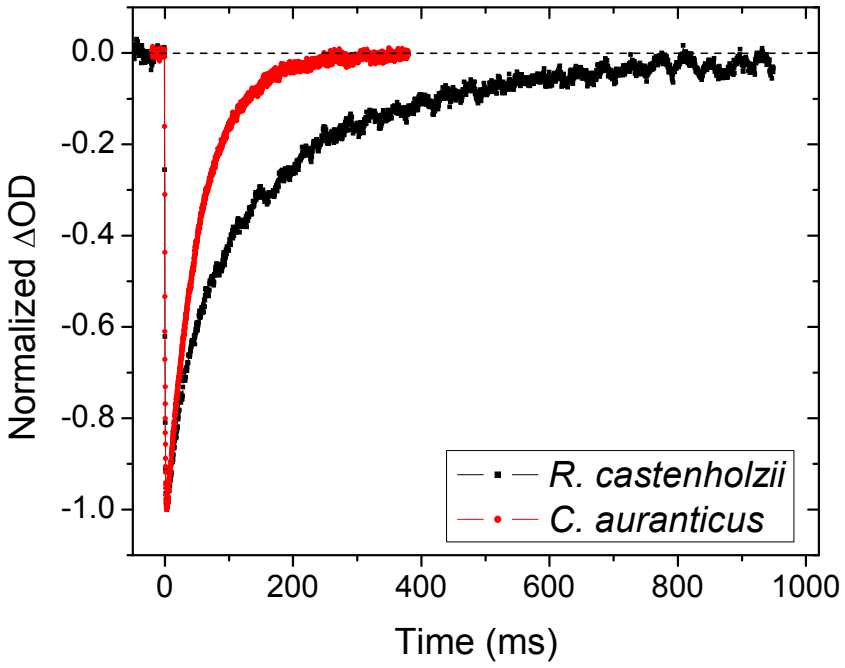

Figure 5.2. Kinetic traces monitored at 865 nm for *R. castenholzii* (black trace) and *C. aurantiacus* (red trace). Each trace was the average of 20 measurements at a rate of 0.067 Hz. The magnitude of bleaching was been normalized for comparative purposes. The kinetics for *C. aurantiacus* could be fit to a single exponential of 45 ms, while the kinetics of *R. castenholzii* required two exponentials, 42 and 1100 ms (70% and 30% amplitude respectively). Both samples contained ~2 μM, 0.02% βDDM, 20 mM Tris, 200 mM NaCl.

REFERENCES

Abdourakhmanov IA, Ganago AO, Erokhin YE, Solov'ev AA and Chugunov VA (1979) Orientation and linear dichroism of the reaction centers from *Rhodopseudomonas sphaeroides* R-26. Biochimica et Biophysica Acta 546: 183-186

Akihito I and Graham RF (2009) On the adequacy of the Redfield equation and related approaches to the study of quantum dynamics in electronic energy transfer. The Journal of Chemical Physics 130: 234110

Akiyama M, Nagashima KVP, Hara M, Wakao N, Tominaga K, Kise H and Kobayashi M (1999) Stoichiometries of LH1/RC determined by the molar ratio of BChl/BPhe analyzed by HPLC in seven species of purple bacteria containing LH1 only. Photomedicine Photobiol 21: 105-110

Andrew G, Alastair TG, Richard JC and Bruno R (2006) Carotenoid stoichiometry in the LH2 crystal: No spectral evidence for the presence of the second molecule in the α/β-apoprotein dimer. FEBS Letters 580: 3841-3844

Axelrod H, Miyashita O and Okamura M (2009) Structure and function of the cytochrome c2:reaction center complex from *Rhodobacter sphaeroides*. In: Hunter CN, Daldal F, Thurnauer MC and Beatty JT (eds) The Purple Phototrophic Bacteria, pp 323-336. Springer, Dordrecht

Bahatyrova S, Frese RN, van der Werf KO, Otto C, Hunter CN and Olsen JD (2004) Flexibility and size heterogeneity of the LH1 light harvesting complex revealed by atomic force microscopy. Journal of Biological Chemistry 279: 21327-21333

Becker M, Nagarajan V, Middendorf D, Parson WW, Martin JE and Blankenship RE (1991) Temperature dependence of the initial electron-transfer kinetics in photosynthetic reaction centers of *Chloroflexus aurantiacus*. Biochimica et Biophysica Acta 1057: 299-312

Bekker A, Holland HD, Wang PL, Rumble D, Stein HJ, Hannah JL, Coetzee LL and Beukes NJ (2004) Dating the rise of atmospheric oxygen. Nature 427: 117-120

Beljonne D, Curutchet C, Scholes GD and Silbey RJ (2009) Beyond förster resonance energy transfer in biological and nanoscale systems. The Journal of Physical Chemistry B 113: 6583-6599

Bergström H, Westerhuis WHJ, Sundström V, van Grondelle R, Niederman RA and Gillbro T (1988) Energy transfer within the isolated B875 light-harvesting

pigment-protein complex of *Rhodobacter sphaeroides* at 77 K studied by picosecond absorption spectroscopy. FEBS Letters 233: 12-16

Blankenship RE (1992) Origin and early evolution of photosynthesis. Photosynthesis Research 33: 91-111

Blankenship RE (2002) Molecular Mechanisms of Photosynthesis. Blackwell Scientific, Oxford

Blankenship RE, Feick R, Bruce BD, Kirmaier C, Holten D and Fuller RC (1983) Primary photochemistry in the facultative green photosynthetic bacterium *Chloroflexus aurantiacus*. Journal of Cellular Biochemistry 22: 251-261

Boonstra AF, Germeroth L and Boekema EJ (1994) Structure of the light harvesting antenna from *Rhodospirillum molischianum* studied by electron microscopy. Biochimica et Biophysica Acta 1184: 227-234

Boonstra AF, Visschers RW, Calkoen F, van Grondelle R, van Bruggen EFJ and Boekema EJ (1993) Structural characterization of the B800-850 and B875 light-harvesting antenna complexes from *Rhodobacter sphaeroides* by electron microscopy. Biochimica et Biophysica Acta 1142: 181-188

Borisov AY, Freiberg AM, Godik VI, Rebane KK and Timpmann KE (1985) Kinetics of picosecond bacteriochlorophyll luminescence in vivo as a function of the reaction center state. Biochimica et Biophysica Acta 807: 221-229

Breton J, Martin JL, Migus A, Antonetti A and Orszag A (1986) Femtosecond spectroscopy of excitation energy transfer and initial charge separation in the reaction center of the photosynthetic bacterium *Rhodopseudomonas viridis*. Proceedings of the National Academy of Sciences 83: 5121-5125

Breton J, Vermeglio A, Garrigos M and Paillotin G (1981) Orientation of the chromophores in the antenna system of *Rhodopseudomonas sphaeroides*. Balaban International Science Services, Philidelphia

Bruce BD, Fuller RC and Blankenship RE (1982) Primary photochemistry in the facultatively aerobic green photosynthetic bacterium *Chloroflexus aurantiacus*. Proceedings of the National Academy of Sciences of the United States of America 79: 6532-6536

Brune DC, King GH, Infosino A, Steiner T, Thewalt MLW and Blankenship RE (1987a) Antenna organization in green photosynthetic bacteria. 2. Excitation transfer in detached and membrane-bound chlorosomes from *Chloroflexus aurantiacus*. Biochemistry 26: 8652-8658

Brune DC, Nozawa T and Blankenship RE (1987b) Antenna organization in green photosynthetic bacteria. 1. Oligomeric bacteriochlorophyll c as a model for the 740 nm absorbing bacteriochlorophyll c in *Chloroflexus aurantiacus chlorosomes*. Biochemistry 26: 8644-8652

Bryant DA, Costas AMG, Maresca JA, Chew AGM, Klatt CG, Bateson MM, Tallon LJ, Hostetler J, Nelson WC, Heidelberg JF and Ward DM (2007) *Candidatus* Chloracidobacterium thermophilum: an aerobic phototrophic acidobacterium. Science 317: 523-526

Bylina EJ, Kirmaier C, McDowell L, Holten D and Youvan DC (1988) Influence of an amino-acid residue on the optical properties and electron transfer dynamics of a photosynthetic reaction centre complex. Nature 336: 182-184

Cherepy NJ, Holzwarth AR and Mathies RA (1995) Near-infrared resonance Raman spectra of *Chloroflexus aurantiacus* photosynthetic reaction centers. Biochemistry 34: 5288-5293

Chuang JI, Boxer SG, Holten D and Kirmaier C (2008) Temperature dependence of electron transfer to the M-side bacteriopheophytin in *Rhodobacter capsulatus* reaction centers. The Journal of Physical Chemistry B 112: 5487-5499

Clayton RK and Clayton BJ (1978) Molar extinction coefficients and other properties of an improved reaction center preparation from *Rhodopseudomonas viridis*. Biochimica et Biophysica Acta 501: 478-487

Cogdell RJ, Gall A and Köhler J (2006) The architecture and function of the light-harvesting apparatus of purple bacteria: from single molecules to in vivo membranes. Quarterly Reviews of Biophysics 39: 227-324

Cogdell RJ and Scheer H (1985) Circular dichroism of light-harvesting complexes from purple phototrophic bacteria. Photochemistry and Photobiology 42: 669-678

Collins AM, Xin Y and Blankenship RE (2009) Pigment organization in the photosynthetic apparatus of *Roseiflexus castenholzii*. Biochimica et Biophysica Acta 1787: 1050-1056

Connolly JS, A. JF and Samuel EB (1982) Fluorescence lifetimes of chlorophyll *a*: solvent, concentration and oxygen dependence. Photochemistry and Photobiology 36: 559-563

Cotton TM and Van Duyne RP (1981) Characterization of bacteriochlorophyll interactions in vitro by resonance Raman spectroscopy. Journal of the American Chemical Society 103: 6020-6026

Deisenhofer J, Epp O, Miki K, Huber R and Michel H (1985) Structure of the protein subunits in the photosynthetic reaction centre of *Rhodopseudomonas viridis* at 3A resolution. Nature 318: 618-624

Dolan PM, Miller D, Cogdell RJ, Birge RR and Frank HA (2001) Linear dichroism and the transition dipole moment orientation of the carotenoid in the LH2 antenna complex in membranes of *Rhodopseudomonas acidophila* strain 10050. The Journal of Physical Chemistry B 105: 12134-12142

Dracheva S, Williams JC, Van Driessche G, Van Beeumen JJ and Blankenship RE (1991) The primary structure of cytochrome c-554 from the green photosynthetic bacterium *Chloroflexus aurantiacus*. Biochemistry 30: 11451-11458

Dracheva SM, Drachev LA, Konstantinov AA, Semenov AY, Skulachev V, P. , Arutjunjan A, M., Shuvalov V, A. and Zaberezhnaya S, M. (1988) Electrogenic steps in the redox reactions catalyzed by photosynthetic reaction-centre complex from *Rhodopseudomonas viridis*. European Journal of Biochemistry 171: 253-264

Du M, Rosenthal SJ, Xie X, DiMagno TJ, Schmidt M, Hanson DK, Schiffer M, Norris JR and Fleming GR (1992) Femtosecond spontaneous-emission studies of reaction centers from photosynthetic bacteria. Proceedings of the National Academy of Sciences of the United States of America 89: 8517-8521

Elstner EF (1982) Oxygen activation and oxygen toxicity. Annual Review of Plant Physiology 33: 73-96

Fathir I, Ashikaga M, Tanaka K, Katano T, Nirasawa T, Kobayashi M, Wang Z-Y and Nozawa T (1998) Biochemical and spectral characterization of the core light harvesting complex 1 (LH1) from the thermophilic purple sulfur bacterium *Chromatium tepidum*. Photosynthesis Research 58: 193-202

Feick R, Shiozawa JA and Ertlmaier A (1995) Biochemical and spectroscopic properties of the reaction center of the green filamentous bacterium, *Chloroflexus aurantiacus*. In: Blankenship RE, Madigan, M.T. and Bauer (ed) Anoxygenic Photosynthetic BacteriaKluwer Academic Publishers, Dordrecht

Feick RG, Fitzpatrick M and Fuller RC (1982) Isolation and characterization of cytoplasmic membranes and chlorosomes from the green bacterium *Chloroflexus aurantiacus*. J. Bacteriol. 150: 905-915

Finkele U, Lauterwasser C, Zinth W, Gray KA and Oesterhelt D (1990) Role of tyrosine M210 in the initial charge separation of reaction centers of *Rhodobacter sphaeroides*. Biochemistry 29: 8517-8521

Förster T (1948) Zwischenmolekulare energiewanderung und fluoreszenz. Annalen der Physik 437: 55-75

Francke C and Amesz J (1995) The size of the photosynthetic unit in purple bacteria. Photosynthesis Research 46: 347-352

Freeman JC and Blankenship RE (1990) Isolation and characterization of the membrane-bound cytochrome c-554 from the thermophilic green photosynthetic bacterium *Chloroflexus aurantiacus*. Photosynthesis Research 23: 29-38

Freiberg A and Timpmann K (1992) Picosecond fluorescence spectroscope of light-harvesting antenna complexes from *Rhodospirillum rubrum* in the 300-4 K temperature range. Comparison with the data on chromatophores. Journal of Photochemistry and Photobiology B: Biology 15: 151-158

Frigaard N-U and Bryant D (2006) Chlorosomes: antenna organelles in photosynthetic green bacteria. In: Shively JM (ed) Complex Intracellular Structures in Prokaryotes, pp 79-114. Springer Berlin Heidelberg

Frigaard N-U, Larsen K, L. and Cox R, P. (1996) Spectrochromatography of photosynthetic pigments as a fingerprinting technique for microbial phototrophs. FEMS Microbiology Ecology 20: 69-77

Frigaard N-U, Li H, Milks KJ and Bryant DA (2004) Nine mutants of *Chlorobium tepidum* each unable to synthesize a different chlorosome protein still assemble functional chlorosomes. Journal of Bacteriology 186: 646-653

Gardiner AT, Cogdell RJ and Takaichi S (1993) The effect of growth conditions on the light-harvesting apparatus in *Rhodopseudomonas acidophila*. Photosynthesis Research 38: 159-167

Georgakopoulou S, Cogdell RJ, van Grondelle R and van Amerongen H (2003) Linear-dichroism measurements on the LH2 antenna complex of *Rhodopseudomonas acidophila* strain 10050 show that the transition dipole moment of the carotenoid rhodopin glucoside is not collinear with the long molecular axis. The Journal of Physical Chemistry B 107: 655-658

Georgakopoulou S, Frese RN, Johnson E, Koolhaas C, Cogdell RJ, van Grondelle R and van der Zwan G (2002) Absorption and CD spectroscopy and modeling of various LH2 complexes from purple bacteria. Biophys. J. 82: 2184-2197

Germeroth L, Lottspeich F, Robert B and Michel H (1993) Unexpected similarities of the B800-850 light-harvesting complex from *Rhodospirillum molischianum* to the B870 light-harvesting complexes from other purple photosynthetic bacteria. Biochemistry 32: 5615-5621

Goedheer JC (1966) Visible absorption and fluorescence of chlorophyll and its aggregates in solution. In: Vernon LP and Seely GR (eds) The Chlorophylls, pp 147-184. Academic Press, New York

Golecki JR and Oelze J (1987) Quantitative relationship between bacteriochlorophyll content, cytoplasmic membrane structure and chlorosome size in *Chloroflexus aurantiacus*. Archives of Microbiology 148: 236-241

Gonçalves RP, Bernadac A, Sturgis JN and Scheuring S (2005) Architecture of the native photosynthetic apparatus of *Phaeospirillum molischianum*. Journal of Structural Biology 152: 221-228

Griebenow K, Müller MG and Holzwarth AR (1991) Pigment organization and energy transfer in green bacteria. 3. Picosecond energy transfer kinetics within the B806-866 bacteriochlorophyll a antenna complex isolated from *Chloroflexus aurantiacus*. Biochimica et Biophysica Acta 1059: 226-232

Hamm P, Gray KA, Oesterhelt D, Feick R, Scheer H and Zinth W (1993) Subpicosecond emission studies of bacterial reaction centers. Biochimica et Biophysica Acta 1142: 99-105

Hanada S, Hiraishi A, Shimada K and Matsuura K (1995) *Chloroflexus aggregans* sp. nov., a Filamentous Phototrophic Bacterium Which Forms Dense Cell Aggregates by Active Gliding Movement. International Journal of Systematic and Evolutionary Microbiology 45: 676-681

Hanada S and Pierson B (2006) The family Chloroflexaceae. In: Dworkin M, Falkow S, Rosenberg E, K-H S and E S (eds) The Prokaryotes, pp 815-842. Springer New York

Hanada S, Takaichi S, Matsuura K and Nakamura K (2002) *Roseiflexus castenholzii* gen. nov., sp. nov., a thermophilic, filamentous, photosynthetic bacterium that lacks chlorosomes. Int J Syst Evol Microbiol 52: 187-193

Holzapfel W, Finkele U, Kaiser W, Oesterhelt D, Scheer H, Stilz HU and Zinth W (1990) Initial electron-transfer in the reaction center from *Rhodobacter sphaeroides*. Proceedings of the National Academy of Sciences 87: 5168-5172

Hunter CN (1995) Genetic manipulation of the antenna complexes of purple bacteria. In: Blankenship RE, Madigan MT and Bauer CE (eds) Anoxygenic Photosynthetic Bacteria, pp 473-501. Kluwer Academic Publishers, Dordrecht

Hunter CN, Daldal F, Thurnauer MC and Beatty JT (2008) The Purple Phototrophic Bacteria. In: Govindjee (ed) Advamces in Photosynthesis and Respiration. Kluwer Academic Publishers, Dordrecht

Itoh S, Uzumaki T, Takaichi S, Iwaki M, Kumazaki S, Itoh K and Mino H (2008) Unidirectional electron transfer in chlorophyll *d*-containing photosystem I reaction center complex of *Acaryochloris marina*. In: Allen J, Gantt E, Golbeck J and Osmond B (eds) Photosynthesis: Energy from the Sun, pp 93-96. Springer Netherlands

Ivancich A, Feick R, Ertlmaier A and Mattioli TA (1996) Structure and protein binding interactions of the primary donor of the *Chloroflexus aurantiacus* reaction center. Biochemistry 35: 6126-6135

Jamieson SJ, Wang P, Qian P, Kirkland JY, Conroy MJ, Hunter CN and Bullough PA (2002) Projection structure of the photosynthetic reaction centre-antenna complex of *Rhodospirillum rubrum* at 8.5 Å resolution. EMBO Journal 21: 3927-3935

Katilius E, Turanchik T, Lin S, Taguchi AKW and Woodbury NW (1999) B-Side electron transfer in a *Rhodobacter sphaeroides* reaction center mutant in which the B-Side monomer bacteriochlorophyll is replaced with bacteriopheophytin. The Journal of Physical Chemistry B 103: 7386-7389

Keppen OI, Tourova TP, Kuznetsov BB, Ivanovsky RN and Gorlenko VM (2000) Proposal of *Oscillochloridaceae* fam. nov. on the basis of a phylogenetic analysis of the filamentous anoxygenic phototrophic bacteria, and emended description of *Oscillochloris* and *Oscillochloris trichoides* in comparison with further new isolates. Int J Syst Evol Microbiol 50: 1529-1537

Kirmaier C, Blankenship RE and Holten D (1986) Formation and decay of radical-pair state $P^{+}I^{-}$ in *Chloroflexus aurantiacus* reaction centers. Biochimica et Biophysica Acta 850: 275-285

Kirmaier C and Holten D (1987) Primary photochemistry of reaction centers from the photosynthetic purple bacteria. Photosynthesis Research 13: 225-260

Kirmaier C and Holten D (1991) An assessment of the mechanism of initial electron transfer in bacterial reaction centers. Biochemistry 30: 609-613

Kirmaier C, Holten D and Parson WW (1985) Temperature and detection-wavelength dependence of the picosecond electron-transfer kinetics measured in *Rhodopseudomonas sphaeroides* reaction centers. Resolution of new spectral and kinetic components in the primary charge-separation process. Biochimica et Biophysica Acta 810: 33-48

Klappenbach J and Pierson B (2004) Phylogenetic and physiological characterization of a filamentous anoxygenic photoautotrophic bacterium '*Candidatus* Chlorothrix halophila' gen. nov., sp. nov., recovered from hypersaline microbial mats. Archives of Microbiology 181: 17-25

Koepke J, Hu X, Muenke C, Schulten K and Michel H (1996) The crystal structure of the light-harvesting complex II (B800-850) from *Rhodospirillum molischianum*. Structure 4: 581-597

Koolhaas MHC, van der Zwan G, Frese RN and van Grondelle R (1997) Red shift of the zero crossing in the CD spectra of the LH2 antenna complex of *Rhodopseudomonas acidophila*: a structure-based study. The Journal of Physical Chemistry B 101: 7262-7270

Kramer HJM, Pennoyer JD, Van Grondelle R, Westerhuis WHJ, Niederman RA and Amesz J (1984a) Low-temperature optical properties and pigment organization of the B875 light-harvesting bacteriochlorophyll-protein complex of purple photosynthetic bacteria. Biochimica et Biophysica Acta 767: 335-344

Kramer HJM, van Grondelle R, Hunter CN, Westerhuis WHJ and Amesz J (1984b) Pigment organization of the B800-850 antenna complex of *Rhodopseudomonas sphaeroides*. Biochimica et Biophysica Acta 765: 156-165

Lakowicz JR (1983) Principle of fluorescence spectroscopy. Plenum Press, New York

Lang HP and Hunter CN (1994) The relationship between carotenoid biosynthesis and the assembly of the light-harvesting LH2 complex in *Rhodobacter sphaeroides*. Biochemical Journal 298: 197-205

Lin X, Murchison HA, Nagarajan V, Parson WW, Allen JP and Williams JC (1994) Specific alteration of the oxidation potential of the electron donor in reaction centers from *Rhodobacter sphaeroides*. Proceedings of the National Academy of Sciences of the United States of America 91: 10265-10269

Marcus RA (1964) Chemical and electrochemical electron-transfer theory. Annual Review of Physical Chemistry 15: 155-196

McDermott G, Prince SM, Freer AA, Hawthornthwaite-Lawless AM, Papiz MZ, Cogdell RJ and Isaacs NW (1995) Crystal structure of an integral membrane light-harvesting complex from photosynthetic bacteria. Nature 374: 517-521

Montaño GA, Bowen BP, LaBelle JT, Woodbury NW, Pizziconi VB and Blankenship RE (2003a) Characterization of *Chlorobium tepidum* chlorosomes: A calculation of bacteriochlorophyll *c* per chlorosome and oligomer modeling. Biophysical Journal 85: 2560-2565

Montaño GA, Wu H-M, Lin S, Brune DC and Blankenship RE (2003b) Isolation and Characterization of the B798 Light-Harvesting Baseplate from the Chlorosomes of *Chloroflexus aurantiacus* Biochemistry 42: 10246-10251

Montaño GA, Xin Y, Lin S and Blankenship RE (2004) Carotenoid and bacteriochlorophyll energy transfer in the B808-866 complex from *Chloroflexus aurantiacus*. The Journal of Physical Chemistry B 108: 10607-10611

Müh F, Schulz C, Schlodder E, Jones MR, Rautter J, Kuhn M and Lubitz W (1998) Effects of zwitterionic detergents on the electronic structure of the primary donor and the charge recombination kinetics of P+QA− in native and mutant reaction centers from *Rhodobacter sphaeroides*. Photosynthesis Research 55: 199-205

Mulkidjanian A, Venturoli G, Hochkoeppler A, Zannoni D, Melandri B and Drachev L (1994) Photosynthetic electrogenic events in native membranes of *Chloroflexus aurantiacus*. Flash-induced charge displacements within the reaction center-cytochromec554 complex. Photosynthesis Research 41: 135-143

Nagarajan V, Parson WW, Gaul D and Schenck C (1990) Effect of specific mutations of tyrosine-(M)210 on the primary photosynthetic electron-transfer process in *Rhodobacter sphaeroides*. Proceedings of the National Academy of Sciences of the United States of America 87: 7888-7892

Nitschke W and Dracheva S (2004) Reaction Center Associated Cytochromes. In: Amezs J, Barber J, Blankenship RE, Norio M and Ort DR (eds) Anoxygenic Photosynthetic Bacteria, pp 775-805.

Novoderezhkin V and Fetisova Z (1999) Exciton delocalization in the B808-866 antenna of the green bacterium *Chloroflexus aurantiacus* as revealed by ultrafast pump-probe spectroscopy. Biophys. J. 77: 424-430

Novoderezhkin VI, Taisova AS, Fetisova ZG, Blankenship RE, Savikhin S, Buck DR and Struve WS (1998) Energy transfers in the B808-866 antenna from the green bacterium *Chloroflexus aurantiacus*. Biophysical Journal 74: 2069-2075

Oelze J (1985) Analysis of bacteriochlorophylls. Methods in Microbiology Volume 18: 257-284

Ogrodnik A, Volk M, Letterer R, Feick R and Michel-Beyerle ME (1988) Determination of free energies in reaction centers of *Rb. sphaeroides*. Biochimica et Biophysica Acta 936: 361-371

Olsen JD, Sockalingum GD, Robert B and Hunter CN (1994) Modification of a hydrogen bond to a bacteriochlorophyll a molecule in the light-harvesting 1 antenna of *Rhodobacter sphaeroides*. Proc. Natl. Acad. Sci. U.S.A. 91: 7124-7128

Olsen JD, Sturgis JN, Westerhuis WHJ, Fowler GJS, Hunter CN and Robert B (1997) Site-directed modification of the ligands to the bacteriochlorophylls of the light-harvesting LH1 and LH2 complexes of *Rhodobacter sphaeroides*. Biochemistry 36: 12625-12632

Ovchinnikov YA, Abdulaev NG, Shmuckler BE, Zargarov AA, Kutuzov MA, Telezhinskaya IN, Levina NB and Zolotarev AS (1988) Photosynthetic reaction centre of *Chloroflexus aurantiacus* Primary structure of M-subunit. FEBS Letters 232: 364-368

Oyaizu H, DeBrunner-Vossbrinck B, Mandelco L, Studier J and Woese C (1987) The green non-sulfur bacteria: a deep branching in the eubacterial line of descent. Systematic and Applied Microbiology 9: 47-53

Palaniappan V, Martin PC, Chynwat V, Frank HA and Bocian DF (1993) Comprehensive resonance Raman study of photosynthetic reaction centers from *Rhodobacter sphaeroides*. Implications for pigment structure and pigment-protein interactions. Journal of the American Chemical Society 115: 12035-12049

Papiz MZ, Prince SM, Howard T, Cogdell RJ and Isaacs NW (2003) The structure and thermal motion of the B800-850 LH2 complex from *Rps. acidophila* at 2.0 Å resolution and 100 K: new structural features and functionally relevant motions. Journal of Molecular Biology 326: 1523-1538

Parson WW and Case GD (1970) In *Chromatium*, a single photochemical reaction center oxidizes both cytochrome C552 and cytochrome C555. Biochimica et Biophysica Acta 205: 232-245

Parson WW, Chu Z-T and Warshel A (1990) Electrostatic control of charge separation in bacterial photosynthesis. Biochimica et Biophysica Acta 1017: 251-272

Picorel R, Belanger G and Gingras G (1983) Antenna holochrome B880 of *Rhodospirillum rubrum* S1. Pigment, phospholipid, and polypeptide composition. Biochemistry 22: 2491-2497

Pierson BK and Castenholz RW (1974) A phototrophic gliding filamentous bacterium of hot springs, *Chloroflexus aurantiacus*, gen. and sp. nov. Archives of Microbiology 100: 5-24

Pierson BK and Thornber JP (1983) Isolation and spectral characterization of photochemical reaction centers from the thermophilic green bacterium *Chloroflexus aurantiacus* strain J-10-f1. Proceedings of the National Academy of Sciences of the United States of America 80: 80-84

Psencik J, Collins AM, Liljeroos L, Torkkeli M, Laurinmaki P, Ansink HM, Ikonen TP, Serimaa RE, Blankenship RE, Tuma R and Butcher SJ (2009) Structure of chlorosomes from the green filamentous bacterium *Chloroflexus aurantiacus*. Journal of Bacteriology 191: 6701-6708

Qian P, Yagura T, Koyama Y and Cogdell RJ (2000) Isolation and purification of the reaction center (RC) and the core (RC-LH1) complex from *Rhodobium marinum*: the LH1 ring of the detergent-solubilized core complex contains 32 bacteriochlorophylls. Plant Cell Physiology 41: 1347-1353

Robert B (2009) Resonance Raman spectroscopy. Photosynthesis Research 101: 147-155

Robert B and Lutz M (1985) Structures of antenna complexes of several *Rhodospirillales* from their resonance Raman spectra. Biochimica et Biophysica Acta 807: 10-23

Roszak AW, Howard TD, Southall J, Gardiner AT, Law CJ, Isaacs NW and Cogdell RJ (2003) Crystal structure of the RC-LH1 core complex from *Rhodopseudomonas palustris*. Science 302: 1969-1972

Sadekar S, Raymond J and Blankenship RE (2006) Conservation of distantly related membrane proteins: photosynthetic reaction centers share a common structural core. Mol Biol Evol 23: 2001-2007

Sauer K, Cogdell RJ, Prince SM, Freer A, Isaacs NW and Hugo S (1996) Structure-based calculations of the optical spectra of the LH2 bacteriochlorophyll-protein

complex from *Rhodopseudomonas acidophila*. Photochemistry and Photobiology 64: 564-576

Savikhin S, Buck DR, Struve WS, Blankenship RE, Taisova AS, Novoderezhkin VI and Fetisova ZG (1998) Excitation delocalization in the bacteriochlorophyll c antenna of the green bacterium *Chloroflexus aurantiacus* as revealed by ultrafast pump-probe spectroscopy. FEBS Letters 430: 323-326

Schägger H and von Jagow G (1987) Tricine-sodium dodecyl sulfate-polyacrylamide gel electrophoresis for the separation of proteins in the range from 1 to 100 kDa. Analytical Biochemistry 166: 368-379

Schägger H and von Jagow G (1991) Blue native electrophoresis for isolation of membrane protein complexes in enzymatically active form. Analytical Biochemistry 199: 223-231

Scheer H (2006) An overview of chlorophylls and bacteriochlorophylls: biochemistry, biophysics, functions and applications. In: Grimm B, Porra RJ, Rüdiger W and Scheer H (eds) Chlorophylls and Bacteriochlorophylls, pp 1-26. Springer Netherlands, Dordrecht

Schenck CC, Blankenship RE and Parson WW (1982) Radical-pair decay kinetics, triplet yields and delayed fluorescence from bacterial reaction centers. Biochimica et Biophysica Acta 680: 44-59

Scheuring S (2006) AFM studies of the supramolecular assembly of bacterial photosynthetic core-complexes. Current Opinion in Chemical Biology 10: 387-393

Schmidt K (1980) A comparative study on the composition of chlorosomes (Chlorobium vesicles) and cytoplasmic membranes from *Chloroflexus aurantiacus* strain Ok-70-fl and *Chlorobium limicola* f. *thiosulfatophilum* strain 6230. Archives of Microbiology 124: 21-31

Shiozawa JA, Lottspeich F and Feick R (1987) The photochemical reaction center of *Chloroflexus aurantiacus* is composed of two structurally similar polypeptides. European Journal of Biochemistry 167: 595-600

Shuvalov VA, Shkuropatov AY, Kulakova SM, Ismailov MA and Shkuropatova VA (1986) Photoreactions of bacteriopheophytins and bacteriochlorophylls in reaction centers of *Rhodopseudomonas sphaeroides* and *Chloroflexus aurantiacus*. Biochimica et Biophysica Acta 849: 337-346

Straley SC, Parson WW, Mauzerall DC and Clayton RK (1973) Pigment content and molar extinction coefficients of photochemical reaction centers from *Rhodopseudomonas spheroides*. Biochimica et Biophysica Acta 305: 597-609

Stryer L (1978) Fluorescence energy transfer as a spectroscopic ruler. Annual Review of Biochemistry 47: 819-846

Sturgis JN, Olsen JD, Robert B and Hunter CN (1997) Functions of conserved tryptophan residues of the core light-harvesting complex of *Rhodobacter sphaeroides*. Biochemistry 36: 2772-2778

Suzuki H, Hirano Y, Kimura Y, Takaichi S, Kobayashi M, Miki K and Wang Z-Y (2007) Purification, characterization and crystallization of the core complex from thermophilic purple sulfur bacterium *Thermochromatium tepidum*. Biochimica et Biophysica Acta 1767: 1057-1063

Takaichi S, Maoka T, Yamada M, Matsuura K, Haikawa Y and Hanada S (2001) Absence of carotenes and presence of a tertiary methoxy group in a carotenoid from a thermophilic filamentous photosynthetic bacterium *Roseiflexus castenholzii*. Plant Cell Physiol. 42: 1355-1362

Thornber JP and Olson JM (1971) Chlorophyll-proteins and reaction center preparations from photosynthetic bacteria, algae and higher plants. Photochemistry and Photobiology 14: 329-341

Timmins PA, Leonhard M, Weltzien HU, Wacker T and Welte W (1988) A physical characterization of some detergents of potential use for membrane protein crystallization. FEBS Letters 238: 361-368

Van Amerongen H, Valkunas L and R VG (2000) Photosynthetic Excitons. World Scientific, Singapore

van Heel M, Harauz G, Orlova EV, Schmidt R and Schatz M (1996) A new generation of the IMAGIC image processing system. Journal of Structural Biology 116: 17-24

van Heel M and Keegstra W (1981) IMAGIC: A fast, flexible and friendly image analysis software system. Ultramicroscopy 7: 113-129

van Vliet P, Zannoni D, Nitschke W and Rutherford WA (1991) Membrane-bound cytochromes in *Chloroflexus aurantiacus* studied by EPR. European Journal of Biochemistry 199: 317-323

Vasmel H, Dorssen RJ, Vos GJ and Amesz J (1986) Pigment organization and energy transfer in the green photosynthetic bacterium *Chloroflexus aurantiacus*. Photosynthesis Research 7: 281-294

Vasmel H, Meiburg RF, Kramer HJM, de Vos LJ and Amesz J (1983) Optical properties of the photosynthetic reaction center of *Chloroflexus aurantiacus* at low temperature. Biochimica et Biophysica Acta 724: 333-339

Venturoli G, Trotta M, Feick R, Melandri AB and Zannoni D (1991) Temperature dependence of charge recombination from the $P^+Q_A^-$, $P^+Q_B^-$ states in photosynthetic reaction centers isolated from the thermophilic bacterium *Chloroflexus aurantiacus*. European Journal of Biochemistry 202: 625-634

Vermeglio A and Clayton RK (1977) Kinetics of electron transfer between the primary and the secondary electron acceptor in reaction centers from *Rhodopseudomonas sphaeroides*. Biochimica et Biophysica Acta 461: 159-165

Visschers RW, Germeroth L, Michel H, Monshouwer R and van Grondelle R (1995) Spectroscopic properties of the light-harvesting complexes from *Rhodospirillum molischianum*. Biochimica et Biophysica Acta 1230: 147-154

Wachtveitl J and Zinth W (2006) Electron transfer in photosynthetic reaction centers. In: Grimm B, Porra R, Rüdiger W and Scheer H (eds) Chlorophylls and Bacteriochlorophylls, pp 445-459. Springer Netherlands, Dordrecht

Watanabe T and Kobayashi M (1991) Electrochemistry of chlorophylls. In: Scheer H (ed) Chlorophylls,, pp 287-315. CRC Press, Boca Raton

Watanabe Y, Feick RG and Shiozawa JA (1995) Cloning and sequencing of the genes encoding the light-harvesting B806-866 polypeptides and initial studies on the transcriptional organization of puf2B, puf2A and puf2C in *Chloroflexus aurantiacus*. Archives of Microbiology 163: 124-130

Wechsler T, Brunisholz R, Suter F, Fuller RC and Zuber H (1985) The complete amino acid sequence of a bacteriochlorophyll *a* binding polypeptide isolated from the cytoplasmic membrane of the green photosynthetic bacterium *Chloroflexus aurantiacus*. FEBS Letters 191: 34-38

Wechsler TD, Brunisholz RA, Frank G, Suter F and Zuber H (1987) The complete amino acid sequence of the antenna polypeptide B806-866-[beta] from the cytoplasmic membrane of the green bacterium *Chloroflexus auranliacus*. FEBS Letters 210: 189-194

Weller R, Bateson MM, Heimbuch BK, Kopczynski ED and Ward DM (1992) Uncultivated cyanobacteria, *Chloroflexus*-like inhabitants, and spirochete-like inhabitants of a hot spring microbial mat. Appl. Environ. Microbiol. 58: 3964-3969

Westerhuis WHJ, Sturgis JN, Ratcliffe EC, Hunter CN and Niederman RA (2002) Isolation, size estimates, and spectral heterogeneity of an oligomeric series of light-harvesting 1 complexes from *Rhodobacter sphaeroides*. Biochemistry 41: 8698-8707

Xin Y, Lin S and Blankenship RE (2007) Femtosecond spectroscopy of the primary charge separation in reaction centers of *Chloroflexus aurantiacus* with selective excitation in the Q_Y and Soret bands. Journal of Physical Chemistry A 111: 9367-9373

Xin Y, Lin S, Montaño G and Blankenship R (2005) Purification and characterization of the B808–866 light-harvesting complex from green filamentous bacterium *Chloroflexus aurantiacus*. Photosynthesis Research 86: 155-163

Yamada M, Zhang H, Hanada S, Nagashima KVP, Shimada K and Matsuura K (2005) Structural and spectroscopic properties of a reaction center complex from the chlorosome-lacking filamentous anoxygenic phototrophic bacterium *Roseiflexus castenholzii*. Journal of Bacteriology 187: 1702-1709

Yang SI, Li J, Cho HS, Kim D, Bocian DF, Holten D and Lindsey JS (2000) Synthesis and excited-state photodynamics of phenylethyne-linked porphyrin-phthalocyanine dyads. Journal of Materials Chemistry 10: 283-296

Young A and Britton G (1993) Carotenoids in Photosynthesis. Chapman and Hall, London, UK

Youvan DC, Alberti M, Begusch H, Bylina EJ and Hearst JE (1984) Reaction center and light-harvesting I genes from *Rhodopseudomonas capsulata*. Proceedings of the National Academy of Sciences 81: 189-192

Zhang FG, Gillbro T, van Grondelle R and Sundström V (1992) Dynamics of energy transfer and trapping in the light-harvesting antenna of *Rhodopseudomonas viridis*. Biophysical Journal 61: 694-703

Zuber H and Cogdell R (2004) Structure and organization of purple bacterial antenna complexes. In: Blankenship RE, Madigan, M.T. and Bauer, C.E. (ed) Anoxygenic Photosynthetic Bacteria, pp 315-348. Kluwer Academic Publishers, Dordrecht

APPENDIX A Curriculum Vitae

Aaron M. Collins

Department of Chemistry
Washington University in St. Louis
St. Louis, MO 63130

Phone: 314-935-9162 (office)
314-591-6740 (cell) Email: amcollin@artsci.wustl.edu

EDUCATION

2005 -	**Ph.D. Candidate, Department of Chemistry,** **Washington University in St. Louis** Thesis: The primary Photochemistry and Light-Harvesting in *Roseiflexus castenholzii* Advisor: Robert E. Blankenship Prospective date of completion May: 2010
2005 - 2008	**A.M. In Chemistry, Department of Chemistry,** **Washington University in St. Louis**
2001 – 2005	**B.S. in Chemistry, University of Connecticut** **(American Chemical Society Accredited)** **B.S. in Biophysics, University of Connecticut** *magna cum laude* Thesis: Construction of a Wavelength Resolved Surface Plasmon Resonance Spectrometer and its Use to Measure Immobilized Protein Stability on a Surface. Advisor: C. Vijaya Kumar

---

RESEARCH INTERESTS

Light-harvesting and energy transfer in anoxygenic photosynthetic bacteria.
Spectroscopic analysis of reconstituted antenna pigment/protein complexes

TEACHING EXPERIENCE

Lecturer, Washington University in St. Louis, (Summer semester, 2009)
Introduction to General Chemistry
- Prepare lectures, assignments, quizzes and exams

Graduate Student Mentor, Washington University in St. Louis (Summer, 2009)
International Genetically Engineered Machine competition (iGEM)

Teaching Assistant, Washington University in St. Louis, (Spring semester, 2007 and 2008)
General Chemistry II – recitation
- Preparation of recitation lectures, correction of assignments, leading of review sessions for exams

Teaching Assistant, Arizona State University, (Spring semester, 2006)
Chemistry and Society
- Preparation of lectures, evaluation of assignments, construction of new laboratory experiments

Teaching Assistant, Arizona State University, (Fall semester, 2005)
General Chemistry Laboratory
- Preparing recitation lectures, supervision experiments, correction of class assignments and reports

HONORS AND AWARDS

Photosynthetic Antenna Research Center (PARC) Scientific Exchange grant ($2500)
Best Graduate Student Presentation - 34nd Midwestern Photosynthesis Conference, Turkey Run, IN, 2008 ($100)
Graduate Assistance in Areas of National Need (GAANN) Fellowship - 2007 ($30,000)
Outstanding Graduate Teaching Award – Chemistry Department, Washington University in St. Louis, 2007 ($100)
Best Student Poster – 32nd Midwestern Photosynthesis Conference, Turkey Run, IN, 2006
Washington University in St. Louis Graduate Academic Scholarship, 2006-2010
ASU Graduate Academic Scholarship, 2005-2006
ASU Graduate Student Award ($3,000)

SOCIETIES

International Society of Photosynthesis Research
American Association for the Advancement of Science

PEER-REVIEWED PUBLICATIONS

van de Meene AML, Olson TL, **Collins AM** and Blankenship RE (2007) Initial Characterization of the Photosynthetic Apparatus of "*Candidatus* Chlorothrix halophila": A Filamentous, Anoxygenic Photoautotroph. *J. Bacteriology* 189: 4196-4203.

Collins AM, Xin Y, and Blankenship RE (2009) Pigment organization in the photosynthetic apparatus of *Roseiflexus castenholzii*. *Biochim. Biophys. Acta.* 1787, 1050-1056.

Psencik J, **Collins AM**, Liljeroos L, Torkkeli M, Laurinmaki P, Ansink HM, Ikonen TP, Serimaa RE, Blankenship RE, Tuma R, and Butcher SJ (2009) Structure of the chlorosomes from green filamentous bacterium *Chloroflexus aurantiacus*. *J. Bacteriology*, 191, 6701-6708

Moulisová V, Luer L, Hoseinkhani S, Brotosudarmo THP, **Collins AM**, Lanzani G, Blankenship RE, and Cogdell RJ (2009), Low light adaptation: Energy transfer processes in different types of light harvesting complexes from *Rhodopseudomonas palustris*. *Biophys. J*. 97, 3019–3028

Modesto-Lopez LB, Thimsen EJ, **Collins AM**, Blankenship RE, and Biswas P, (2010) Electrospray-assisted characterization and deposition of chlorosomes to fabricate a light-harvesting nano-bio device. *Energy Environ. Sci*., 3, 216–222

Collins AM, Kevin E. Redding KE and Blankenship RE (2009) Fluorescence Modulation in *Heliobacterium modesticaldum.* Manuscript accepted. *Photosyn. Res.*

Collins AM, Kirmaier C, Holten D, Blankenship RE (2009) Reaction Center kinetics and energetics in *Roseiflexus castenholzii.* Manuscript in Preparation.

Niedzwiedzki DM, **Collins AM**, Lafountain AM, Enriquez MM, Frank HA, Blankenship RE, (2009), Spectroscopic Studies of Carotenoid-to-Bacteriochlorophyll

Energy Transfer in LHRC Photosynthetic Complex from *Roseiflexus castenholzii*. Manuscript in Review

PRESENTATIONS

2010

Aaron M. Collins, Qun Tang, Pu Qian, C. Neil Hunter, David F. Bocian, and Robert E. Blankenship [Talk]. The Light-Harvesting Architecture of *Roseiflexus castenholzii*, PARC Seminar at Washington University. St. Louis, MO, USA

2009

Aaron M. Collins, Christine Kirmaier, Qun Tang, David F. Bocian, Dewey Holten, and Robert E. Blankenship [poster]. Light Harvesting and Electron Transfer in *Roseiflexus castenholzii*, 35th Midwestern Photosynthesis Meeting, Turkey Run State Park, Marshall, IN, USA

Aaron M. Collins, Christine Kirmaier, Dewey Holten and Robert E. Blankenship [Poster] Reaction Center Kinetics and Energetics in *Roseiflexus castenholzii*. Gordon Research Conference on Photosynthesis, Bryant University, Smithfield, RI, USA

2008

Aaron M. Collins, Yueyong Xin, Robert E. Blankenship [Talk] Characterization of the Core Complex from *Roseiflexus Castenholzii*, 34th Midwestern Photosynthesis Meeting, Turkey Run State, Park, Marshall, IN, USA

Aaron M. Collins, Yueyong Xin, Robert E. Blankenship [Poster] Antenna Organization of the Chlorosome-lacking Filamentous Anoxygenic Phototroph *Roseiflexus castenholzii*, Gordon Research Conference on Photosynthesis, Mount Holyoke College, South Hadley, MA, USA

Aaron M. Collins and Robert E. Blankenship [Talk] Departmental Seminar - Theory and Examples of use of Circular Dichroism, Bioforum, Washington University in St. Louis, St. Louis, MO, USA

Aaron M. Collins and Robert E. Blankenship [Talk] Antenna Organization and Electron Transfer in Heliobacteria, Mini-symposium in honor of Howard Gest, Washington University, St. Louis, MO, USA

2007

Aaron M. Collins and Robert E. Blankenship [Poster]
Variable Fluorescence in Heliobacteria, 33th Midwestern Photosynthesis Meeting, Turkey Run State, Park, Marshall, IN, USA

Aaron M. Collins, Yueyong Xin, Robert E. Blankenship [Poster]
Reconstitution of the Light Harvesting Antenna from *Chloroflexus aurantiacus*, 14th International Congress on Photosynthesis, Glasgow, UK

Aaron M. Collins and Robert E. Blankenship [Talk]
A Brief Introduction to Chlorosomes, 14th International Congress on Photosynthesis, Satellite Meeting on Antennas, Drymen, Glasgow, UK

2006

Martin F. Hohmann-Marriott, Aaron M. Collins and Robert E. Blankenship [Poster]. Variable Fluorescence in Green-Sulfur Bacteria, 32nd Midwestern Photosynthesis Meeting, Turkey Run State, Park, Marshall, IN, USA

JOURNAL OF BACTERIOLOGY, June 2007, p. 4196–4203 Vol. 189, No. 11
0021-9193/07/$08.00+0 doi:10.1128/JB.01711-06

Initial Characterization of the Photosynthetic Apparatus of "*Candidatus* Chlorothrix halophila," a Filamentous, Anoxygenic Photoautotroph▽†

Allison M. L. van de Meene,[1] Tien Le Olson,[1] Aaron M. Collins,[2] and Robert E. Blankenship[2]*

Department of Chemistry and Biochemistry, P.O. Box 871604, Arizona State University, Tempe, Arizona 85287-1604,[1] and Departments of Biology and Chemistry, Washington University, St. Louis, Missouri 63130[2]

Received 6 November 2006/Accepted 27 February 2007

"*Candidatus* Chlorothrix halophila" is a recently described halophilic, filamentous, anoxygenic photoautotroph (J. A. Klappenbach and B. K. Pierson, Arch. Microbiol. 181:17–25, 2004) that was enriched from the hypersaline microbial mats at Guerrero Negro, Mexico. Analysis of the photosynthetic apparatus by negative staining, spectroscopy, and sodium dodecyl sulfate-polyacrylamide gel electrophoresis indicated that the photosynthetic apparatus in this organism has similarities to the photosynthetic apparatus in both the *Chloroflexi* and *Chlorobi* phyla of green photosynthetic bacteria. The chlorosomes were found to be ellipsoidal and of various sizes, characteristics that are comparable to characteristics of chlorosomes in other species of green photosynthetic bacteria. The absorption spectrum of whole cells was dominated by the chlorosome bacteriochlorophyll *c* (BChl *c*) peak at 759 nm, with fluorescence emission at 760 nm. A second fluorescence emission band was observed at 870 nm and was tentatively attributed to a membrane-bound antenna complex. Fluorescence emission spectra obtained at 77 K revealed another complex that fluoresced at 820 nm, which probably resulted from the chlorosome baseplate complex. All of these results suggest that BChl *c* is present in the chlorosomes of "*Ca*. Chlorothrix halophila," that BChl *a* is present in the baseplate, and that there is a membrane-bound antenna complex. Analysis of the proteins in the chlorosomes revealed an ~6-kDa band, which was found to be related to the BChl *c* binding protein CsmA found in other green bacteria. Overall, the absorbance and fluorescence spectra of "*Ca*. Chlorothrix halophila" revealed an interesting mixture of photosynthetic characteristics that seemed to have properties similar to properties of both phyla of green bacteria when they were compared to the photosynthetic characteristics of *Chlorobium tepidum* and *Chloroflexus aurantiacus*.

Photosynthesis is a fundamental biological process that converts light energy into chemical energy. The organic products of photosynthesis are used by nonphotosynthesizing organisms for energy. Photosynthetic products include food products and fossil fuels, the legacy of ancient photosynthesis. There are different types of photosynthesis, including oxygenic photosynthesis, which occurs in cyanobacteria, algae, and plants, and anoxygenic photosynthesis, which occurs in purple bacteria, two groups of green bacteria, and heliobacteria (3).

Green photosynthetic bacteria can perform photosynthesis at the lowest light intensities of all photosynthetic organisms, even at light intensities that occur at the bottom of the sea near hydrothermal vents (1). This feat is accomplished with pigment-packed antenna systems called chlorosomes, which capture photons and transfer their energy to other pigment-protein antenna systems and then to reaction centers where photochemistry takes place (4).

In general, the architecture of chlorosomes is similar in all species of green photosynthetic bacteria. These structures are ellipsoidal, between 70 and 260 nm long, between 40 and 100 nm wide, and between 10 and 60 nm thick (31, 32). The interior of a chlorosome contains approximately 200,000 molecules of bacteriochlorophyll *c* (BChl *c*), BChl *d*, or BChl *e* packaged as oligomers with some BChl *a* and carotenoids and a small number of proteins (4). This array of pigments is thought to be surrounded by a lipid monolayer envelope (31). In the cell, the chlorosome attaches to the inner leaflet of the cytoplasmic membrane, where at the site of attachment a proteinaceous baseplate sits on the chlorosome. This baseplate contains the CsmA baseplate protein, which binds BChl *a*, as well as carotenoids (22). Antenna complexes and reaction centers are stored in the cytoplasmic membrane next to the chlorosome.

There are two phyla of green photosynthetic bacteria: the *Chlorobi* (14) and the *Chloroflexi* (13). The *Chlorobi* are green sulfur bacteria, and the *Chloroflexi* are filamentous anoxygenic phototrophs, which were previously called the green nonsulfur bacteria (24). While both groups contain chlorosomes, the compositions of their pigment-protein antenna systems and reaction centers differ. The *Chlorobi* contain an Fe-S type of reaction center similar to photosystem I (12) and a pigment-protein antenna complex called the BChl *a* protein or the Fenna-Matthews-Olson (FMO) protein (9, 20). The *Chloroflexi* contain a pheophytin-quinone type of reaction center similar to the reaction centers present in photosystem II and the purple phototrophic bacteria (11). The *Chloroflexi* also have a pigment-protein antenna complex called the B808-866 antenna

* Corresponding author. Mailing address: Departments of Biology and Chemistry, Campus Box 1229, Washington University, St. Louis, MO 63130. Phone: (314) 935-7971. Fax: (314) 935-4432. E-mail: Blankenship@wustl.edu.

† Supplemental material for this article may be found at http://jb.asm.org/.

▽ Published ahead of print on 16 March 2007.

Biochimica et Biophysica Acta 1787 (2009) 1050–1056

Contents lists available at ScienceDirect

Biochimica et Biophysica Acta

journal homepage: www.elsevier.com/locate/bbabio

Pigment organization in the photosynthetic apparatus of *Roseiflexus castenholzii*

Aaron M. Collins, Yueyong Xin, Robert E. Blankenship *

Department of Biology, Washington University, St Louis, MO 63130, USA
Department of Chemistry, Washington University, St Louis, MO 63130, USA

ARTICLE INFO

Article history:
Received 20 January 2009
Received in revised form 23 February 2009
Accepted 26 February 2009
Available online 9 March 2009

Keywords:
Roseiflexus castenholzii
Light harvesting
Pigment organization

ABSTRACT

The light-harvesting–reaction center (LHRC) complex from the chlorosome-lacking filamentous anoxygenic phototroph (FAP), *Roseiflexus castenholzii* (*R. castenholzii*) was purified and characterized for overall pigment organization. The LHRC is a single complex that is comprised of light harvesting (LH) and reaction center (RC) polypeptides as well as an attached *c*-type cytochrome. The dominant carotenoid found in the LHRC is keto-γ-carotene, which transfers excitation to the long wavelength antenna band with 35% efficiency. Linear dichroism and fluorescence polarization measurements indicate that the long wavelength antenna pigments absorbing around 880 nm are perpendicular to the membrane plane, with the corresponding Q_y transition dipoles in the plane of the membrane. The antenna pigments absorbing around 800 nm, as well as the bound carotenoid, are oriented at a large angle with respect to the membrane. The antenna pigments spectroscopically resemble the well-studied LH2 complex from purple bacteria, however the close association with the RC makes the light harvesting component of this complex functionally more like LH1.

Published by Elsevier B.V.

1. Introduction

Photosynthetic organisms have evolved to capture sunlight utilizing a variety of light harvesting architectures and pigment compositions that are highly diverse and have evolved to adapt to very different light intensity and light quality environments. Significant progress has been made in elucidating the structure–function relationships of the LH, RC and photosynthetic electron transport complexes among the various classes of phototrophs [1]. However, among the anoxygenic phototrophs, the purple bacteria are by far the best understood and other groups are less well characterized [2–4].

The phylum *Chloroflexi* contains filamentous anoxygenic phototrophs (FAPs) which are typified by *Chloroflexus* (*Cf.*) *aurantiacus* and harvest light primarily using bacteriochlorophyll (BChl) *c* located in the chlorosome [5]. The photosynthetic apparatus of most recently isolated species has not yet been characterized [6–8]. Among these, the newly described *Roseiflexus castenholzii* is one of just a few known FAPs that lack chlorosomes [9,10]. Recently, a crude RC preparation from *R. castenholzii* was described which has similar absorption characteristics to the RC of *Cf. aurantiacus* and protein sequence homology both to *Cf. aurantiacus* and to purple bacteria [11]. This same report determined that the *puf* gene arrangement was in the order of *pufB*, *-A*, *-L*, *-M*, and *-C*. This is more analogous to the arrangement of the *puf* operon in purple bacteria rather than that in *Cf. aurantiacus*, which have the same genes located on two distinct operons, *puf1* and *puf2* [12]. The genome sequences of several FAPs, including both *Cf. aurantiacus* and *R. castenholzii* have recently been determined [13].

Cf. aurantiacus contains, in addition to the peripheral chlorosome, a membrane-bound light-harvesting complex (B808–866) that is in close association with the RC. The B808–866 complex, named according to its Q_y absorption maxima, is thought to contain 3 BChl *a* per two antenna polypeptides, which are similar to the α- and β-subunits of LH1 and LH2 from purple bacteria [14,15]. The absorbance of the antenna resembles LH2, however, the close association with the RC suggests that its function is related to LH1 [16,17]. The Q_y transitions of the 866 nm pigments were determined to be approximately in the plane of the membrane while the 808 nm transitions are oriented at ~45° to the membrane plane [16,18]. *R. castenholzii* lacks chlorosomes but also contains a membrane-bound antenna that is generally similar to that found in *Cf. aurantiacus*, however its absorbance maxima are at about 800 and 880 nm [9,11].

Chloroflexi are the earliest branching phylum of bacteria that contains phototrophs, so they may have a central importance in understanding the origin and evolution of photosynthesis [19]. However, with the exception of *Cf. aurantiacus*, relatively little has been done to characterize this very diverse group of bacteria. The following objectives for the present analysis are: (a) to purify the LHRC complex from *R. castenholzii* and (b) provide initial characterization the LHRC complex in terms of pigment composition and organization. Our results demonstrate an overall similarity between the antenna pigments in *R. castenholzii* and *Cf. aurantiacus*, but with

* Corresponding author. Laboratory Sciences 401B, Department of Chemistry, Washington University, St. Louis, MO 63130-4899, USA. Tel.: +1 314 935 7971; fax +1 314 935 5125.
E-mail address: Blankenship@wustl.edu (R.E. Blankenship).

0005-2728/$ – see front matter. Published by Elsevier B.V.
doi:10.1016/j.bbabio.2009.02.027

JOURNAL OF BACTERIOLOGY, Nov. 2009, p. 6701–6708 Vol. 191, No. 21
0021-9193/09/$12.00 doi:10.1128/JB.00690-09

Structure of Chlorosomes from the Green Filamentous Bacterium *Chloroflexus aurantiacus*▽†

Jakub Pšenčík,[1] Aaron M. Collins,[2] Lassi Liljeroos,[3] Mika Torkkeli,[4] Pasi Laurinmäki,[3] Hermanus M. Ansink,[3]‡ Teemu P. Ikonen,[4]§ Ritva E. Serimaa,[4] Robert E. Blankenship,[2] Roman Tuma,[3,5] and Sarah J. Butcher[3]*

Department of Chemical Physics and Optics, Faculty of Mathematics and Physics, Charles University, Prague, Czech Republic[1]; *Department of Chemistry, Washington University, St. Louis, Missouri*[2]; *Institute of Biotechnology and Department of Biological and Environmental Sciences, University of Helsinki, Helsinki, Finland*[3]; *Department of Physical Sciences, University of Helsinki, Helsinki, Finland*[4]; *and The Astbury Centre for Structural Molecular Biology, University of Leeds, Leeds, United Kingdom*[5]

Received 27 May 2009/Accepted 18 August 2009

The green filamentous bacterium *Chloroflexus aurantiacus* employs chlorosomes as photosynthetic antennae. Chlorosomes contain bacteriochlorophyll aggregates and are attached to the inner side of a plasma membrane via a protein baseplate. The structure of chlorosomes from *C. aurantiacus* was investigated by using a combination of cryo-electron microscopy and X-ray diffraction and compared with that of *Chlorobi* species. Cryo-electron tomography revealed thin chlorosomes for which a distinct crystalline baseplate lattice was visualized in high-resolution projections. The baseplate is present only on one side of the chlorosome, and the lattice dimensions suggest that a dimer of the CsmA protein is the building block. The bacteriochlorophyll aggregates inside the chlorosome are arranged in lamellae, but the spacing is much greater than that in *Chlorobi* species. A comparison of chlorosomes from different species suggested that the lamellar spacing is proportional to the chain length of the esterifying alcohols. *C. aurantiacus* chlorosomes accumulate larger quantities of carotenoids under high-light conditions, presumably to provide photoprotection. The wider lamellae allow accommodation of the additional carotenoids and lead to increased disorder within the lamellae.

Chlorosomes (5, 13) are light-harvesting complexes found in three different phyla of photosynthetic bacteria. *Chloroflexus aurantiacus* belongs to the filamentous anoxygenic phototrophs (green nonsulfur bacteria) comprising members of the phylum *Chloroflexi*. All members of the green sulfur bacteria (phylum *Chlorobi*) contain chlorosomes. Very recently, a phototropic chlorosome-containing organism was found in the phylum *Acidobacteria* (9).

Chlorosomes are oblong bodies attached to the inner side of the cytoplasmic membrane. A unique property of chlorosomes is that their main pigment, bacteriochlorophyll (BChl) *c*, *d*, or *e*, is organized in the form of an aggregate. A similar self-assembled aggregate can form in the absence of proteins and exhibits spectral and excitonic properties similar to those of pigments in the native chlorosomes (for a review, see reference 3). The BChl aggregates were suggested to form lamellar structures in chlorosomes of green sulfur bacteria with lamellar spacing between 2 and 3 nm, depending on the main BChl (BChl *c* or *e*) and the prevailing esterifying alcohol (38, 39). In this model, the lamellar layers are maintained by nonspecific hydrophobic interactions of the interdigitated esterifying alcohols, while the in-layer arrangement is mediated through specific interactions between the stacked chlorin rings. In BChl *c*-containing chlorosomes of *Chlorobaculum tepidum* (formerly *Chlorobium tepidum*), the lamellar system (spacing, ~2 nm) often remains parallel for the whole length of the chlorosome (33, 38). In *Chlorobaculum tepidum* the lamellae exhibit considerable curvature, which was initially attributed to undulation (38), but recent end-on micrographs revealed a variety of curved lamellar structures, such as lamellar tubules or multilayered wraps, as well as undulations (33). Recently, when chlorosomes from a *Chlorobaculum tepidum* mutant with well-ordered BChl aggregates were used as a model for electron microscopy (EM) and nuclear magnetic resonance experiments, it was proposed that BChl aggregates form concentric nanotubes with the pigments arranged in helical spirals (14).

In contrast, chlorosomes from BChl *e*-containing bacteria (e.g., *Chlorobium phaeovibrioides*) contain lamellar pigments that are organized into small domains with random orientations. It has been proposed that this arrangement improves the absorption of photons with different polarizations (39). This, together with aggregation-induced enlargement of the oscillator strength, enables the bacteria to survive under extremely low-light conditions. At this point it is unclear whether these domains also exhibit a multilayer tubular arrangement. The data suggest that while the lamellar nature of BChl aggregates seems to be conserved, the higher-order structure of chlorosomes may be different in different species.

Chlorosomes attach to the cytoplasmic membrane via a crystalline baseplate that contains BChl *a* and carotenoids and acts

* Corresponding author. Mailing address: Institute of Biotechnology and Department of Biological and Environmental Sciences, University of Helsinki, Helsinki, Finland. Phone: 358 919159563. Fax: 358 919159930. E-mail: sarah.butcher@helsinki.fi.

† Supplemental material for this article may be found at http://jb.asm.org/.

‡ Present address: Free University of Amsterdam Medical Centre, Amsterdam, The Netherlands.

§ Present address: EMBL Hamburg, c/o DESY, Notkestraße 85, 22603 Hamburg, Germany.

▽ Published ahead of print on 28 August 2009.

Low Light Adaptation: Energy Transfer Processes in Different Types of Light Harvesting Complexes from *Rhodopseudomonas palustris*

Vladimíra Moulisová,[†] Larry Luer,[‡§] Sajjad Hoseinkhani,[‡] Tatas H. P. Brotosudarmo,[†] Aaron M. Collins,[¶] Guglielmo Lanzani,[‖] Robert E. Blankenship,[¶] and Richard J. Cogdell[†*]

[†]Faculty of Biomedical and Life Sciences, University of Glasgow, Glasgow, United Kingdom; [‡]CNR/INFM ULTRAS, Department of Physics, Politecnico di Milano, Milan, Italy; [§]IMDEA Nanociencia, Facultad de Ciencias, Módulo C-IX, Ciudad Universitaria de Cantoblanco, Madrid, Spain; [¶]Departments of Biology and Chemistry, Washington University in St. Louis, St. Louis, Missouri; and [‖]Italian Institute of Technology and Department of Physics, Politecnico di Milano, Milan, Italy

ABSTRACT Energy transfer processes in photosynthetic light harvesting 2 (LH2) complexes isolated from purple bacterium *Rhodopseudomonas palustris* grown at different light intensities were studied by ground state and transient absorption spectroscopy. The decomposition of ground state absorption spectra shows contributions from B800 and B850 bacteriochlorophyll (BChl) *a* rings, the latter component splitting into a low energy and a high energy band in samples grown under low light (LL) conditions. A spectral analysis reveals strong inhomogeneity of the B850 excitons in the LL samples that is well reproduced by an exponential-type distribution. Transient spectra show a bleach of both the low energy and high energy bands, together with the respective blue-shifted exciton-to-biexciton transitions. The different spectral evolutions were analyzed by a global fitting procedure. Energy transfer from B800 to B850 occurs in a mono-exponential process and the rate of this process is only slightly reduced in LL compared to high light samples. In LL samples, spectral relaxation of the B850 exciton follows strongly nonexponential kinetics that can be described by a reduction of the bleach of the high energy excitonic component and a red-shift of the low energetic one. We explain these spectral changes by picosecond exciton relaxation caused by a small coupling parameter of the excitonic splitting of the BChl *a* molecules to the surrounding bath. The splitting of exciton energy into two excitonic bands in LL complex is most probably caused by heterogenous composition of LH2 apoproteins that gives some of the BChls in the B850 ring B820-like site energies, and causes a disorder in LH2 structure.

INTRODUCTION

Absorption of solar energy by photoactive pigments and energy transfer through a cascade of antenna complexes to the photosynthetic reaction center (RC) represent the earliest reactions in photosynthesis. In purple photosynthetic bacteria, there are two main types of light harvesting complexes, LH1 and LH2 (1). The crystal structures of a few of these LH complexes isolated from purple nonsulfur bacteria have been solved by x-ray crystallography, e.g., the LH2 complex from *Rhodopseudomonas* (*Rps.*) *acidophila* 10050 (2), the LH2 from *Rhodospirillum molischianum* (3), the LH3 (LH2 version from low light) from *Rps. acidophila* 7050 (4) and the LH1-RC complex (core-complex, LH1 with photosynthetic reaction center) from *Rhodopseudomonas palustris* (5). The LH2 complex from *Rps. acidophila* consists of nine α- and β-apoprotein dimers arranged in a highly symmetric ring. Each heterodimer binds three BChl *a* molecules, one which is monomeric and two of which are strongly coupled. The overall complex contains nine monomeric and 18 strongly coupled BChl *a* molecules. The nine monomeric BChls absorb in the NIR at 800 nm and are called B800, the 18 tightly coupled BChls absorb at 850 nm (B850). The LH1 complex isolated from the *Rps. palustris* consists of 15 α/β-heterodimer subunits that form an ellipse that surrounds the RC. LH1 only has the tightly coupled BChl *a* molecules absorbing at 875 nm (B875). Light energy absorbed by B800 is transferred to B850, then on to B875 in LH1 from where it is finally transferred to BChls in RC (6).

The knowledge of these structures has allowed the energy transfer (ET) processes that take place in and between them to be understood in great detail (7). It has been found that some purple bacteria adapt to growth at lower light intensities by synthesizing LH complexes with modified spectral properties (8). It is not yet clear what the differences are in the ET processes taking place in these complexes in comparison to their high light (HL) counterparts. When growing at low light (LL) intensities, the bacterium *Rps. palustris* changes the spectral properties of its LH2 complexes. Compared to the HL form of LH2 the absorption spectrum of LL LH2 complexes has a lower, broader absorption at 850 nm and a broader, relatively higher absorption peak at 800 nm (9,10). Tadros et al. (11) and Tadros and Waterkamp (12) identified multiple genes encoding LH2 α- and β-apoproteins in *Rps. palustris*. Different members of this multigene family are expressed depending on the growth conditions (13,14). It has also been shown that both the HL and LL LH2 complexes from *Rps. palustris* contain multiple antenna apoprotein types, suggesting the possibility of LH2 rings with mixed populations of polypeptides giving different spectral properties to B850 BChls (15). This idea was supported by a resonance Raman spectroscopy study on LL LH2 complexes,

Submitted July 24, 2009, and accepted for publication September 10, 2009.

*Correspondence: gbta18@udcf.gla.ac.uk

Editor: Leonid S. Brown.

0006-3495/09/12/3019/10 $2.00

doi: 10.1016/j.bpj.2009.09.023

Electrospray-assisted characterization and deposition of chlorosomes to fabricate a biomimetic light-harvesting device

Luis B. Modesto-Lopez,[a] Elijah J. Thimsen,[a] Aaron M. Collins,[b] Robert E. Blankenship[b] and Pratim Biswas*[a]

Received 21st July 2009, Accepted 16th September 2009
First published as an Advance Article on the web 20th October 2009
DOI: 10.1039/b914758f

Photosynthesis is an efficient process by which solar energy is converted into chemical energy. Green photosynthetic bacteria such as *Chloroflexus aurantiacus* have supramolecular antenna complexes called chlorosomes attached to their cytoplasmic membrane that increase the cross section for light absorption even in low-light conditions. Self-assembled bacteriochlorophyll pigments in the chlorosome interior play a key role in the efficient transfer and funneling of the harvested energy. In this work it was demonstrated that chlorosomes can be rapidly and precisely size-characterized online in real time using an electrospray-assisted mobility-based technique. Chlorosomes were electrospray-deposited onto TiO_2 nanostructured films with columnar morphology to fabricate a novel biomimetic device to overcome the solvent compatibility issues associated with biological particles and synthetic dyes. The assembled unit retained the viability of the chlorosomes, and the harvesting of sunlight over a broader range of wavelengths was demonstrated. It was shown that the presence of chlorosomes in the biomimetic device had a 30-fold increase in photocurrent.

Introduction

Solar energy is a plentiful resource distributed over the surface of the earth and is already used to generate electricity trough photovoltaic devices. In recent years, dye-sensitized solar cells (DSSCs) based on a metal oxide film,[1] typically a titanium dioxide (TiO_2) nanostructured thin film, have been increasingly investigated to overcome the high-cost of fabrication of silicon-based photovoltaic devices. Key challenges for these DSSCs reside in increasing the photon collection efficiency over a broad spectrum of wavelengths in the visible regime, and in retarding the charge recombination process. In our previous studies, a TiO_2 nanostructured film with columnar morphology[2] was observed to be more efficient both in preventing the electron-hole recombination process and in enhancing the electron transport across the film than a granular morphology in a DSSC. A TiO_2 film made of vertically aligned nanostructured columns results in a higher interfacial area between the hole carrier (an electrolyte or a conductive polymer) and the electron acceptor (TiO_2) materials with highly-efficient electron transport properties.

When it comes to solar energy harvesting, nature provides valuable knowledge of the materials, of their functionality, and of the assembly mechanisms to produce efficient light-harvesting structures such as the ones found in plants and photosynthetic bacteria. A novel approach to develop light-harvesting devices to generate electricity, based on the concept of biomimetics, is to combine engineered nanostructured TiO_2 films having an efficient electron transport morphology, nano-columns or nano-wires, with robust natural light-harvesting supramolecular structures.

[a]*Aerosol and Air Quality Research Laboratory, Department of Energy, Environmental and Chemical Engineering, Washington University in Saint Louis, Campus Box 1180, Saint Louis, MO, 63130, USA. E-mail: pratim.biswas@wustl.edu; Fax: +1-(314)-935-5464; Tel: +1-(314)-935-5482*
[b]*Departments of Chemistry and Biology, Washington University in Saint Louis, Campus Box 1137, Saint Louis, MO, 63130, USA*

Broader context

Dye-sensitized solar cells (DSSCs) have been touted as lower cost alternates to silicon-based photovoltaic devices. One of the challenges is to improve the energy conversion efficiency of DSSCs by extending the absorption at longer wavelengths. One approach is to extract the highly efficient natural photosynthetic components from green bacteria and incorporate them into robust nanostructured systems to fabricate engineered biomimetic hybrid devices. This paper reports a generalized fabrication methodology of a multilayered biomimetic light-harvesting device that combines a nanostructured TiO_2 film with columnar morphology with natural light-harvesting supramolecular structures, called chlorosomes, found in green bacteria. The key aspect was the use of an electrospray system to aerosolize the chlorosomes, and then deposit them using electric fields. The incompatibility issue of the dye (organic solvent) and biological components (aqueous solvents) was overcome by the sequential process: aerosolization, drying in flight, followed by deposition. An online, real time mobility-based technique was used to determine the size and charge characteristics of chlorosomes. The results of photocurrent as a function of wavelength show a thirty fold increase in photocurrent when the chlorosomes were incorporated into the solar cell. The approaches demonstrated in this work have broader applicability in the characterization and sequential deposition of components to fabricate biomimetic solar cell devices.

Photosynth Res
DOI 10.1007/s11120-010-9554-8

REGULAR PAPER

Modulation of fluorescence in *Heliobacterium modesticaldum* cells

Aaron M. Collins · Kevin E. Redding · Robert E. Blankenship

Received: 16 December 2009 / Accepted: 14 April 2010

Abstract In what appears to be a common theme for all phototrophs, heliobacteria exhibit complex modulations of fluorescence yield when illuminated with actinic light and probed on a time scale of μs to minutes. The fluorescence yield from cells of *Heliobacterium modesticaldum* remained nearly constant for the first 10–100 ms of illumination and then rose to a maximum level with one or two inflections over the course of many seconds. Fluorescence then declined to a steady-state value within about one minute. In this analysis, the origins of the fluorescence induction in whole cells of heliobacteria are investigated by treating cells with a combination of electron accepters, donors, and inhibitors of the photosynthetic electron transport, as well as varying the temperature. We conclude that fluorescence modulation in *H. modesticaldum* results from acceptor-side limitation in the reaction center (RC), possibly due to charge recombination between P_{800}^{+} and A_0^{-}.

Keywords *Heliobacterium modesticaldum* · Fluorescence modulation · Fluorescence induction

Abbreviations

RC	Reaction center
[4Fe–4S]	4-Iron–4-sulfur
PMS	Phenazine methosulfate
BChl	Bacteriochlorophyll
PS1	Photosystem 1
A_0	Primary acceptor in the RC
F_0	Basal fluorescence level
F_v	Variable fluorescence

Introduction

Since the discovery of heliobacteria in 1983 by Gest and Favinger (Gest and Favinger 1983), notable progress has been made in elucidating their physiology and pigment composition, as well as energy transfer within the antenna of their photosystem and characteristics of the electron transport chain (for recent reviews see (Heinnickel and Golbeck 2007; Neerken and Amesz 2001; Oh-oka 2007). In addition to this, the genome of *Heliobacterium modesticaldum* (*H. modesticaldum*) has recently been sequenced and annotated (Sattley et al. 2008). Heliobacteria are obligate heterotrophs and are unique in that they facilitate light-harvesting using the pigment, bacteriochlorophyll (BChl) *g*, whose tetrapyrrole group is essentially an isomer of Chl *a*, in which the double bond in ring B has been moved to the ethylidine functional group at the C-8[1] position; it is also esterified with farnesol rather than phytol (Mizoguchi et al. 2005). The most recent measurements

Electronic supplementary material The online version of this article (doi:10.1007/s11120-010-9554-8) contains supplementary material, which is available to authorized users.

A. M. Collins · R. E. Blankenship (✉)
Departments of Biology and Chemistry, Washington University in St. Louis, Campus Box 1137, St. Louis, MO 63130, USA
e-mail: blankenship@wustl.edu

K. E. Redding
Institute de Biologie Physico-Chimique, 13 rue Pierre et Marie Curie, Paris 75005, France

Present Address:
K. E. Redding
Department of Chemistry and Biochemistry, Arizona State University, Tempe, AZ 85281, USA

Published online: 12 May 2010